

NQ

3 9 5 7 6

U M I
MICROFILMED 1999

INFORMATION TO USERS

This manuscript has been reproduced from the microfilm master. UMI films the text directly from the original or copy submitted. Thus, some thesis and dissertation copies are in typewriter face, while others may be from any type of computer printer.

The quality of this reproduction is dependent upon the quality of the copy submitted. Broken or indistinct print, colored or poor quality illustrations and photographs, print bleedthrough, substandard margins, and improper alignment can adversely affect reproduction.

In the unlikely event that the author did not send UMI a complete manuscript and there are missing pages, these will be noted. Also, if unauthorized copyright material had to be removed, a note will indicate the deletion.

Oversize materials (e.g., maps, drawings, charts) are reproduced by sectioning the original, beginning at the upper left-hand corner and continuing from left to right in equal sections with small overlaps. Each original is also photographed in one exposure and is included in reduced form at the back of the book.

Photographs included in the original manuscript have been reproduced xerographically in this copy. Higher quality 6" x 9" black and white photographic prints are available for any photographs or illustrations appearing in this copy for an additional charge. Contact UMI directly to order.

UMI[®]

Bell & Howell Information and Learning
300 North Zeeb Road, Ann Arbor, MI 48106-1346 USA
800-521-0600

UNIVERSITY OF ALBERTA

**LATE QUATERNARY GLACIATION AND POSTGLACIAL EMERGENCE,
SOUTHERN EUREKA SOUND, HIGH ARCTIC CANADA**

by

COLM Ó COFAIGH



A thesis submitted to the Faculty of Graduate Studies and Research in partial fulfilment
of the requirements for the degree of Doctor of Philosophy

Department of Earth and Atmospheric Sciences

Edmonton, Alberta

Spring 1999



National Library
of Canada

Acquisitions and
Bibliographic Services

395 Wellington Street
Ottawa ON K1A 0N4
Canada

Bibliothèque nationale
du Canada

Acquisitions et
services bibliographiques

395, rue Wellington
Ottawa ON K1A 0N4
Canada

Your file *Votre référence*

Our file *Notre référence*

The author has granted a non-exclusive licence allowing the National Library of Canada to reproduce, loan, distribute or sell copies of this thesis in microform, paper or electronic formats.

The author retains ownership of the copyright in this thesis. Neither the thesis nor substantial extracts from it may be printed or otherwise reproduced without the author's permission.

L'auteur a accordé une licence non exclusive permettant à la Bibliothèque nationale du Canada de reproduire, prêter, distribuer ou vendre des copies de cette thèse sous la forme de microfiche/film, de reproduction sur papier ou sur format électronique.

L'auteur conserve la propriété du droit d'auteur qui protège cette thèse. Ni la thèse ni des extraits substantiels de celle-ci ne doivent être imprimés ou autrement reproduits sans son autorisation.

0-612-39576-6

Canada

UNIVERSITY OF ALBERTA

LIBRARY RELEASE FORM

Name of Author: Colm Ó Cofaigh
Title of Thesis: Late Quaternary Glaciation and Postglacial
Emergence, Southern Eureka Sound,
High Arctic Canada
Degree: Doctor of Philosophy
Year this Degree Granted: Spring 1999

Permission is hereby granted to the University of Alberta Library to reproduce single copies of this thesis and to lend or sell such copies for private, scholarly or scientific research purposes only.

The author reserves all other publication and other rights in association with the copyright in the thesis, and except as hereinbefore provided, neither the thesis nor any substantial portion thereof may be printed or otherwise reproduced in any material form whatever without the author's prior written permission.

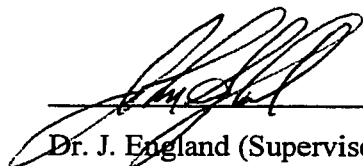
Colm Ó Cofaigh
Colm Ó Cofaigh
30 Hilton Ave. N.W.
Calgary, Alberta
Canada T2K 2H2.

December 1, 1998

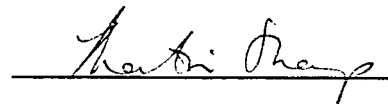
University Of Alberta

Faculty Of Graduate Studies And Research


The undersigned certify that they have read, and recommend to the Faculty of Graduate Studies and Research for acceptance, a thesis entitled "Late Quaternary Glaciation and Postglacial Emergence, Southern Eureka Sound, High Arctic Canada" submitted by Colm Ó Cofaigh in partial fulfillment of the requirements for the degree of Doctor of Philosophy.



Dr. J. England (Supervisor)



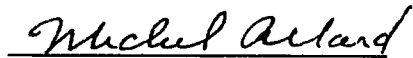
Dr. M. Sharp



Dr. N. Rutter



Dr. D. Vitt



Dr. M. Allard

October 30, 1998

This thesis is dedicated with love and gratitude to Ma and Da (Joan and Tomás Ó Cofaigh) who have been anchors of support throughout my life and always encouraged me to pursue my dreams.

ABSTRACT

Eureka Sound is the inter-island channel separating Ellesmere and Axel Heiberg islands, High Arctic Canada. This thesis reconstructs the glacial and sea level history of southern Eureka Sound through surficial geological mapping, studies of glacial sedimentology and geomorphology, surveying of raised marine shorelines, radiocarbon dating of marine shells and driftwood and surface exposure dating of erratics and bedrock. Granite dispersal trains, shelly till and ice-moulded bedrock record westerly-flow of warm-based, regional ice into Eureka Sound from a source on southeastern Ellesmere Island during the late Wisconsinan. Regional ice was coalescent with local ice domes over Raanes and northern Svendsen peninsulas. Marine limit (dating ≤ 9.2 ka BP; ≤ 9.9 ka cal BP) is inset into the dispersal trains and records early Holocene deglaciation of regional ice. Collectively these data indicate an extensive ice-cover in southern Eureka Sound during the Last Glacial Maximum. Ice-divides were located along the highlands of central Ellesmere and Axel Heiberg islands, from which ice converged on Eureka Sound, and subsequently flowed north and south along the channel.

Deglaciation was characterised by a two-step retreat pattern, likely triggered by eustatic sea level rise and abrupt early Holocene warming. Initial break-up and radial retreat of ice in Eureka Sound and the larger fiords, preceded terrestrial stabilisation along coastlines and inner fiords. Location of deglacial depocentres was predominantly controlled by fiord bathymetry. Regionally, two-step deglaciation is reflected by prominent contrasts in glacial geomorphology between the inner and outer parts of many fiords. Glacial sedimentological and geomorphological evidence indicates spatial variation in basal thermal regime between retreating trunk glaciers.

Holocene emergence of up to 150 m asl along southern Eureka Sound is recorded by raised marine deltas, beaches and washing limits. Emergence curves exhibit marked contrasts in the form and rate of initial unloading. Isobases drawn on the 8.5 ka shoreline for greater Eureka Sound demonstrate that a cell of highest emergence extends along the length of the channel, and closes in the vicinity of the entrance to Norwegian Bay. The isobase pattern indicates a distinct loading centre over the sound, and in conjunction with glacial geological evidence, suggests that the thickest late Wisconsinan ice lay over the channel.

ACKNOWLEDGEMENTS

Financial support for this research was provided by the Canadian Circumpolar Institute (BAR grants), the Quaternary Research Association (Young Research Workers Awards), and the Natural Sciences and Engineering Research Council of Canada (Grant #A6608 to J. England). Chlorine-36 analyses and additional radiocarbon dating were provided by Dr. Marek Zreda, University of Arizona, through grants from the National Science Foundation in support of his on-going High Arctic research program. Radiocarbon dating was also provided by the Geological Survey of Canada, Ottawa, and Isotrace, University of Toronto. I would like to particularly acknowledge the assistance of Dr. Roger McNeely, GSC Radiocarbon Dating Laboratory, Ottawa. Thanks also to Dr. Serge Occhietti, Université du Québec à Montréal, for amino acid analyses. Conducting my research on southwestern Ellesmere Island would have been impossible without the superb logistical support of the Polar Continental Shelf Project. Björn Tenbrüggen, Celesa Horvath and Shul Gorden provided dedicated field assistance and great company. A University of Alberta PhD Scholarship, Dissertation Fellowship and Andrew Stewart Memorial Graduate Prize are also gratefully acknowledged.

Although this thesis has been a long journey, it has also been a fantastic learning experience, and many people have helped me along the road. Thank you to my supervisor, Dr. John England, for taking me on as a graduate student and giving me the opportunity to work on Ellesmere Island. He inspired me to pursue Arctic research through a talk he gave at a departmental research symposium way back in the far away days of 1994. Ever since, working with John has been a truly memorable experience (in the best sense!) and I have learned much along the way. Thanks John for the numerous stimulating discussions, exhaustive reviews, encouragement, friendship, for helping to show me that the pursuit of rigorous science is also immensely enjoyable, and all your hospitality.

Dr. Martin Sharp has also been an integral part of my time at U of A, and played a large role in making it so intellectually stimulating and enjoyable. Thanks Martin for all the discussions, chapter reading, support and encouragement over the years. You have taught me to always try to strive for excellence in work, and to keep an open mind. Geography 631 was one of the highlights of my years at U of A. Also particular thanks to Dr. John Shaw. From encouraging me to come to Canada all those years ago while driving around the back roads of Northern Ireland in a minivan, to assisting and giving feedback during write-up, you have always given freely of your time, shown me fairness and encouragement, and put up with numerous "But what ifs...?". I will always be grateful. Also thanks to Drs. Nat Rutter and Bruce Rains for discussion on aspects of this thesis over the years, as well as Doug Hodgson (Geological Survey of Canada, Ottawa) and Dr. Dave Evans (University of Glasgow).

Special thanks to Drs. Don Lemmen and Jan Bednarski, Geological Survey of

Canada, Calgary. They have consistently gone out of their way to help, and always made time for me whenever I entered their respective offices with one of my numerous questions or problems. No matter how puzzled, annoyed or down I've been before our discussions, I have always left their offices encouraged and clearer. Without their hospitality, assistance and encouragement the last two years would have been daunting indeed.

I look back with many fond memories on my time at U of A due to my interaction with many of the other graduate students in the department. In particular, Shul, Bjorn, James, John, Anthony, Scott, Monique, Kim and Nigel. Special thanks to Rod Smith and Sandra Mackay-Smith for their friendship and hospitality over the years. Also thanks to Andy Podor for his assistance during the first field season on Ellesmere and his friendship.

I would particularly like to thank the late Kent Holden, my friend, office mate, and colleague during my first three years at U of A. Kent was one of the finest people it has been my good fortune to meet since coming to Canada, and was always there for me through support, discussion, or just listening. I well remember the hours of endless discussion, puzzlement and laughs we had doing Geography 631 together that first year. Thanks Kent for everything. You are sorely missed.

Finally, three people have played a larger role than any others in helping me to complete this thesis, particularly in the last torturous months. Firstly, my parents (Tomás and Joan Ó Cofaigh) who have been behind me every step of the way, for as long as I can remember. Their love, continual support, senses of humour and remembering that "everything passes" have kept me going through it all. Thank you. I hope I can make you both proud.

To Celesa Horvath, the biggest thank you of all. More than any other person you have been there for me constantly over the last four and a half years. Your support, love, humour and hugs have kept me going through the darkest days and ensured that this thesis finally sees the light. Even though you have had to deal with your own thesis, as well as a full-time job, you have made our home a haven from work and stress and always helped me to remember that I would get through. I will be forever grateful. We move together into a new day.

TABLE OF CONTENTS

CHAPTER ONE

Introduction	1
1.1 OBJECTIVES	1
1.2 STRUCTURE	4
1.3 REFERENCES	8

CHAPTER TWO

Late Wisconsinan glaciation of southern Eureka Sound, High Arctic Canada: evidence for extensive Inuitian ice during the Last Glacial Maximum	12
2.1 INTRODUCTION	12
2.1.1 Previous Work	15
2.1.2 Regional Setting	17
2.2 DATA PRESENTATION	17
2.2.1 Distribution of erratics	17
<i>Raanes Peninsula and Bay Fiord</i>	17
<i>Adjacent areas</i>	21
2.2.2 Glacial geomorphology	22
<i>Raanes Peninsula and northwestern Svendsen Peninsula</i>	22
<i>Bay Fiord</i>	25
<i>Stor Island</i>	26
2.2.3 Marine Limit	27
2.2.4 Chronology	29
<i>Pre-Holocene radiocarbon dates</i>	29
<i>Holocene radiocarbon dates</i>	31
<i>Cosmogenic Chlorine-36</i>	33
2.3 DISCUSSION	35
2.3.1 Age of granite dispersal trains in southern Eureka Sound	35

2.3.2 Last Glacial Maximum	36
<i>Ice configuration and dynamics</i>	36
2.3.3 Deglaciation	40
2.3.4 Implications	42
<i>Significance of landscape zonation in fiords</i>	42
<i>Late Wisconsinan glaciation of northern Eureka Sound</i>	43
<i>Origin of Eureka Sound and its tributaries</i>	45
<i>Late Wisconsinan glaciation of the western Arctic Archipelago</i>	47
2.4 REFERENCES	49

CHAPTER THREE

Geomorphic and sedimentary signatures of early Holocene deglaciation in High Arctic fiords, Ellesmere Island: implications for thermal regime and ice dynamics during deglaciation	58
3.1 INTRODUCTION	58
3.2 STARFISH BAY	59
3.2.1 Sector A	63
<i>Geomorphology and sedimentary sequences</i>	63
<i>Interpretation</i>	67
<i>Marine limit and radiocarbon chronology</i>	69
3.2.2 Sector B	70
<i>Geomorphology</i>	70
<i>Marine limit and radiocarbon chronology</i>	72
<i>Interpretation</i>	72
3.2.3 Sector C	72
<i>Geomorphology and sedimentology</i>	72
<i>Marine limit and radiocarbon chronology</i>	73
<i>Interpretation</i>	73
3.3 BLIND FIORD	74
3.3.1 Sector A	74

<i>Geomorphology</i>	74
<i>Marine limit and radiocarbon chronology</i>	76
3.3.2 Sector B	76
<i>Geomorphology</i>	76
<i>Marine limit and radiocarbon chronology</i>	78
3.2.3 Sector C	78
<i>Geomorphology</i>	78
<i>Marine limit and radiocarbon chronology</i>	78
<i>Interpretation</i>	80
3.4 DISCUSSION	82
3.4.1 Controls on Early-Holocene Deglacial Sedimentation and Ice-retreat	82
<i>Fiord Topography</i>	82
<i>Basal Thermal Regime</i>	83
3.4.2 Implications	84
3.5 REFERENCES	87

CHAPTER FOUR

Holocene emergence and shoreline delevelling, southern Eureka Sound, High Arctic Canada	94
4.1 INTRODUCTION	94
4.2 STUDY AREA	98
4.3 LATE WISCONSINAN GLACIATION OF SOUTHERN EUREKA SOUND	98
4.4 METHODOLOGY	99
4.4.1 Surveying technique and definition of marine limit	99
4.5 MARINE LIMIT: ELEVATION AND PATTERN	99
4.6 RELATIVE SEA LEVEL CURVES	101
4.6.1 Blind Fiord	101
4.6.2 Starfish Bay	106

4.6.3 Irene Bay	107
4.7 POSTGLACIAL ISOBASES 8.5 KA BP	109
4.8 DISCUSSION	111
4.8.1 Initial postglacial emergence	111
4.8.2 Postglacial Isobases	113
4.9 REFERENCES	115

CHAPTER FIVE

Conclusions	120
5.1 LATE WISCONSINAN GLACIATION OF SOUTHERN EUREKA SOUND	120
5.2 CONTROLS ON EARLY HOLOCENE DEGLACIAL SEDIMENTATION AND ICE DYNAMICS	122
5.3 POSTGLACIAL EMERGENCE OF SOUTHERN EUREKA SOUND ..	124
5.4 RECOMMENDATIONS FOR FUTURE RESEARCH	124
5.5 REFERENCES	127

APPENDIX A: CHAPTER 2 RADIOCARBON AND CHLORINE-36 DATES	132
APPENDIX B: CHAPTER 3 RADIOCARBON DATES	145
APPENDIX C: CHAPTER 4 RADIOCARBON DATES	148

LIST OF FIGURES

Figure	Follows page
1.1	Location map, Queen Elizabeth Islands 1
1.2	Location map, southern Eureka Sound 1
2.1	Location map, Queen Elizabeth Islands and northwest Greenland 10
2.2	Location map, southern Eureka Sound 10
2.3	Distribution of granite erratics and ice-flow directional indicators 13
2.4	Granite dispersal trains, Ellesmere and Axel Heiberg islands, distribution of granite erratics above marine limit, western Arctic islands, and extent of Shield rocks on Ellesmere and Devon islands 13
2.5	Glacial geomorphology, southern Eureka Sound 16
2.6	Marine limit elevations, southern Eureka Sound 20
2.7	Pre-Holocene radiocarbon and Chlorine-36 dates, southern Eureka Sound 21
2.8	Holocene radiocarbon dates, southern Eureka Sound 22
2.9	Palaeogeography of the Last Glacial Maximum, southern Eureka Sound 26
2.10	Early Holocene deglacial dates, Eureka Sound and Nansen Sound 29
3.1	Location map, Queen Elizabeth Islands and northwest Greenland 47
3.2	Location map, southwestern Ellesmere Island and the study area 47
3.3	Starfish Bay, sector boundaries, glacial geomorphology, marine limit elevations and radiocarbon date locations 47
3.4	Starfish Bay, Sector A, glacial geomorphology and marine limit elevations . . . 48
3.5	Stratigraphic log from morainal bank, Starfish Bay, Sector A 48
3.6	Lithofacies in morainal bank, Starfish Bay, Sector A 48
3.7	Starfish Bay, Sector A, marine limit elevations and glacial geomorphology 52
3.8	Blind Fiord, sector boundaries, glacial geomorphology, marine limit elevations

	and radiocarbon date locations	55
3.9	Lateral meltwater channels, central Blind Fiord, Sector B	56
3.10	Blind Fiord, Sector C, glacial geomorphology and marine limit elevations	57
4.1	Location map, Queen Elizabeth Islands	72
4.2	Location map, southern Eureka Sound	72
4.3	Marine limit elevations, southern Eureka Sound	75
4.4	Marine limit elevations and radiocarbon date locations, Blind Fiord, Starfish Bay and Irene Bay	76
4.5	Emergence curves: Blind Fiord; Head of Starfish Bay; Irene Bay	76
4.6	Postglacial isobases (8.5 ka BP), greater Eureka Sound	80

CHAPTER ONE

Introduction

This thesis concerns the nature of high latitude Quaternary glaciation and sea level change. Its objective is the reconstruction of the glacial and sea level history of southern Eureka Sound, High Arctic Canada (Figs. 1.1 and 1.2), focussing in particular on the Ellesmere Island side of the channel, and including Stor Island (Fig. 1.2). Southern Eureka Sound constitutes one of the remaining gaps in reconstructions of Quaternary glaciation and postglacial emergence in the Queen Elizabeth Islands. Previous work is restricted to that of Hodgson (1985) in several fiord heads along the east side of the study area. The proximity of the study area to Norwegian Bay (Fig. 1.1) makes it a key location for linking the glacial and sea level records of the alpine sector of the Queen Elizabeth Islands (*e.g.*, Andrews 1970; Hodgson 1985; England 1992, 1998; Lemmen *et al.* 1994; Bell 1996; Bednarski 1998) to that of the central and western parts of the Arctic Archipelago (Balkwill *et al.* 1974; Hodgson 1982, 1989; Dyke *in press* a and b). Over 60 new radiocarbon dates and 6 surface exposure dates are presented, which constrain the onset of the last glaciation, initial deglaciation, and the pattern of Holocene emergence.

1.1 OBJECTIVES

The aims of this research are:

- (1) To determine the extent of late Wisconsinan glaciation in southern Eureka Sound with respect to whether there was an extensive *Inuitian Ice Sheet* (Blake 1970), or a more restricted *Franklin Ice Complex* (England 1976a). Particular emphasis will be placed on determining the significance of the “drift-belt” as first mapped and formally defined on western Ellesmere Island by Hodgson (1985), with regard to whether this represents the late Wisconsinan limit or a recessional ice margin.
- (2) To investigate whether there is evidence for (a) older, pre-late Quaternary glaciations (cf. Lemmen and England 1992; Bell 1992; Bednarski 1995), as well as evidence for (b) a “full glacial sea” (cf. England 1983, 1992, 1997).

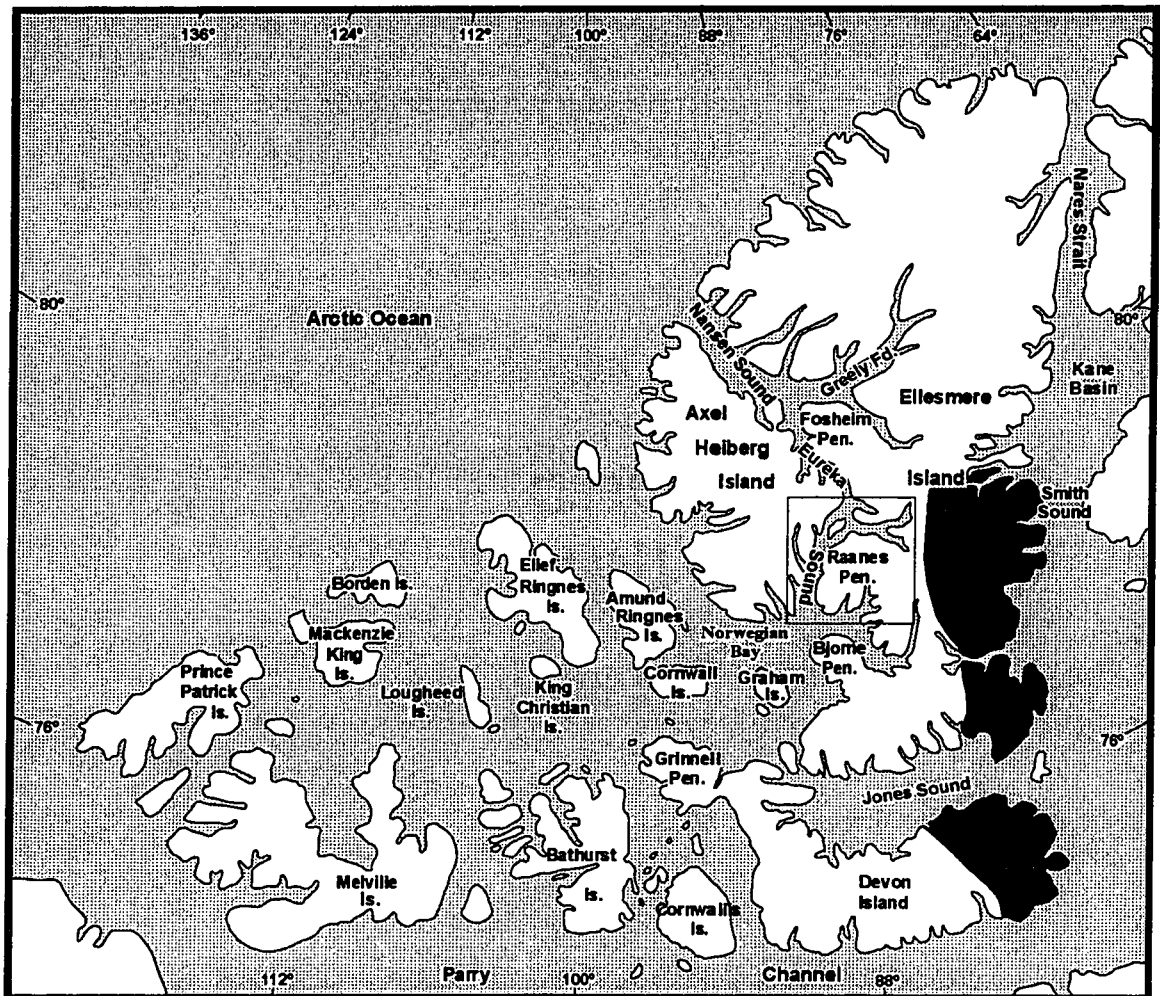


Figure 1.1: Queen Elizabeth Islands, Canada, location of study area (box), and extent of Canadian Shield bedrock on Ellesmere and Devon islands (black shading).

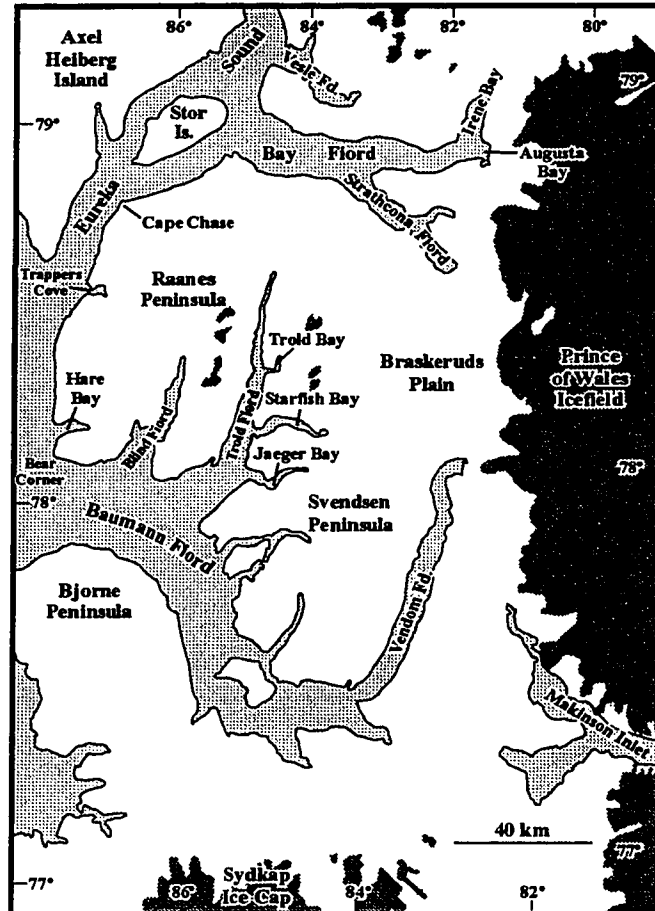


Figure 1.2: Southern Eureka Sound showing contemporary ice cover (dark shading) and location of placenames referred to in text.

- (3) To determine the controls on early Holocene deglacial sedimentation and ice dynamics in High Arctic fiords, and investigate how inter-fiord variations in deglacial landform/sediment associations directly reflect variations in these controls.
- (4) To determine the magnitude and chronology of postglacial emergence across the study area, as well as the pattern of Holocene shoreline develevelling, and examine how these relate to patterns of Holocene emergence in northern Eureka Sound (cf. Hodgson 1985; England 1992, 1997; Bell 1996).

As part of objectives (1) and (2a), a major component of this research is to determine the distribution, age and source of granite erratics in the study area. Hodgson (1985) noted granite erratics within inner Irene Bay, and granites were observed further west on Stor Island by Troelsen (1952) (Figs. 1.1 and 1.2). Along northern Eureka Sound, Bell (1992) also documented granite erratics, and hypothesised that they came from the Shield of southeastern Ellesmere Island. He proposed that the glaciations responsible for erratic deposition were late Tertiary/early Quaternary in age on the basis of amino acid ratios from associated shelly till. However, the distribution of granite erratics further south, across Raanes and Svendsen peninsulas, and through Bay Fiord, remains largely unknown. If granite erratics are present in southern Eureka Sound, a key question pertains to their source, with regard to whether they were deposited by northward flowing Laurentide ice from the Canadian mainland, or by westward-flowing Ellesmere Island ice.

1.2 STRUCTURE

The thesis is written in paper format and is divided into three main chapters, in addition to the introduction and conclusions. The three papers are thematic and focus on the principal aspects of the glacial and sea level history of the study area. Each paper is discussed briefly below.

Chapter 2: *Late Wisconsinan glaciation of southern Eureka Sound, High Arctic Canada: evidence for extensive Inuitian ice during the Last Glacial Maximum.* (Objectives #1 and #2, above).

(A version of this paper will be submitted for publication to Quaternary Science Reviews.)

This paper presents a reconstruction of the extent and chronology of late Wisconsinan glaciation in southern Eureka Sound, focussing on the Ellesmere Island side of the channel, and Stor Island (Fig. 1.1) Previous work in Eureka Sound is limited predominantly to the northern part of the channel, where radically different reconstructions of the glacial history have been proposed. These range from a limited expansion of local ice caps and glaciers during the Last Glacial Maximum, with more extensive, pre-late Wisconsinan regional ice (*e.g.*, Hodgson 1985; England 1987, 1990, 1992; Bell 1992, 1996), to a late Wisconsinan *Innuitian Ice-Sheet* (*e.g.*, Blake 1970; Hodgson 1985; Bednarski 1998; England 1998, *in press*). Along southern Eureka Sound, ice extent, chronology and dynamics of retreat are unknown, with the exception of the fiord heads to the east (Hodgson 1985).

This paper therefore addresses the glacial history of southern Eureka Sound, focussing in particular on the distribution and age of prominent granite erratic dispersal trains, and the timing and pattern of deglaciation. It is based on geomorphological mapping (air photos and ground traverse), sedimentological investigation of glaciogenic and raised marine deposits, surveying of raised marine shorelines, radiocarbon dating of molluscs and driftwood from raised marine deposits and till, as well as surface exposure dating of erratics and bedrock surfaces using cosmogenic Chlorine-36 (in collaboration with M. Zreda, University of Arizona).

Chapter 3: Geomorphic and sedimentary signatures of early Holocene deglaciation in High Arctic fiords, Ellesmere Island: implications for thermal regime and ice dynamics during deglaciation. (Objective # 3, above).

(A version of this paper has been published in Canadian Journal of Earth Sciences.)

This paper presents an integrated study of glacial geomorphology, sedimentology, marine limit elevations and radiocarbon dating from two adjacent fiords on southwestern Ellesmere Island, Starfish Bay and Blind Fiord (Fig. 1.2). Both fiords exhibit marked contrasts in their deglacial landform/sediment associations. These contrasts are attributed to inter-fiord variations in early Holocene deglacial ice dynamics and basal thermal regime, which controlled the type and location of deglacial landform/sediment associations in the two fiords. The objective of the paper is to highlight the influences of fiord bathymetry and basal thermal

regime on early Holocene deglacial ice dynamics and sedimentation. The paper also discusses implications for regional reconstructions of late Wisconsinan glaciation in an area where marked contrasts in weathering, and presence or absence of glacial landforms, occur (*e.g.*, Hodgson 1985; England 1987, 1990; Lemmen *et al.* 1994; Bell 1996). These differences have previously been linked to the extent of late Wisconsinan glaciation (*e.g.*, England 1987, 1990; Bell 1996). With few exceptions to date (*e.g.*, Lemmen *et al.* 1994), such integrated studies have been rare in the Canadian High Arctic. Previous research has tended to focus on the extent of late Wisconsinan glaciation (*e.g.*, Blake 1970, 1992; England 1976a, 1998; Evans 1990; Bell 1996), and the pattern of Holocene emergence (*e.g.*, Blake 1975, 1993; England 1976b, 1992), or more rarely on sedimentological studies of emergent glaciomarine deposits (*e.g.*, Bednarski 1988; Stewart 1991; Aitken and Bell 1998).

This paper is based primarily on geomorphological mapping, sedimentological investigation of glaciogenic and raised marine deposits, particularly the internal structure of ice-contact landforms, and radiocarbon dating of associated marine shells to establish a deglacial chronology

Chapter 4: *Holocene emergence and shoreline delevelling, southern Eureka Sound, High Arctic Canada* (Objective #4, above).

(A version of this paper will be submitted for publication to *Géographie physique et Quaternaire*.)

This paper focuses on the magnitude and chronology of postglacial emergence throughout the study area. The reconstruction is based on surveying of raised marine shorelines and radiocarbon dating of associated marine shells and driftwood. Previous work on this topic from northern Eureka Sound (*e.g.*, Hodgson 1985; England 1992, 1997; Bell 1996), highlighted several unique aspects of postglacial emergence there including: (a) emergence of ≥ 150 m asl (*e.g.*, Bell 1996; Bednarski 1998) which is the highest recorded in the Queen Elizabeth Islands. The magnitude of this emergence has been used as support for a regional ice sheet during the late Wisconsinan (*cf.* Blake 1970, 1992; Walcott 1972; Tushingham 1991; England and Ó Cofaigh 1998; England *in press*); (b) England (1992, 1997) presented evidence which indicates that initial emergence in northern Eureka Sound was slow (1

m/century). He argued that this was inconsistent with the presence of a regional ice sheet over the eastern Queen Elizabeth Islands during the late Wisconsinan, and that together with isobases drawn on the 8ka shoreline, implies a possible neotectonic contribution to uplift. This neotectonic hypothesis is supplanted by his revision to a more extensive regional ice cover during the late Wisconsinan (England, 1998, *in press*).

This paper presents new data from southern Eureka Sound where similarly high *deglacial* shorelines (>140 m asl) are recorded. It attempts to integrate these new data with previously published work (see above) on Holocene emergence from northern Eureka Sound with the objective of reconstructing the pattern of Holocene shoreline delevelling for Eureka Sound as a whole.

1.3 REFERENCES

- Aitken, A.E. and Bell, T.J. (1998). Holocene glacimarine sedimentation and macrofossil palaeoecology in the Canadian High Arctic: environmental controls. *Marine Geology*, **145**, 151-171.
- Andrews, J.T. (1970). *A geomorphic study of postglacial uplift with particular reference to Arctic Canada*. Institute of British Geographers, London, England, Special Publication No. 2, 156p.
- Balkwill, H.R., Roy, K.J., Hopkins, W.S. and Sliter, W.V. (1974). Glacial features and pingos, Amund Ringnes Island, Arctic Archipelago. *Canadian Journal of Earth Sciences*, **11**, 1319-1325.
- Bednarski, J. (1988). The geomorphology of glaciomarine sediments in a high arctic fiord. *Géographie physique et Quaternaire*, **42**, 65-74.
- Bednarski, J. (1995). Glacial advances and stratigraphy in Otto Fiord and adjacent areas, Ellesmere Island, Northwest Territories. *Canadian Journal of Earth Sciences*, **32**, 52-64.
- Bednarski, J. (1998). Quaternary history of Axel Heiberg Island bordering Nansen Sound, Northwest Territories, emphasising the last glacial maximum. *Canadian Journal of Earth Sciences*, **35**, 520-533.
- Bell, T. (1992). *Glacial and sea level history of western Fosheim Peninsula, Ellesmere Island, Arctic Canada*. Unpublished PhD thesis, University of Alberta, Edmonton, 172pp.
- Bell, T. (1996). Late Quaternary glacial and sea level history of Fosheim Peninsula, Ellesmere Island, Canadian High Arctic. *Canadian Journal of Earth Sciences*, **33**, 1075-1086.
- Blake, W.R., Jr. (1970). Studies of glacial history in arctic Canada. I. Pumice, radiocarbon dates, and differential postglacial uplift in the eastern Queen Elizabeth Islands. *Canadian Journal of Earth Sciences*, **7**, 634-664.
- Blake, W.R., Jr. (1975). Radiocarbon age determinations and postglacial emergence at Cape Storm, southern Ellesmere Island, Arctic Canada. *Geografiska Annaler*, **57A**, 1-71.

- Blake, W.R., Jr. (1992). Holocene emergence at Cape Herschel, east central Ellesmere Island, Arctic Canada: implications for ice sheet configuration. *Canadian Journal of Earth Sciences*, **29**, 1958-1980.
- Blake, W.R., Jr. (1993). Holocene emergence along the Ellesmere Island coasts of northernmost Baffin Bay. *Norsk Geologisk Tidsskrift*, **73**, 147-160.
- Dyke, A. S. (*in press*, a). The last glacial maximum and deglaciation of Devon Island: Support for an Innuitian Ice Sheet. *Quaternary Science Reviews*.
- Dyke, A. S. (*in press*, b). Holocene deleveling of Devon Island, Arctic Canada: Implications for ice sheet geometry. *Canadian Journal of Earth Science*.
- England, J. (1976a). Late Quaternary glaciation of the eastern Queen Elizabeth Islands, Northwest Territories, Canada: alternative models. *Quaternary Research*, **6**, 185-202.
- England, J. (1976b). Postglacial isobases and uplift curves from the Canadian and Greenland High Arctic. *Arctic and Alpine Research*, **8**, 61-78.
- England, J. (1983). Isostatic adjustments in a full glacial sea. *Canadian Journal of Earth Sciences*, **20**, 895-917.
- England, J. (1987). Glaciation and the evolution of the Canadian high arctic landscape. *Geology*, **15**, 419-424.
- England, J. (1990). The late Quaternary history of Greely Fiord and its tributaries, west-central Ellesmere Island. *Canadian Journal of Earth Sciences*, **27**, 255-270.
- England, J. (1992). Postglacial emergence in the Canadian High Arctic: integrating glacioisostasy, eustasy and late deglaciation. *Canadian Journal of Earth Sciences*, **29**, 984-999.
- England, J. (1997). Unusual rates and patterns of Holocene emergence, Ellesmere Island, Arctic Canada. *Journal of the Geological Society*, London, **154**, 781-792.
- England, J. (1998). Support for the Innuitian Ice Sheet in the Canadian High Arctic during the Last Glacial Maximum. *Journal of Quaternary Science*, **13**, 275-280.
- England, J. (*in press*) Coalescent Greenland and Innuitian ice during the Last Glacial Maximum: revising the Quaternary of the Canadian High Arctic. *Quaternary Science Reviews*.

- England, J. and Ó Cofaigh, C. (1998). Deglacial sea level along Eureka Sound: the effects of ice retreat from a central basin to alpine margins (abstract). *Joint Meeting of the Geological Association of Canada and Mineralogical Association of Canada*, Quebec, Canada.
- Evans, D.J.A. (1990). The last glaciation and relative sea history of northwest Ellesmere Island, Canadian High Arctic. *Journal of Quaternary Science*, **5**, 67-82.
- Hodgson, D.A. (1982). *Surficial materials and geomorphological processes, western Sverdrup and adjacent islands, District of Franklin*. Geological Survey of Canada, Paper 81-9, 37p.
- Hodgson, D.A. (1985). The last glaciation of west-central Ellesmere island, Arctic Canada. *Canadian Journal of Earth Sciences*, **22**, 347-368.
- Hodgson, D.A. (1989). Quaternary geology of the Queen Elizabeth Islands. In: Fulton, R.J. (ed.), *Quaternary Geology of Canada and Greenland*. Geological Survey of Canada, Geology of Canada, no. 1, 441-477.
- Hodgson, D.A. (1990). Were erratics moved by glaciers or icebergs to Prince Patrick Island, western Arctic Archipelago, Northwest Territories? *Geological Survey of Canada, Paper 90-1D*, 67-70.
- Lemmen, D.S. and England, J. (1992). Multiple glaciations and sea level changes, northern Ellesmere Island, high arctic Canada. *Boreas*, **21**, 137-152.
- Lemmen, D.S., Aitken, A.E. and Gilbert, R. (1994). Early Holocene deglaciation of Expedition and Strand fiords, Canadian High Arctic. *Canadian Journal of Earth Sciences*, **31**, 943-958.
- Stewart, T.G. (1991). Glacial marine sedimentation from tidewater glaciers in the Canadian High Arctic. In: Anderson, J.B. and Ashley, G.M. (eds.), *Glacial Marine Sedimentation; Paleoclimatic Significance*. Geological Society of America Special Paper 261, pp. 95-105.
- St. Onge, D. (1965). *La geomorphologie de l'île Ellef Ringnes Territoires du Nord-Ouest, Canada*. Geographical Branch, Paper 38, 58p.
- Troelsen, J.C. (1952). Geological investigations in Ellesmere Island. *Arctic*, **5**, 199-210.

- Tushingham, A. M. (1991). On the extent and thickness of the Innuitian Ice-Sheet: a postglacial-adjustment approach. *Canadian Journal of Earth Sciences*, **28**, 231-239.
- Walcott, R.I. (1972). Late Quaternary vertical movements in eastern North America: quantitative evidence of glacio-isostatic rebound. *Reviews of Geophysics and Space Physics*, **10**, 849-884.

CHAPTER TWO

Late Wisconsinan glaciation of southern Eureka Sound, High Arctic Canada: evidence for extensive Inuitian ice during the Last Glacial Maximum

2.1 INTRODUCTION

This paper is the first detailed study of the late Wisconsinan glacial history of southern Eureka Sound, Queen Elizabeth Islands, Arctic Canada (Figs. 2.1 and 2.2). Blake (1970) originally proposed the existence of an *Inuitian Ice Sheet* during the late Wisconsinan in this region on the basis of a broad, southwestwards-oriented corridor of maximum Holocene emergence extending from Eureka Sound to Bathurst Island. He argued that this emergence directly reflected the crustal response to removal of a pan-archipelago ice sheet, which was coalescent with the *Laurentide Ice Sheet* to the south and the *Greenland Ice Sheet* to the northeast. A persistent problem with this reconstruction has been the lack of direct stratigraphic and chronologic evidence for such an ice sheet along its proposed axis in Eureka Sound. To date, the only detailed Quaternary investigations in this region are from the northern part of the sound, and these have advocated a restricted late Wisconsinan ice cover (England 1987, 1990, 1992; Bell 1992, 1996), although recent work challenges that interpretation (Bednarski 1998; England 1998, *in press*).

This paper focuses on the largely unstudied southern part of Eureka Sound. It significantly extends previous work to the north (England 1987, 1990, 1992; Bell 1992, 1996; Bednarski 1995, 1998), and links studies conducted in the fiord heads of west-central Ellesmere Island (Hodgson 1985) to recent Quaternary investigations in Norwegian Bay (Hättestrand and Stroeven 1996)(Figs. 2.1 and 2.2). It thus connects the Quaternary record of the alpine sector of the Queen Elizabeth Islands (Ellesmere and Axel Heiberg islands) (*e.g.*, Hodgson 1985; Blake 1992a, 1993; Lemmen *et al.* 1994; Bell 1996; Bednarski 1998; England, 1997, 1998) to that of the central and western Arctic archipelago (*e.g.*, Fyles 1965; Balkwill *et al.* 1974; Hodgson 1982, 1989, 1990; Praeg 1989; Hättestrand and Stroeven 1996; Dyke *in press* a and b). The focus of this paper is predominantly on the Ellesmere Island side of the channel, specifically Bay Fiord, Raanes Peninsula and northwestern

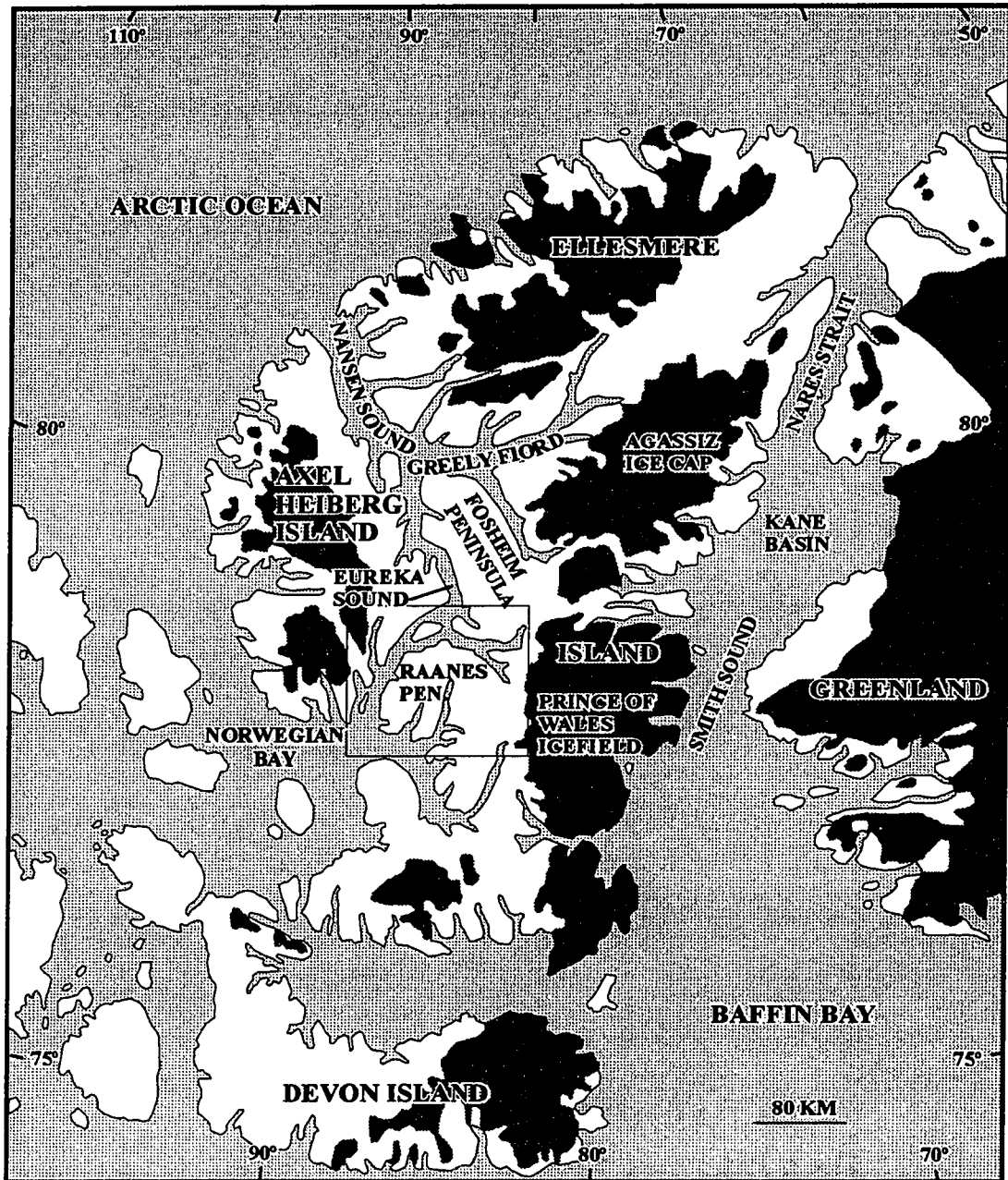


Figure 2.1: Eastern Queen Elizabeth Islands and northwest Greenland showing location of the study area (box) and contemporary ice cover (dark shading).

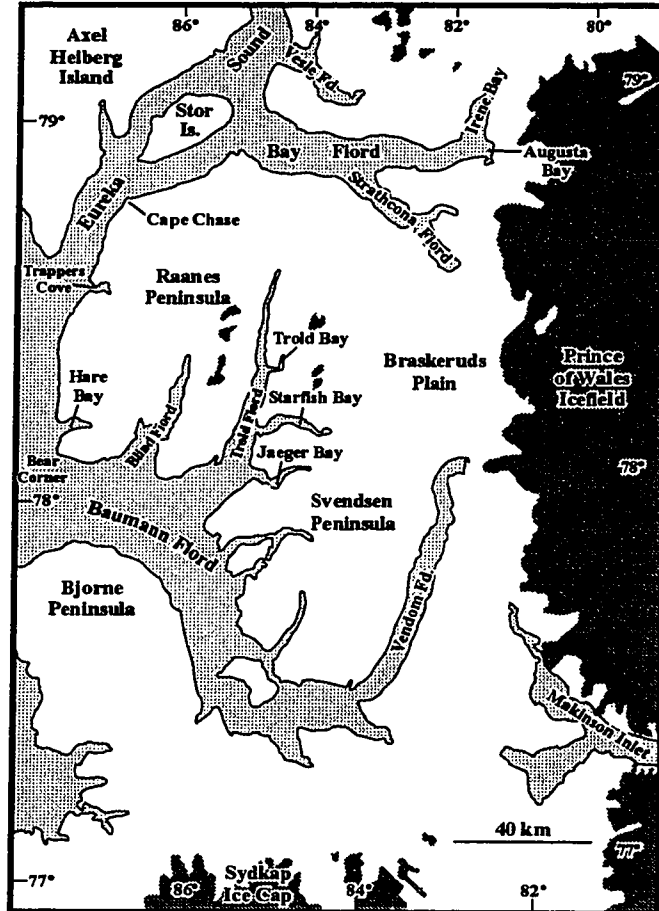


Figure 2.2: Southern Eureka Sound showing contemporary ice cover (dark shading) and location of placenames referred to in text.

Svendsen Peninsula, as well as Stor Island (Figs. 2.1 and 2.2). Emphasis is placed on the reconstruction of late Wisconsinan ice configuration, dynamics and chronology.

The reconstruction presented here is based upon surficial geological and geomorphological mapping, sedimentological investigations of glaciogenic and raised marine deposits, radiocarbon dating of marine shells and driftwood, and surface exposure dating of bedrock and erratics using cosmogenic Chlorine-36.

In this paper the term Last Glacial Maximum refers to the period of *maximum* ("full-glacial") ice cover, prior to the onset of initial deglaciation. On western Ellesmere and Axel Heiberg islands, AMS radiocarbon dates on shell fragments from till and outwash provide maximum ages for the Last Glacial Maximum and indicate that it occurred sometime after 28-27 ka BP (Bednarski 1998; This paper), and possibly as late as <20 ka BP based on an AMS date on sub-till organic detritus (Blake 1992b). Deglaciation was underway by 10-11 ka BP (Hodgson *et al.* 1991; Bednarski 1995, 1998). On eastern Ellesmere Island, AMS dates on shell fragments in till indicate that the Last Glacial Maximum may have occurred <19 ka BP (England 1998).

2.1.1 Previous Work

Early investigations into the glacial history of greater Eureka Sound noted the presence of crystalline erratics (dominantly granite, gneiss and quartzite) derived from a source to the east, probably under the Prince of Wales Icefield (Troelsen 1952; Fyles, *in* Jenness 1962; Tozer 1963)(Fig. 2.2), as well as evidence for high relative sea levels of 150-160 m asl (Schei 1904; Farrand and Gadja 1962). Several workers (*e.g.*, Fyles *in* Jenness 1962; Boesch 1963; Hattersley-Smith 1969) also noted elevational differences with respect to the degree of weathering and preservation of glacial landforms, and postulated that these reflected variations in the magnitude of different regional glaciations, with the last being the most restricted. These early observations broadly define contrasting reconstructions over the last three decades concerning the extent of late Wisconsinan glaciation in the Queen Elizabeth Islands which have essentially been divided between proponents of an extensive *Innuitian Ice Sheet* (*e.g.*, Blake 1970, 1972, 1977; 1992a and b; Blake *et al.* 1996; de Freitas 1990; Tushingham 1991; Hughes and Hughes 1994; Funder and Hansen 1996; Hättstrand and

Stroeven 1996; Bednarski 1998; England 1998, *in press*; Dyke *in press* a and b; Zreda *et al.* 1994, *in press*), and proponents of a more restricted ice cover, the *Franklin Ice Complex* (*e.g.*, England 1976, 1978, 1983, 1987, 1990, 1992, 1996; England and Bradley 1978; Bednarski 1986; Lemmen 1989; Evans 1990; Bell 1996).

Eureka Sound has been a key area in this debate, and it provides a good illustration of the issues around which these contrasting reconstructions have centred: (1) the large amount of postglacial emergence in the region (~150 m), and whether this represents a solely glacioisostatic response to the removal of a large regional ice load (*cf.* Blake 1970; Tushingham; 1991), or reflects a smaller ice load possibly coupled to neotectonic adjustments (*cf.* England 1992, 1997; Bell 1996); (2) the significance of a well defined “drift belt” (Hodgson 1985) of glacial landforms and sediments at the heads of many fiords on western Ellesmere and Axel Heiberg islands (Hodgson 1985; England 1990, Lemmen *et al.* 1994; Ó Cofaigh Chapter 3, this volume), with respect to whether this marks the limit of late Wisconsinan glaciation (Hodgson 1985; England 1990), or a stillstand during retreat of a more extensive ice cover (Hodgson 1985); (3) a sparsity of fresh glacial landform/sediment assemblages beyond this drift belt in many locations (*e.g.*, England 1987, 1990; Lemmen *et al.* 1994; Bell 1996; Ó Cofaigh Chapter 3, this volume), coupled with a greater degree of weathering in many outer fiords and at higher elevations (Boesch 1963; England 1987; England and Bradley 1978; England *et al.* 1981; Bell 1996). Granite erratics and shelly till beyond the drift belt demonstrate past glacial inundation of fiords and inter-island channels, but were assigned by proponents of limited ice to older (late Tertiary/early Quaternary) glaciations based on morphostratigraphy and amino acid ratios (Lemmen and England 1992; Bell 1992). However, Ó Cofaigh (1997) proposed a late Wisconsinan age on the basis of the association of granite dispersal trains with deglacial sediments of early Holocene age, and more recently England (1998, *in press*) has proposed a similar age based on inferred regional glaciological implications of extensive ice during the late Wisconsinan along eastern Ellesmere Island.

This paper is the first detailed glacial geologic study of granite dispersal trains in Bay Fiord and across southern Raanes Peninsula, and its objectives are to define their extent and age. The location of the study area, which is largely situated beyond the drift belt of the inner

fiords, tests conflicting reconstructions of ice extent in southern Eureka Sound during the late Wisconsinan, and links Quaternary reconstructions on Ellesmere and Axel Heiberg islands (*e.g.*, England 1992; Bell 1996; Bednarski 1998) with the glacial record of the central and western Arctic (*e.g.*, Balkwill *et al.* 1974; Hättestrand and Stroeven 1996; Dyke *in press a* and *b*)

2.1.2 Regional Setting

Eureka Sound is the inter-island channel separating Ellesmere and Axel Heiberg islands and extends from Norwegian Bay in the south to Nansen Sound in the north (Figs. 2.1 and 2.2). Stor Island occupies the central part of the sound, whereas Raanes Peninsula and Bay Fiord border the central and southern coasts (Fig. 2.2). Geologically the study area is dominated by north-northeast striking limestone, sandstone, siltstone and shale of Ordovician, Carboniferous, Triassic and Tertiary age, with local igneous dykes (Trettin 1991a). Precambrian granite outcrops 60 km to the east and underlies the Prince of Wales Icefield (Fig. 2.2). Uplands in the field area reach >1000 m asl and are dissected by fiords and valleys, aligned both parallel to bedrock structure (*e.g.*, Troid Fiord) and cross-cutting it (*e.g.*, Bay Fiord). Contemporary ice cover is limited to small, upland ice-caps, although the study area is bordered to the east and west by extensive icefields on Ellesmere (Prince of Wales Icefield) and Axel Heiberg islands (Figs. 2.1 and 2.2).

2.2 DATA PRESENTATION

2.2.1 Distribution of erratics

Raanes Peninsula and Bay Fiord

The most diagnostic erratic in the study area is granite, dominantly pink and red. Individual erratics, often striated, range in size from small pebbles to large angular boulders (>3 m in diameter), and exhibit varying degrees of weathering ranging from partially grussified to fresh. However, no elevational differences were noted in their weathering characteristics. Granite erratics and associated ice-moulded bedrock extend westwards across the study area from the present ice-margin of the Prince of Wales Icefield which overlies the Canadian Shield of southeastern Ellesmere Island (Figs 2.3 and 2.4). In many locations, granites form part of a

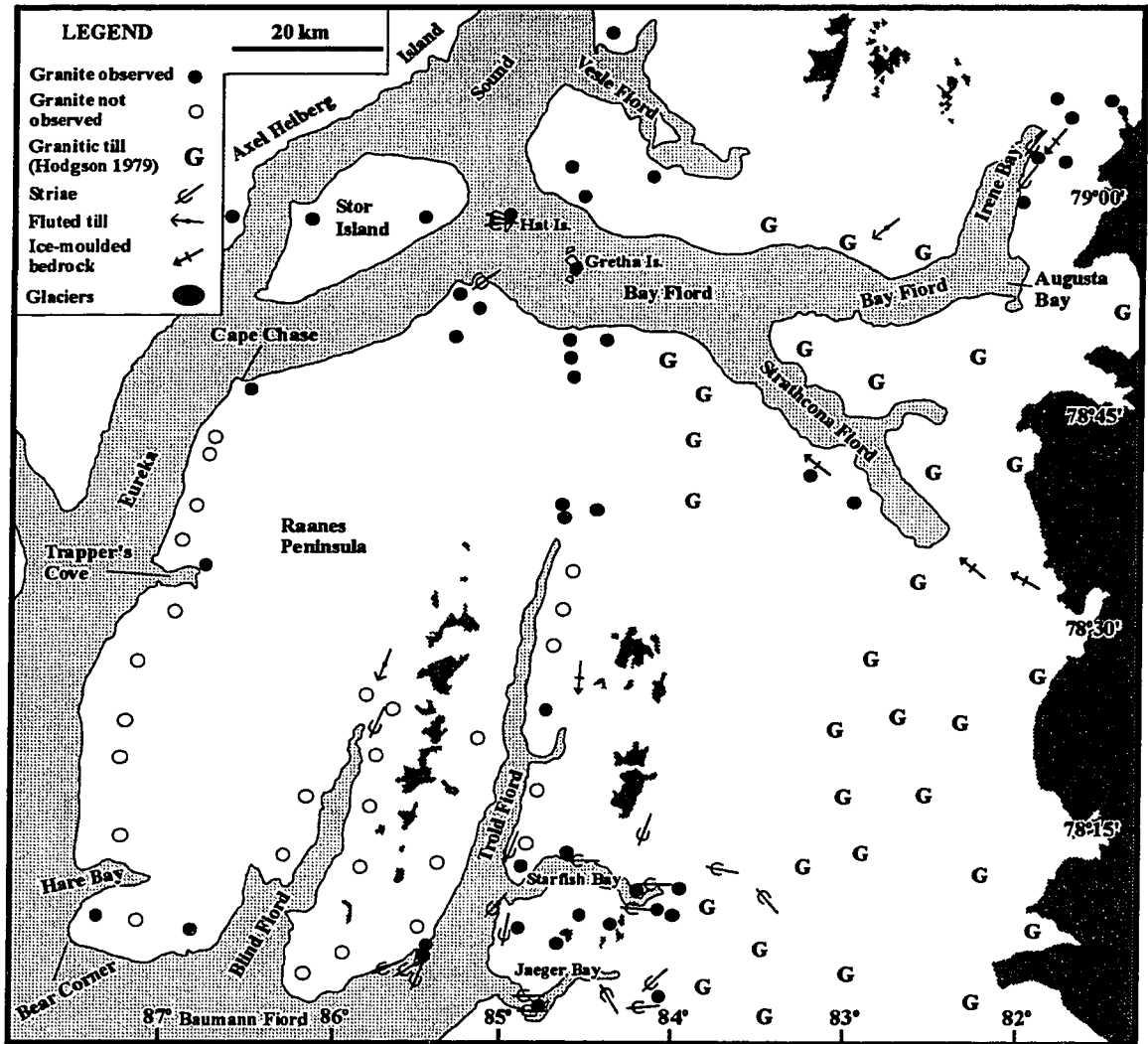


Figure 2.3: Distribution of granite erratics above marine limit and ice-flow directional indicators (striae, flutings, ice-moulded bedrock) in the study area. Each circle represents a control point where granites were either observed (closed circle) or not observed (open circle). Distribution of granitic till ("G") is from Hodgson (1979).

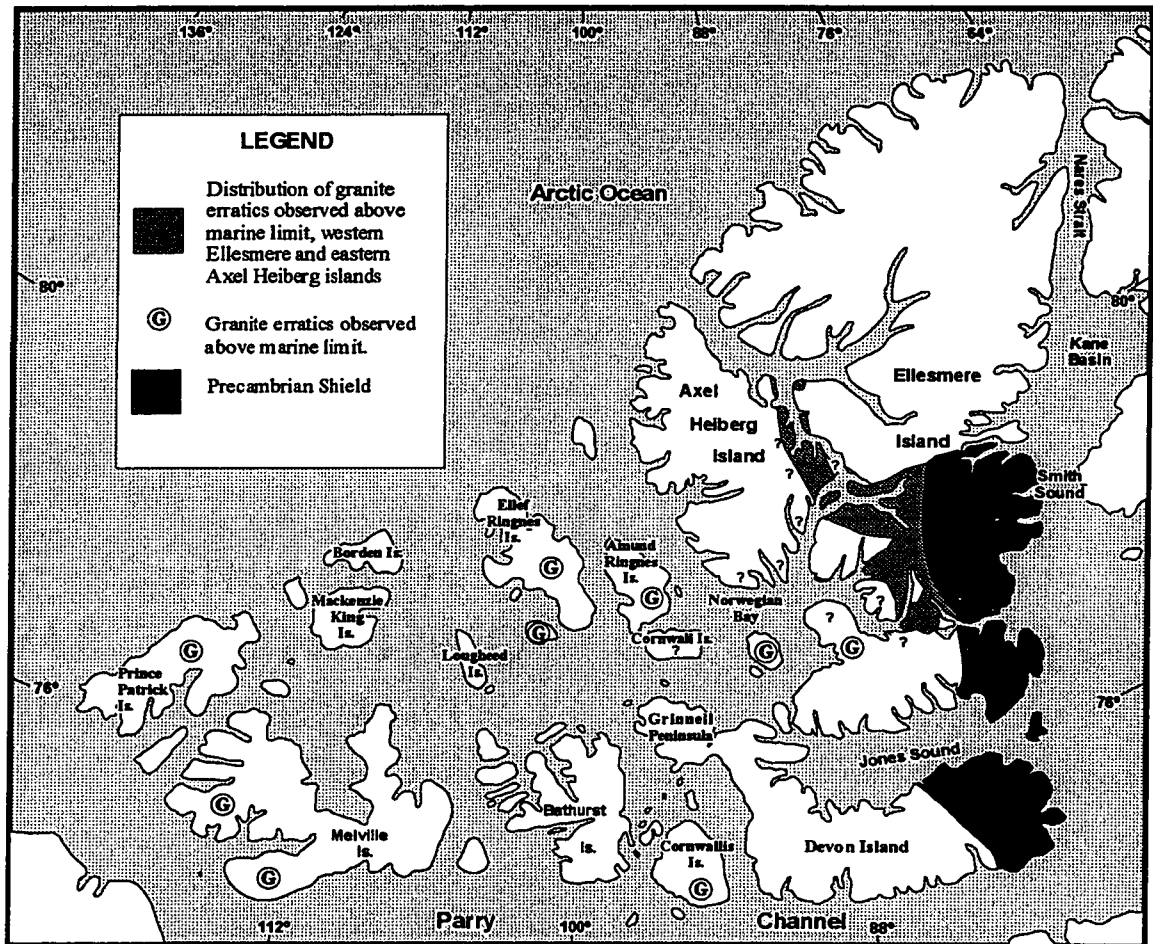


Figure 2.4: Granite dispersal trains, western Ellesmere and eastern Axel Heiberg islands (grey stipple), distribution of granite erratics above marine limit throughout western Arctic islands ("G"), and extent of Canadian Shield rocks on Ellesmere and Devon islands (black shading). Sources of erratic data: Ó Cofaigh (this volume), St. -Onge (1965); Balkwill *et al.* (1974); Hodgson (1973, 1979, 1990, 1992, *pers. comm.* 1996); Bell (1992); Bednarski (1996); Dyke (*in press*). Source of bedrock data: Trettin (1991a).

silty diamict containing shell fragments. This diamict is interpreted as till on account of its regional continuity above marine limit, presence of numerous erratics, often striated, and its stratigraphic position directly overlying ice-moulded and striated bedrock indicating westerly ice-flow, which is similar to the trajectory inferred from the granites themselves.

Tertiary fluvial deposits have been reported on western Ellesmere Island by several workers (*e.g.*, Fyles 1989; Hodgson *et al.* 1991; Bell 1992). Texturally, they are commonly sandy, but localised beds of rounded pebble to cobble gravel have been recorded at the head of Strathcona Fiord (Fyles 1989), and these contain granite (John Fyles, *personal communication* 1998). These gravels lie in the path of any ice advancing westwards through the Bay Fiord system from the Prince of Wales Icefield, and would therefore likely be glacially-eroded and re-deposited. It is important to note however, that the fluvial pebble and cobble gravels contrast texturally with a capping, regionally extensive diamict (2-3 m thick), containing numerous striated, subangular-angular granite boulders, in some cases up to 3 m in diameter, which forms the surficial unit at many localities across western Ellesmere Island (*cf.* Fyles 1989; Hodgson *et al.* 1991; Bell 1992). It is probable therefore, that granite erratics across the study area record glacial erosion and transport from the Canadian Shield under Prince of Wales Icefield, as well as a subsidiary component of pebble-cobble sized clasts from Tertiary fluvial deposits which were overridden and subsumed during westerly ice-flow.

The distribution of granites displays a distinct pattern across the study area (Fig. 2.3). A major dispersal train extends westwards from the present margin of the Prince of Wales Icefield through Irene Bay and Strathcona Fiord along the central axis of Bay Fiord to Stor Island (Figs. 2.3 and 2.4). The principal source of this dispersal train is the Canadian Shield beneath the Prince of Wales Icefield, as granite does not outcrop farther west (Trettin 1991a). Along the south side of central and outer Bay Fiord, granites occur on summits as high as 722 m asl, and extend as far west as Cape Chase in Eureka Sound (Fig. 2.3). They also occur close to the summit of Stor Island (480 m asl)(Troelsen 1952). On the north side of Bay Fiord, granites were observed on the highest summit (764 m asl) separating Bay and Vesle Fiords (Fig. 2.3), and on uplands immediately north of the mouth of Vesle Fiord. The northward extension of this dispersal train along the east coast of Axel Heiberg Island and

western Fosheim Peninsula (Fig. 2.4) was mapped by Bell (1992), who hypothesised that it emanated from Bay Fiord. This is confirmed by the present work.

Abundant granites, commonly up to 1 m in diameter, occur to at least 500 m asl in uplands immediately north of the head of Troid Fiord (Fig. 2.3). By contrast, south of the fiord head, only one granite was observed on summits bordering the east side of Troid Fiord to almost as far south as Starfish Bay. Granites were not observed on summits separating Troid and Blind fiords, however, they reappear at the mouth of Troid Fiord where they are rare. Finally, an extensive north to south helicopter traverse was undertaken along summits bordering the east side of Eureka Sound, from Cape Chase to Bear Corner (Figs. 2.2 and 2.3). Granite erratics were observed only at Cape Chase, Trapper's Cove (see below), and rarely between Hare Bay and Blind Fiord (Fig. 2.3). In inner Trapper's Cove, one granite was found on a recessional moraine 15 m above local marine limit, although granites are common in adjacent raised marine sediments.

In the southern part of the study area, granites are ubiquitous above marine limit in Starfish and Jaeger bays (Fig. 2.3), and are common on intervening summits (up to 1036 m asl). Widespread granitic till extends eastwards to the margin of the Prince of Wales Icefield (Hodgson 1979), indicating that this is the source of the erratics (Fig. 2.3). However, along the north shore of outer Baumann Fiord from Troid Fiord westwards to Eureka Sound, granites are rare and limited to the mouth of Troid Fiord and west of Blind Fiord.

Adjacent areas

South of Baumann Fiord, D. Hodgson (*personal communication* 1996) recorded granite erratics above marine limit on southern Bjorne Peninsula. Hodgson (1979) also mapped discontinuous granitic till between Makinson Inlet and Baumann Fiord, as well as extensive areas of granitic till >300 m asl along the west and east sides of Vendom Fiord. Granitic till can be traced to Vendom Fiord head and extends across Braskeruds Plain to the contemporary ice-margin (Hodgson 1973, 1979)(Fig. 2.4).

On a regional scale, granite erratics have been observed on many islands in the western Arctic Archipelago. In Norwegian Bay, Balkwill *et al.* (1974) documented granites up to 1m in diameter above marine limit on Amund Ringnes Island, and St.-Onge (1965)

similarly recorded granites on Ellef-Ringes Island (Fig. 2.4). However, to the south, granite erratics are absent above marine limit on Grinnell Peninsula, Devon Island (Dyke *in press a*) and Bathhurst Island (Bednarski 1996).

In summary two granite dispersal trains are recognised in the study area. The first is centred along the axis of Bay Fiord (Fig. 2.4), and extends northward along the east coast of Axel Heiberg Island and western Fosheim Peninsula to Nansen Sound (cf. Fyles *in* Jenness 1962; Bell 1992). The second granite dispersal train extends through Starfish and Jaeger bays, and discontinuously along the north side of outer Baumann Fiord (Fig. 2.4). No southward (lateral) termination in the extent of this dispersal train was observed in the study area, and based on the occurrence of granite erratics further to the south and southeast (Hodgson 1973, 1979, *personal communication* 1996), it is possible that it forms part of a larger dispersal train which extends generally through Baumann Fiord and across Bjorne Peninsula.

2.2.2 Glacial geomorphology

The pattern of glacial landforms in the study area is illustrated on Fig. 2.5. Key aspects are highlighted in the following section which describes Raanes and northwestern Svendsen peninsulas (Starfish and Jaeger bays), followed by Bay Fiord and Stor Island.

Raanes Peninsula and northwestern Svendsen Peninsula

Fresh, fiord-parallel striae and roches moutonnées in carbonate bedrock record westerly-flowing trunk glaciers in Starfish and Jaeger bays (Fig. 2.5). A southwesterly deflection in the orientation of striae at the mouth of Starfish Bay demonstrates coalescence with trunk ice in Troid Fiord, and south-southwest oriented striae at the mouth of the latter fiord indicate that this coalescent ice then flowed into Baumann Fiord. Throughout the field area, ice-moulded bedrock is frequently overlain by massive diamict with striated and faceted clasts, including granite, which is interpreted as till. The diamict in turn, is typically succeeded by fossiliferous raised marine sediment in the form of beaches, deltas and extensive accumulations of silt, which are particularly common at fiord heads (*e.g.*, Troid Fiord, Starfish Bay and Jaeger Bay).

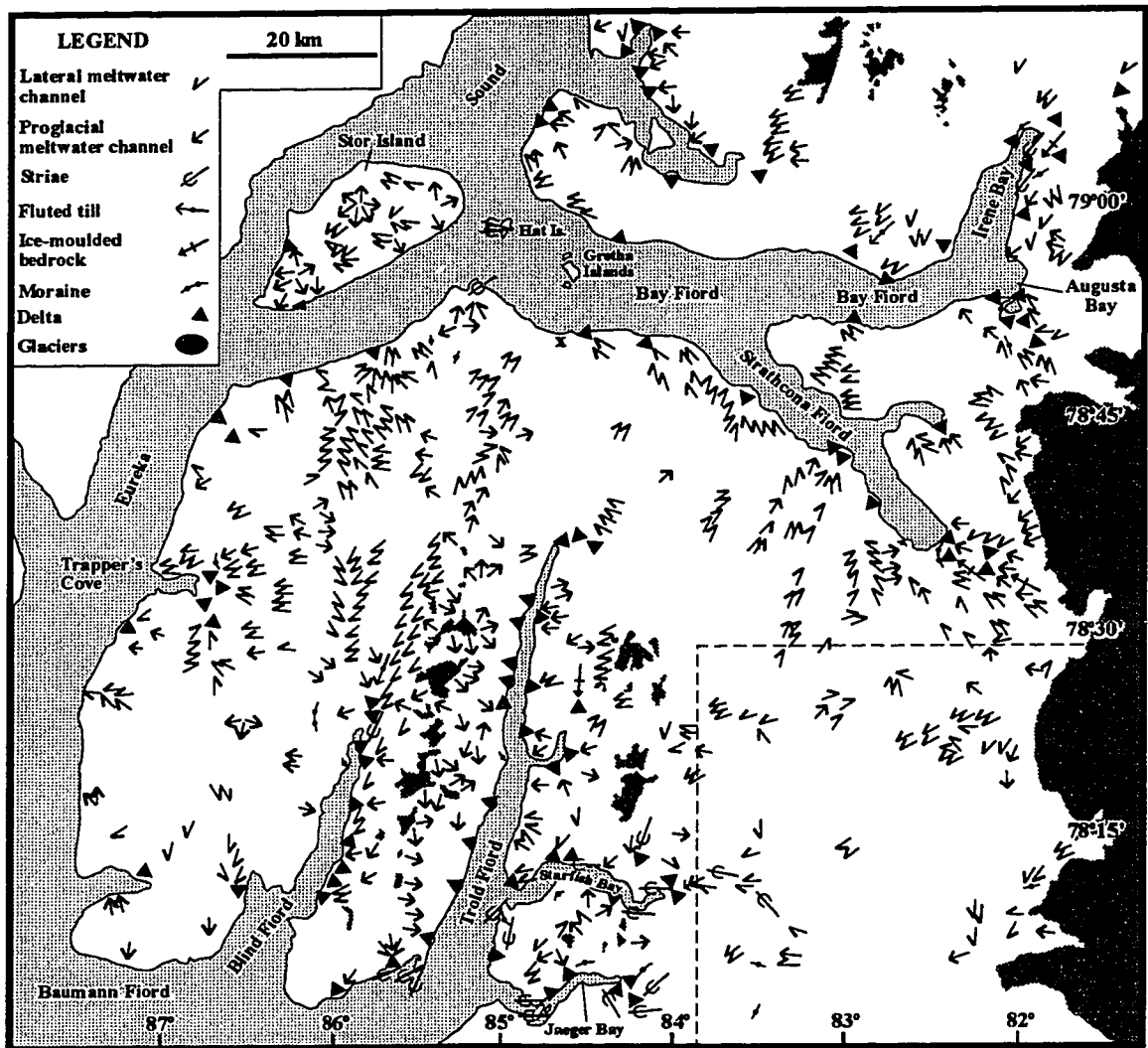


Figure 2.5: Glacial geomorphology, southern Eureka Sound. Dashed line encompasses area after Hodgson (1979).

West of Troid Fiord, lateral meltwater channels record radial, ice-marginal retreat towards the interior of Raanes Peninsula (Fig. 2.5). Channels are particularly well developed in strike-aligned fiords and valleys (*e.g.*, Blind Fiord), where they grade to raised deltas and beaches which mark local marine limit. Lateral meltwater channels incised into till and bedrock are also well developed on northern Raanes Peninsula along Eureka Sound and outer Bay Fiord, where they demonstrate onshore ice retreat, generally perpendicular to the present coastline (Fig. 2.5).

Ice-marginal landforms (moraines, lateral meltwater channels and kame deltas) marking the progressive retreat of a trunk glacier are rare throughout Troid Fiord, probably due to its cliffed topography. However, the passage of ice through the outer fiord is recorded by fresh, fiord-parallel striae and till, overlain by raised marine deposits (Fig. 2.5). Lateral meltwater channels are also not widely developed along the cliffed, west coast of Raanes Peninsula bordering Eureka Sound, particularly north and south of Trapper's Cove (Fig. 2.5). Where they do occur, however, they demonstrate easterly ice retreat, generally perpendicular to the coast. Channels, arcuate moraines and associated glaciomarine deltas are well developed in Trapper's Cove, and similarly document the easterly recession of ice from Eureka Sound into the interior of Raanes Peninsula (Fig. 2.5).

At many locations, ice-moulded bedrock and/or lateral meltwater channels do not terminate on land, but rather can be traced to the coastline or to fiord mouths where they record the extension of ice offshore (*e.g.*, Troid Fiord, Starfish Bay, Jaeger Bay, Trapper's Cove, northern Raanes Peninsula). Moraines and ice-contact deltas thus mark *recessional* positions formed during deglaciation. A particularly prominent belt of ice-contact depositional landforms is present at fiord heads and marks a major stillstand during retreat (*cf.* the "drift belt" of Hodgson 1985; Ó Cofaigh Chapter 3, this volume).

Glacial landforms are poorly developed along outer Baumann Fiord immediately west of Blind Fiord, and are limited to proglacial meltwater channels that descend to marine limit and rare dissected accumulations of deltaic sand. Locally, shelly till forms a patchy veneer on uplands. Sandstone tors, *felsenmeer* and shattered to grussified gabbro erratics of local provenance occur throughout the area, although it is noteworthy that relatively unweathered

gabbro erratics are also present. Well developed flights of raised beaches trim coastal uplands and extend to washing limits marking local marine limit (≥ 138 - ≥ 142 m asl).

Thick (granitic) till is limited to northern Raanes Peninsula along the Bay Fiord and Eureka Sound coasts. Limestone-rich till containing granite erratics is common throughout Starfish and Jaeger bays. Elsewhere, till is present as a patchy veneer, or there are occasional sparse erratics. Nowhere was more than one basal till observed in stratigraphic section, and this always forms the lowermost unit of such sequences.

Bay Fiord

Bay Fiord extends eastwards from Stor Island and comprises in its inner part, the tributaries of Strathcona Fiord and Irene and Augusta bays (Fig. 2.2). A prominent belt of ice-contact landforms and sediments at the heads of these three tributaries documents a major stillstand during deglaciation (Hodgson 1985). Ice-moulded and striated carbonate bedrock, recording westerly ice-flow, underlies these landforms and can be traced westwards to the mouth of Bay Fiord. This ice-flow is also recorded by fluted till along the north shore of inner Bay Fiord (Fig. 2.5). Ice-moulded bedrock is commonly overlain by granitic till and/or fossiliferous raised marine silt (see Section 2.2.1 above). At the fiord mouth, evidence for flow of trunk ice into Eureka Sound is present on Hat Island, where granitic till overlies striated carbonate bedrock (Fig. 2.5). Stoss-side striae orientations record westerly ice flow towards Stor Island. Similar ice-moulded and striated bedrock overlain by granitic till and raised beaches occurs at the mouth of Bay Fiord on its south side (Fig. 2.5), and documents southwesterly flow of trunk ice from Bay Fiord into Eureka Sound.

Lateral meltwater channels, graded to raised deltas and beaches in central and outer Bay Fiord, record easterly receding trunk ice, and, along the south side of the fiord, retreat towards the interior of Raanes Peninsula (Fig. 2.5). On the south central side of the fiord, occasional mounds of gravel outwash (inferred to be kames), containing numerous fragmented shells, occur at 170-200 m asl, well above local marine limit (112-120 m asl). Further east, in inner Bay and central Strathcona fiords, lateral channels graded to large ice-contact deltas and gravel berms marking local marine limit document successive stages in the eastwards retreat of trunk ice.

Finally, on the south side of outer Bay Fiord ("x" Fig. 2.5), a section (18 m high by ~60 m across) of raised marine silt contains abundant paired valves of *Astarte borealis* and occasional *Mya truncata*. The silt has been over-folded from the south-southeast and the top of the fold crudely truncated. Deformation decreases to the north (coastwards) across section, but small-scale deformation of individual silt and sand units in the form of chevron folding and normal faulting is common. This deformation is interpreted as glaciotectonic because of the lateral decrease in deformation across-section towards the coast, which is the opposite to that which might be expected from the onshore grounding of an iceberg, and the subsequent truncation.

Stor Island

The pattern of lateral and proglacial meltwater channels and associated raised marine deltas (Fig. 2.5) demonstrates ice retreat into the interior of the island. That this succeeded the breakup of ice in Eureka Sound is suggested by prominent lateral meltwater channels graded to marine limit (>145 - ≤151 m asl) along the north coast of the island. The location of these channels indicates that they formed at the margin of down-wasting trunk ice in Eureka Sound which was wrapped around the north coast of Stor Island, and retreating generally eastwards towards inner Bay Fiord.

On the west coast of Stor Island, a large delta occurs at the mouth of a valley draining the interior (Fig. 2.5). A 15 m high section at the base of the delta exposes a sequence of gravel, diamict and sand. The lowermost 8 m consists predominantly of poorly-sorted, massive gravel with occasional a(t) b(i) imbrication. This gravel is succeeded by 3 m of alternating beds of massive silty diamict and massive boulder gravel, which dip coastward and wedge out up-slope. The section is capped by 3 m of horizontally-bedded fine sand with abundant paired valves of *M. truncata*, *A. borealis*, *Hiatella arctica* and occasional *Clinocardium ciliatum*.

Lowermost gravel was deposited from traction, probably in a subaerial environment, given the presence of a(t) b(i) imbrication. Overlying wedges of diamict and boulder gravel are inferred to be sediment gravity flow deposits on account of their wedge-like geometry and bedding dips. Such alternations of massive, poorly sorted gravel to diamict could reflect an

ice-proximal depositional environment (cf. Stewart 1991; Aitken and Bell 1998), although it is noteworthy that till is absent from the sequence. In contrast, uppermost fine sands are better sorted and contain abundant macrofauna, and may record the onset of more distal sedimentation. Alternatively, the sediments could equally represent a non-glacial, transgressive sequence, with initial subaerial fluvial sedimentation, followed by sediment gravity flows from the valley sides, subsequent submergence and faunal colonisation.

2.2.3 Marine Limit

Marine limit refers to the maximum elevation attained by the sea along a glacioisostatically depressed coastline. Its elevation at a site is a function of both distance from the former edge of the ice sheet (which is a measure of the ice thickness over the site), date of deglaciation and eustatic sea level rise (Andrews 1970). In areas where former glaciers contacted the sea, marine transgression behind the former ice margin occurs concurrently with ice retreat, and hence accurate recognition and dating of marine limit allows the timing of deglaciation to be established. Throughout the study area, marine limit is marked by following features: (1) The highest raised marine delta or beach; (2) The lowest altitude of undisturbed till or felsenmeer (washing limits). Such washing limits are commonly marked by a notch cut in the till with a well sorted sediment veneer below, or by an abrupt textural transition between poorly sorted bouldery till/felsenmeer, and well sorted washed sediment below; (3) The highest elevation at which well preserved marine shells were found. The latter provides only a minimum estimate on marine limit. It was not used in areas where shelly till outcrops.

The highest marine limit observed in the study area occurs on the north coast of Stor Island at $>145 - \leq 151$ m asl (Fig. 2.6). High marine limits >140 m asl also occur along the south coast of Raanes Peninsula between Eureka Sound and Troid Fiord (Fig. 2.6). Fiords on southern Raanes Peninsula and northwestern Svendsen Peninsula (Blind Fiord, Troid Fiord, Starfish Bay, Jaeger Bay) exhibit a consistent drop in marine limit from mouth to head. For example, in Troid Fiord, marine limit falls from 143 m asl at the fiord mouth to 98 m asl at the head, whereas in Starfish Bay it falls from 113 to 80 m asl.

Along the east side of Eureka Sound, north of Hare Bay, marine limit is recorded by deltas at the mouths of valleys reaching the coast. In inner Trapper's Cove, ice-contact deltas

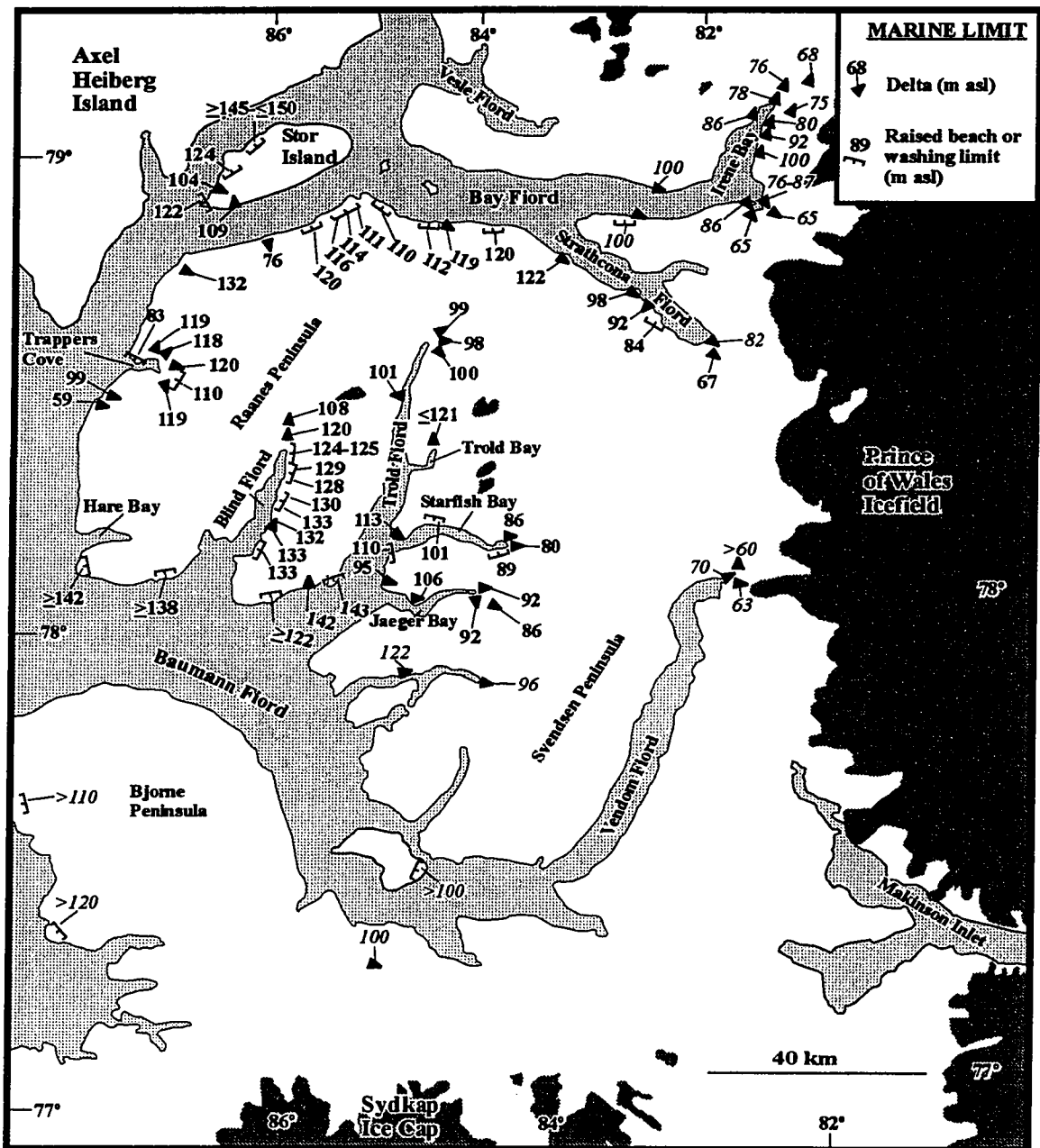


Figure 2.6: Marine limit elevations (m asl) marked by the uppermost delta, washing limit or raised beach, southern Eureka Sound. Italicised marine limit elevations are from Hodgson (1985).

grade to relative sea levels at 118-120 m asl (Fig. 2.6). This contrasts with the outer cove and Eureka Sound coast, where marine limit is marked by raised beaches at 83 m asl (minimum), and deltas immediately to the south at 99 m asl (Fig. 2.6). The north coast of Raanes Peninsula, along Eureka Sound and Bay Fiord, is characterised by a highly variable marine limit which ranges from 76 to 120 m asl in outer and central Bay Fiord respectively, before falling progressively to 65-87 m asl at the heads of Strathcona Fiord and Irene Bay (Fig. 2.6). Regionally therefore, marine limit exhibits an overall decrease in elevation eastwards from Eureka Sound to the fiords heads. However, this decrease is variable over short distances.

2.2.4 Chronology

Pre-Holocene radiocarbon dates

Twelve radiocarbon dates were obtained by Accelerator Mass Spectrometry (AMS) on individual, glacially-redeposited, shell fragments from till and coarse outwash (Fig. 2.7 and Table A.1; see Appendix A for Chapter 2 tables). To avoid a mixture of different-aged shells, only individual fragments were dated. Such dates provide a *maximum* age on the glacier advance responsible for shell transport, and hence the youngest dates are the most instructive with respect to the timing of glaciation. With the exception of one date (27.3 ka BP; AA-23605; Site 3, Fig. 2.7 and Table A.1), these ages are all >30 ka BP, and are thus probably minimum ages given the possibility of contamination by younger carbon (Bradley 1985). For example, shells with finite radiocarbon ages of >30 ka BP from Nansen Sound to the north were inferred to be Pliocene on the basis of their amino acid ratios (Bednarski 1995). Thus the validity of radiocarbon dates >30 ka BP from the study area is regarded as uncertain, although others have assumed a finite age for such dates (Blake 1992b).

Only two samples of paired valves in growth position from the study area provided pre-Holocene radiocarbon dates. Both samples consisted of single valves of *H. arctica*, collected from 15 m asl at the top of the section on the west coast of Stor Island described above (Section 2.2.2). The first sample dated 46,850±2800 BP (AA-23585; Site 8, Fig. 2.7 and Table A.1), whereas the second dated 47,790±350 (AA-27489). Hodgson (1985) reported a date of 30,100±750 BP on whole and fragmented valves collected from the surface of gravelly silt mantling weathered bedrock (108 m asl) in Baumann Fiord (GSC-2700; Site

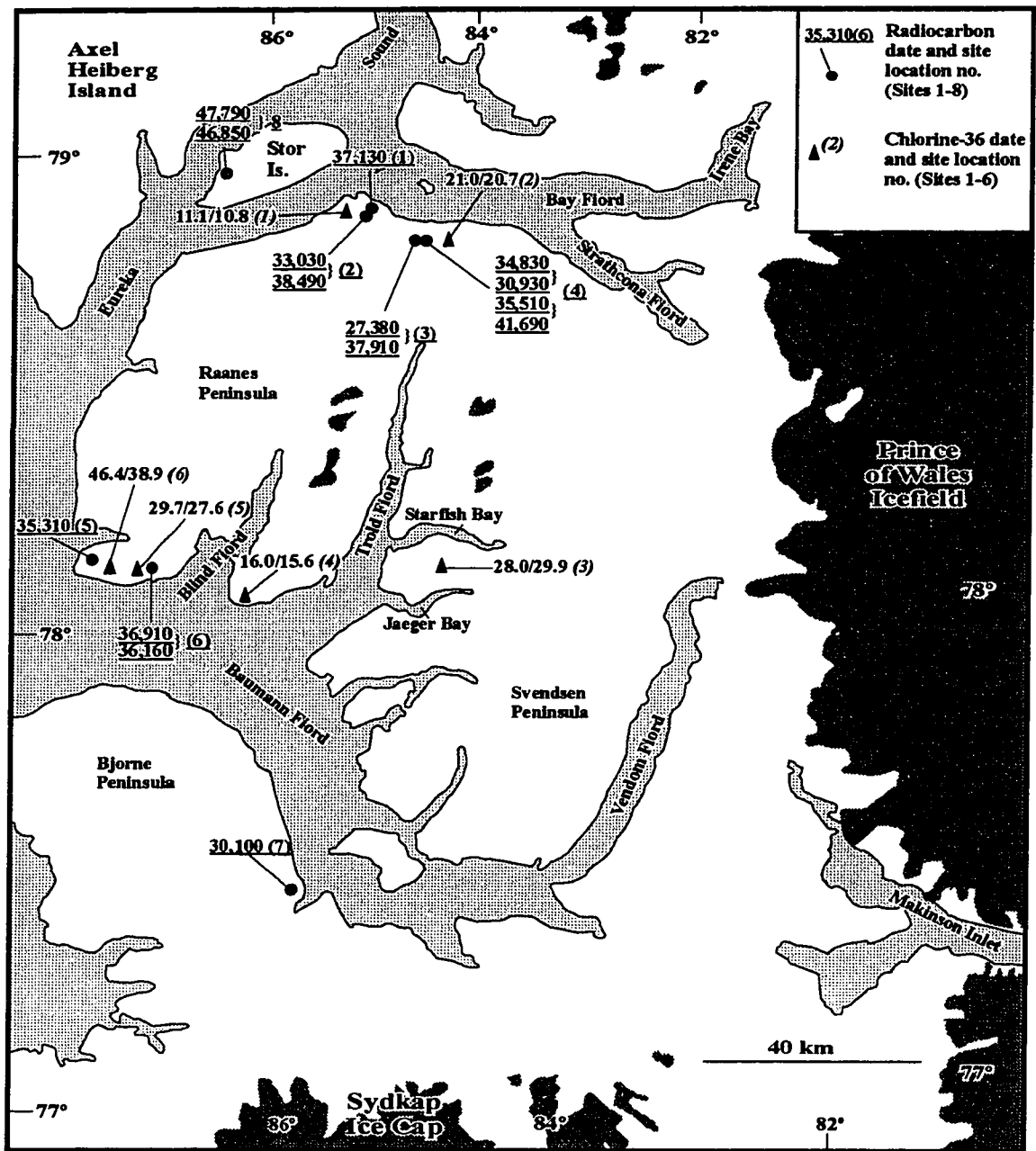


Figure 2.7: Pre-Holocene radiocarbon and Chlorine-36 dates, southern Eureka Sound.

7, Fig. 2.7 and Table A.1). He interprets this sample as having been either glacially-transported or deposited during an earlier marine episode and preserved beyond the limit of late Quaternary glaciation (Hodgson 1985, Table 1).

Holocene radiocarbon dates

Holocene radiocarbon dates obtained on raised marine shells and driftwood are listed in Table A.2 and important dates are shown on Fig. 2.8. The oldest deglacial date in the study area is from outer Trold Fiord, and was obtained on a sample of paired valves of *Portlandia arctica* from the base of a morainal bank which overlies till and striated bedrock. This yielded an AMS radiocarbon date of 9200 ± 110 BP [10150 (9940) 9690 cal BP¹](TO-5604; Site 56, Fig. 2.8 and Table A.2). Paired valves of *P. arctica* from the top of the bank gave an AMS date of 8840 ± 80 BP [9810 (9510) 9380 cal BP](TO-5592; Site 55). Down-fiord from this site, two individual fragments of *H. arctica* from beaches at the fiord mouth provided AMS ages of 8725 ± 65 BP [9600 (9430) 9250 cal BP] and 8645 ± 60 BP [9500 (9370) 9180 cal BP] respectively (AA-23583 and AA-23591; Sites 42 and 43, Fig. 2.8 and Table A.2). The beaches directly overly striated bedrock recording flow of Trold Fiord ice into Baumann Fiord. Further west, at Bear Corner, a surface collection of whole valves and fragments of *M. truncata* and *H. arctica* from a raised beach dated 8750 ± 100 BP [9760 (9440) 9200 cal BP](GSC-6028; Site 27). Localised patches of shelly granitic till (see TO-5602; Site 5, Fig. 2.7 and Table A.1) occur above marine limit throughout this area. Paired valves of *P. arctica* from ice-contact deltas in Trapper's Cove yielded AMS ages of 9030 ± 70 BP [9930 (9810) 9540 cal BP] and 8925 ± 70 BP [9850 (9630) 9460 cal BP](AA-23587 and AA-23593; Sites 23 and 24, respectively, Fig. 2.8 and Table A.2). All these dates are from recessional deglacial sediments and are thus minimum dates on initial deglaciation.

Along the north and west coasts of Raanes Peninsula dates of 8245 ± 90 BP [9140 (8910) 8540 cal BP](AA-23592; Site 25, Fig. 2.8 and Table A.2); 7745 ± 60 BP [8380 (8260) 8090 cal BP](AA-23590; Site 21) and 7180 ± 65 BP [7840 (7660) 7530 cal BP](AA-23598; Site 18) were obtained from ice-contact deposits which formed subsequent to deglaciation

¹ All ¹⁴C dates were calibrated using CALIB 3.0 (Stuiver and Reimer 1993). Calibrated dates are reported to 2 standard deviations.

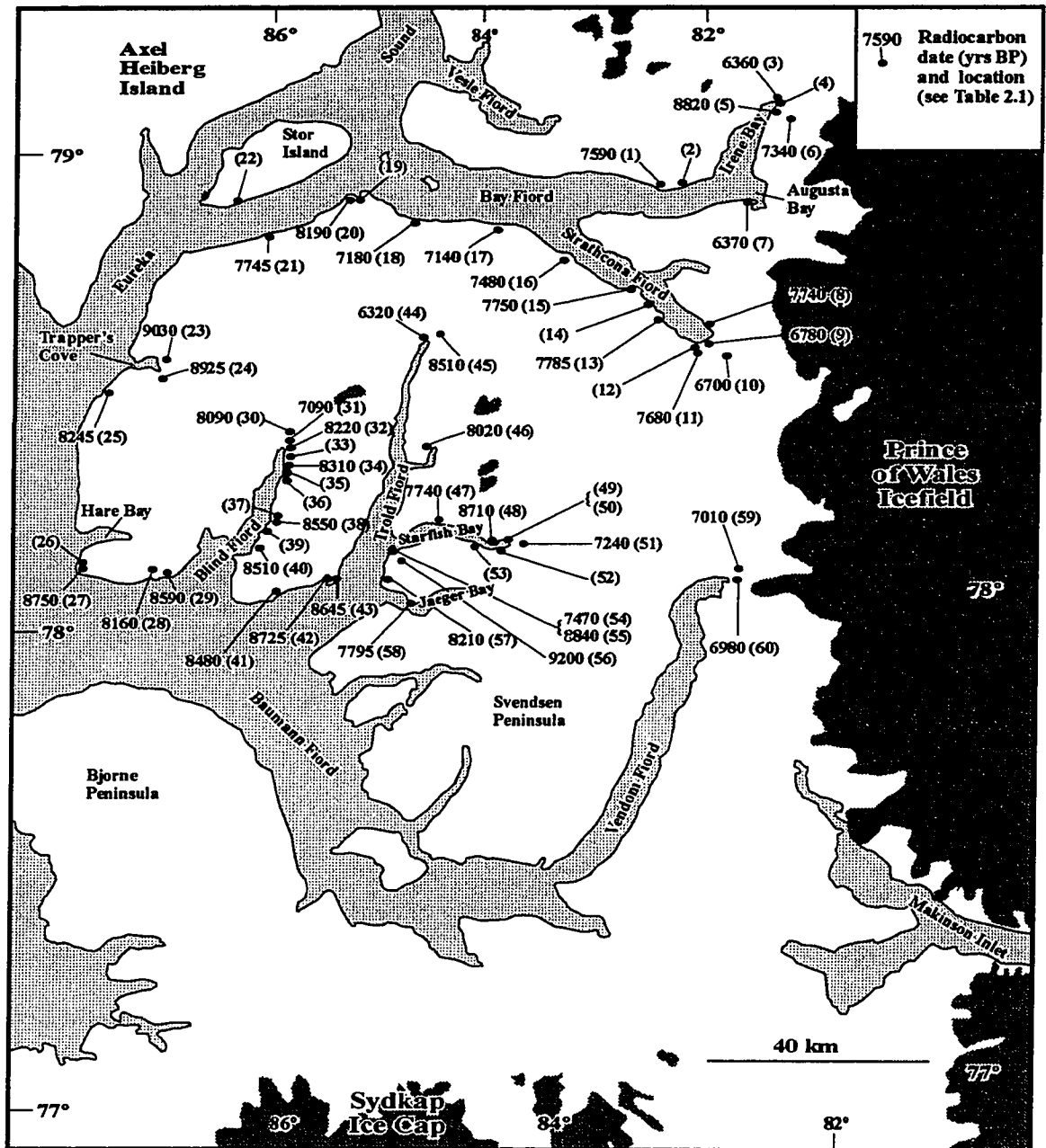


Figure 2.8: Holocene radiocarbon dates, southern Eureka Sound

of the adjacent fiords. However, several fiords in the region exhibit early Holocene dates from sites at both their heads and outer fiords; Starfish Bay 8710 ± 120 BP [9730 (9420) 9060 cal BP](GSC-2719; Site 48, Fig. 2.8 and Table A.2) in the inner fiord, and 8840 ± 80 BP [9810 (9510) 9380 cal BP](TO-5592, Site 55) at the fiord mouth; Blind Fiord 8310 ± 80 BP [9210 (8950) 8630 cal BP](TO-5608; Site 34) in the inner fiord, and 8590 ± 70 BP [9460 (9330) 9060 cal BP](TO-5862, Site 29) at the fiord mouth; Trapper's Cove 9030 ± 70 BP [9930 (9810) 9540 cal BP](AA-23587; Site 23) at the fiord head, and 8245 ± 90 [9140 (8910) 8540 cal BP](AA-23592, Site 25) south of the fiord mouth; and Bay Fiord 8820 ± 90 BP [9810 (9490) 9340 cal BP](GSC-1978; Site 5) at the fiord head (Irene Bay) and 8190 [8970 (8740) 8540 cal BP](AA-23588; Site 20) at the mouth.

Cosmogenic Chlorine-36

Reaction of cosmic rays with nuclei of K, Ca, and Cl atoms in exposed rock surfaces results in the development and accumulation of ^{36}Cl over time (Phillips 1995). Some ^{36}Cl is produced in the subsurface, but the production rate there is 2-3 orders of magnitude lower than that derived from cosmic ray activity at the surface (Lowe and Walker 1997). Therefore, once a surface is exposed, it commences a much higher rate of ^{36}Cl production. If the subsurface and cosmic ray production rates are known, the exposure time can be calculated from the amount of accumulated ^{36}Cl (see Phillips 1995). The range of the technique is from a few thousand to one million years, and it is thus potentially of great utility for distinguishing between surfaces of different age. In the Canadian High Arctic, ^{36}Cl dating has been used on eastern Ellesmere Island to date late Quaternary striated bedrock surfaces, glacial erratics and moraines (Zreda *et al.* 1994, *in press*). There, ^{36}Cl dates on Holocene surfaces correspond to radiocarbon ages on the same surfaces (Zreda *et al.* *in press*).

Samples of erratics (4) and igneous bedrock (2) were collected for ^{36}Cl dating, in order to constrain the age of the dispersal trains and glaciated terrain distal to the "drift-belt" (Hodgson 1985) (Fig. 2.7 and Table A.3). Erratic samples were obtained from the granite dispersal trains in the study area (see above), and consisted of three granite boulders and one gabbro. Two bedrock samples were collected from outer Baumann Fiord, east and west of

the mouth of Blind Fiord respectively. Sample preparation and dating was carried out by Dr. M. Zreda, University of Arizona.

Two samples were obtained from granite boulders of the Bay Fiord dispersal train. The first sample was collected at 158 m asl from the south side of the fiord mouth (Site 1, Fig. 2.7 and Table A.3). This boulder rested on a veneer of granitic shelly till directly overlying striated bedrock recording southwesterly flow of trunk ice from Bay Fiord into Eureka Sound. This dated $11,100 \pm 1100 / 10,800 \pm 1100$ BP². Raised beaches are inset around this ice-moulded bedrock and mark marine limit at 111-116 m asl. A sample of *H. arctica* from a beach at 98 m asl dated 8190 ± 60 BP [8970 (8740) 8540 cal BP](AA-23588; Site 20, Fig. 2.8 and Table A.2) and provides a minimum estimate for deglaciation and establishment of marine limit. A second erratic sample was collected at 155 m asl along the south shore of central Bay Fiord and dated $21,000 \pm 2100 / 20,700 \pm 2100$ BP (Site 2, Fig. 2.7 and Table A.3).

A third sample was collected from a granite boulder on a summit at 762 m asl between Starfish and Jaeger bays. This sample was from the granite dispersal train in the southern part of the study area, which crosses northern Svendsen and southern Raanes peninsulas. It dated $28,000 \pm 2800 / 29,900 \pm 3000$ BP (Site 3, Fig. 2.7 and Table A.3). Further west, along the north coast of outer Baumann Fiord, a sample was collected from a gabbro dyke at 381 m asl. This dated $16,000 \pm 1600 / 15,600 \pm 1600$ BP (Site 4, Fig. 2.7 and Table A.3). The surrounding area is mantled by a diamict with occasional shell fragments. The shell fragments are inferred to be glacially-redeposited on account of their fragmented nature and elevation (>260 m asl), which is considerably higher than marine limit in this area (143 m asl), and thus the enclosing diamict is interpreted as till.

Finally, two samples were collected west of the mouth of Blind Fiord (Sites 5 and 6, Fig. 2.7 and Table A.3). The first was from a gabbro dyke at 234 m asl which dated $29,700 \pm 3000 / 27,600 \pm 2800$ ka BP, whereas the second was from a gabbro erratic resting on sandstone bedrock at 324 m asl, which dated $46,400 \pm 4600 / 38,900 \pm 3900$ BP. Throughout this

² Chlorine-36 dates are reported as two figures, both in calendar years BP. The first age assumes zero erosion, while the second age assumes erosion of 5 mm/ka. The latter value is arbitrarily chosen as the upper limit of possible erosion (M. Zreda *pers. comm.* 1998). Neither age assumes any pre-exposure of the sample.

area, shelly till with rare granite erratics forms a patchy veneer locally above marine limit. AMS radiocarbon dates on shell fragments from this till yielded ages of 35-36 ka BP (sites 5, 6a and 6b; Fig. 2.7 and Table A.1) and conventional and AMS dates on shells associated with marine limit (≥ 138 - ≤ 142 m asl), inset into the till, provided ages of 8750 ± 100 BP [9760 (9440) 9200 cal BP](GSC-6028; Site 27, Fig. 2.8 and Table A.2) and 8590 ± 70 BP [9460 (9330) 9060 cal BP](TO-5862; Site 29).

2.3 DISCUSSION

2.3.1 Age of granite dispersal trains in southern Eureka Sound

Granite dispersal trains and associated fine-grained shelly till and ice-moulded bedrock record regional westerly ice-flow from the Prince of Wales Icefield to Eureka Sound via Bay Fiord, and across northern Svendsen and southern Raanes peninsulas. Marine limit is superimposed onto both dispersal trains in the form of raised deltas and beaches, and records deglaciation of the granite-carrying regional ice. Throughout southern Eureka Sound all radiocarbon dates indicate that marine limit is early Holocene. Evidence for pre-Holocene raised marine shorelines was not found. Similarly, glacial geologic evidence exists for only one glacial cycle in southern Eureka Sound. This implies that the ice responsible for deposition of the granite erratics retreated during the early Holocene, and therefore the dispersal trains are late Wisconsinan in age. There is no litho- or morphostratigraphic evidence to ascribe deposition of the dispersal trains, or parts thereof, to different glaciations (Bell 1992).

The only samples of paired bivalves which yielded pre-Holocene radiocarbon ages in the study area were obtained from a site on the west coast of Stor Island (see above). There is no direct stratigraphic relationship between these samples (15 m asl) and local marine limit (124 m asl) at this site. Available radiocarbon dates on marine limit elsewhere on Stor Island and along the Eureka Sound coast of northern Raanes Peninsula (Fig. 2.8) are all Holocene. Therefore these sediments may record a small pocket of older marine deposits which survived subsequent glacial overriding during the late Wisconsinan. A maximum age for this advance through Bay Fiord is provided by a radiocarbon date obtained on a glacially-redeposited shell fragment from glaciofluvial outwash in central Bay Fiord (AA-23605; Site 3, Fig. 2.7 and

Table A.1) which indicates that trunk ice advanced westwards into Eureka Sound <27.3 ka BP.

Age estimates on these dispersal trains are also provided by Chlorine-36 surface-exposure dates on three granite erratics, one gabbro erratic and two bedrock outcrops. Three of these samples, two granite erratics from Bay Fiord (Sites 1 and 2, Fig. 2.7 and Table A.3) and one bedrock outcrop from outer Baumann Fiord (Site 4, Fig. 2.7 and Table A.3) reinforce the above interpretation of a late Wisconsinan age. The three remaining samples yielded pre-late Wisconsinan ages of 27-29 ka BP (Sites 3 and 5, Fig. 2.7 and Table A.1), and 46/38 ka BP (Site 6, Fig. 2.7 and Table A.1). These dates could indicate deglaciation during the mid-Wisconsinan, and therefore that the sites were not subsequently ice-covered during the late Wisconsinan, although the lack of glacial geologic evidence for pre-late Wisconsinan glaciation (see above) argues against this. Alternatively they may indicate some prior exposure of the samples, in which case they would therefore represent maximum dates.

2.3.2 Last Glacial Maximum

Ice configuration and dynamics

In southern Eureka Sound, granite dispersal trains, shelly till and striated bedrock record regional, westerly flow of warm-based ice during the Last Glacial Maximum, (1) along the axis of Bay Fiord, and (2) across northern Svendsen and southern Raanes peninsulas, both emanating from a divide in the vicinity of the present Prince of Wales Icefield (Fig. 2.9). This flow overtopped summits at 1036 m asl between Starfish and Jaeger bays, and at 764 m asl between Bay and Vesle fiords. The intervening, predominantly granite-free, area of Raanes Peninsula was also ice-covered at this time (Fig 2.9), as evidenced by the pattern of deglacial landforms, in particular lateral meltwater channels, and by the timing of deglaciation which regionally is early Holocene (see sections 2.3.2 and 2.3.5 above).

The Bay Fiord dispersal train exhibits a crudely convergent flow pattern and appears to be focussed along the fiord axis. This suggests that Bay Fiord was a major conduit for ice-flow draining an expanded Prince of Wales Icefield during the Last Glacial Maximum, and was bordered to the south by locally-nourished ice in the interior of Raanes Peninsula (Fig. 2.9). Such a reconstruction is particularly likely, given that the topographic effect of this deep

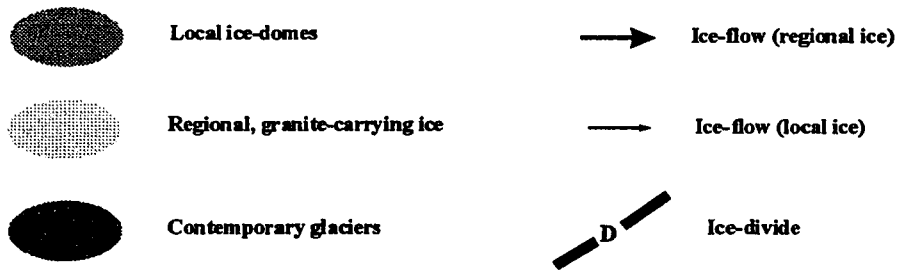
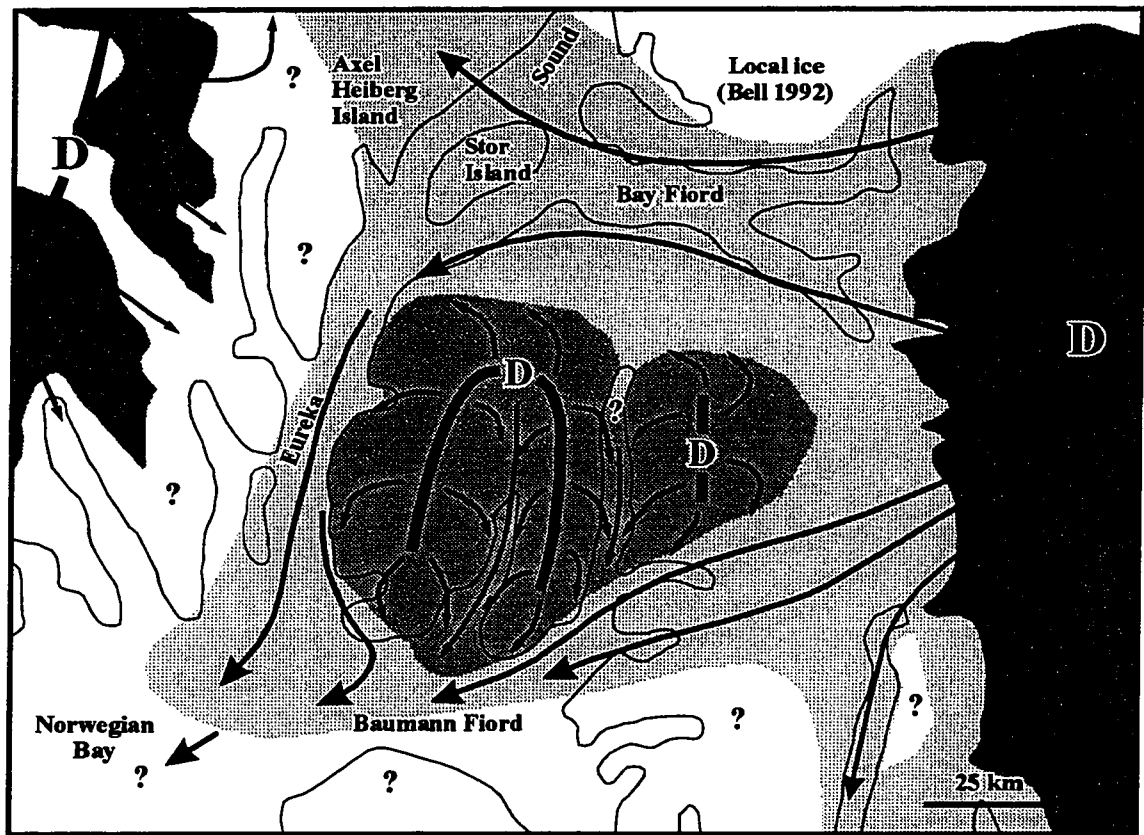


Figure 2.9: Proposed palaeogeography of the Last Glacial Maximum in southern Eureka Sound, showing location of ice-divides, extent of local and regional (granite-carrying) ice and associated principal ice-flow directions.

fiord (>300 m water depth) would have been to focus westerly-flowing ice from the Prince of Wales Icefield, and so promote development of preferential flow along its axis.

The pattern of granites and striae throughout Bay Fiord and central and southern Eureka Sound, indicates that granite-carrying ice exited Bay Fiord, overtopped Stor Island, and flowed north and south along Eureka Sound (Fig. 2.9)(cf. Fyles *in* Jenness 1965; Bell 1992). Bell (1992) mapped the northward extension of this flow (although he inferred a much older age; see below) along eastern Axel Heiberg Island and northwestern Fosheim Peninsula, and traced its limit to the entrance to Nansen Sound. South of Cape Chase, granites are absent from summits along the Raanes Peninsula coast of Eureka Sound until immediately south of Hare Bay. This suggests that granite-carrying ice was kept offshore along the central axis of the sound by the presence of Raanes Peninsula ice along the coast (Fig. 2.9). Rare granites in shelly till south of Hare Bay may record the onshore flow of Eureka Sound ice, which was able to expand across the lower elevation terrain. Alternatively, they could be part of the granite dispersal train across northern Svendsen and southern Raanes peninsulas.

Granite erratics are ubiquitous in Starfish and Jaeger bays, but they exhibit a dramatic decrease at the mouth of Troid Fiord, and are rare westwards to Eureka Sound (section 2.2.1 above). This pattern may record outflow of ice from Troid Fiord, which deflected granite-carrying ice flowing across northwestern Svendsen Peninsula off-shore into Baumann Fiord. The deflected ice would probably have coalesced with southerly-flowing trunk ice exiting Eureka Sound, and flowed southwestwards towards Norwegian Bay (Fig. 2.9).

An extensive ice cover is therefore inferred for the Last Glacial Maximum in southern and central Eureka Sound. This consisted of expanded ice-caps from Ellesmere and Axel Heiberg islands which were coalescent along the length of Eureka Sound, and likely extended continuously northwards through Nansen Sound, as Bednarski (1998) reports infilling of the latter by ice during the Last Glacial Maximum. The westerly ice-flows which deposited the granite dispersal trains emanated from an ice-divide to the east of the study area, probably roughly coincident with the contemporary divide under the Prince of Wales Icefield (Fig. 2.9). Easterly flow from this same divide occurred during the Last Glacial Maximum, and was coalescent with Greenland ice infilling Nares Strait (Blake *et al.* 1992; England 1998, *in press*; Zreda *et al.* *in press*). Westerly flow towards Eureka Sound was also likely mirrored

by a component of easterly flow from a divide over central Axel Heiberg Island. Subsequent flow of coalescent ice to the north and south along Eureka Sound then occurred.

Minimum estimates on ice thickness in Eureka Sound during the Last Glacial Maximum are provided by the elevations of granite erratics. Granites occur at 722 m asl at the mouth of Bay Fiord, and at 764 m asl between Bay and Vesle fiords, providing minimum elevations for the former ice surface in outer Bay Fiord. Water depths in the outer fiord reach 422 m immediately southeast of the Gretha Islands (Fig. 2.3)(all charted water depths are from Department of Fisheries and Oceans, 1979). This indicates a former ice thickness of *at least* 1186 m where Bay Fiord ice entered Eureka Sound. North of Stor Island, along the east coast of Axel Heiberg Island, Bell (1992) reports granites on summits at 725 m asl adjacent to Eureka Sound (local water depth up to 353 m), indicating a minimum ice thickness of 1086 m. However, Koerner *et al.* (1987) proposed that the ice divide over the Agassiz Ice Cap during the Wisconsinan was only 200 m thicker than today (currently 500-800 m, Koerner 1989). Similarly, glaciological modelling of an *Innuitian Ice Sheet*-type glacier cover in the Canadian High Arctic by Reeh (1984) results in a main ice-divide ~700-1000 m thick, located along the highlands of eastern Ellesmere Island, with local domes up to 2300 m asl over the present ice-caps. Proposed *maximum* ice thicknesses are 1500 and 2000 m (ice-margins placed along the 200 and 600 m sea-depth contours respectively), and these occur *west* of the main divide in the vicinity of Fosheim Peninsula/Eureka Sound (Reeh 1984, Fig. 4) and Norwegian Bay.

Collectively, this suggests that although the thickest ice may have been located in Eureka Sound (an interpretation supported by the pattern of postglacial emergence, see section 2.2.3 above, and Ó Cofaigh Chapter 4, this volume), the ice divides which fed this were situated on the alpine highlands to the east and west (Fig. 2.9). No evidence was found for ice-flow into southern Eureka Sound from Norwegian Bay. The reconstruction of late Wisconsinan glaciation advocated here most closely approximates the *Innuitian Ice Sheet* model of Blake (1970).

2.3.3 Deglaciation

Deglaciation of southern Eureka Sound commenced prior to 9200±110 BP [10150 (9940) 9690 cal BP](Section 2.2.4 above; Fig. 2.8 and Table A.2), and trunk ice had vacated the sound by 9030±70 BP [9930 (9810) 9540 cal BP]. Several fiords exhibit early Holocene radiocarbon dates at their heads, in addition to the outer fiords (Section 2.2.4 above; Fig. 2.8 and Table A.2). This indicates that these fiords were characterised by rapid retreat of trunk glaciers back to the fiord heads.

Along the north and west coasts of Raanes Peninsula, glacial geomorphic evidence demonstrates ice-retreat generally perpendicular to the present coastline, following break-up in the adjacent fiords. Radiocarbon dates from ice-contact deposits indicate a period of ice-marginal stabilisation in the vicinity of the present coastline until (locally) as late as 7180±65 BP [7840 (7660) 7530 cal BP], prior to retreat into the interior of Raanes Peninsula. Low marine limits at the mouths of some valleys along the coast in these areas (Fig. 2.6) also suggest the presence of locally persisting glaciers which excluded the sea.

The style of deglaciation reconstructed from the available radiocarbon and geomorphic evidence indicates a two-step retreat pattern. Initial break-up and radial retreat by calving of trunk glaciers in the larger fiords and inter-island channels commenced prior to 9.2 ka BP, and this initial phase of retreat was rapid in some fiords (cf. Ó Cofaigh Chapter 3, this volume). This was followed by terrestrial stabilisation in the narrower and shallower inner fiords, and along coastlines adjacent to the larger channels, preceding recession back to the present ice-margin or peninsula interiors. Regionally, evidence for a two-step pattern to early Holocene deglaciation has been presented for western Axel Heiberg and eastern Ellesmere islands (Lemmen *et al.* 1994; England *in press*).

The earliest radiocarbon date on the deglaciation of southern Eureka Sound is 9200±110 BP [10150 (9940) 9690 cal BP](Fig. 2.8 and Table A.2). Earlier deglacial dates of 11,660±80 BP [13,510 (13,250) 13,040 cal BP] and 10,300±100 BP [11,950 (11,460) 11,010 cal BP](Fig. 2.10 and Table A.4) have been reported to the north from outer Nansen Sound/Otto Fiord (Bednarski, 1995, 1998), whereas Hodgson *et al.* (1991) report a date of 10,600 BP [12,420 (12,110) 11,610 cal BP] from Fosheim Peninsula (Fig. 2.10 and Table A.4). This implies either (1) an asymmetry in the timing of initial deglaciation at the two ends

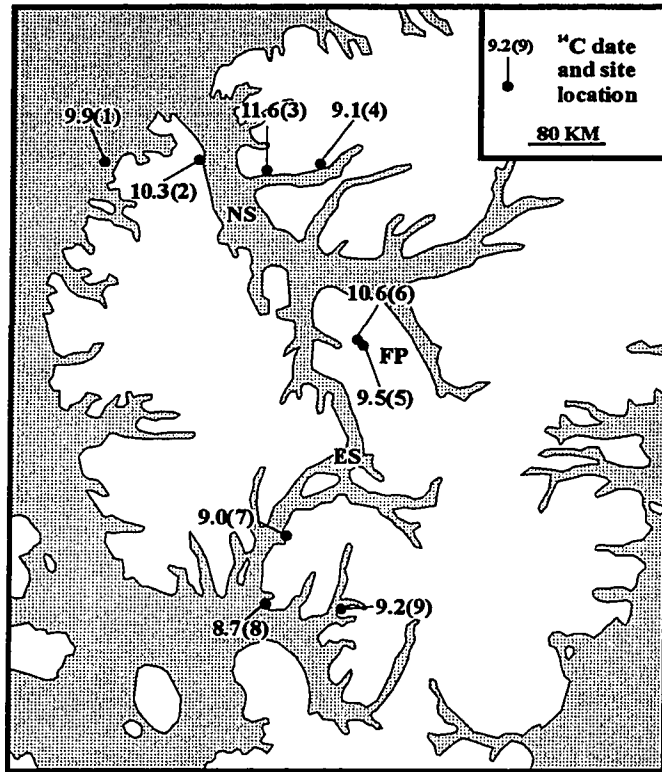


Figure 2.10: Early Holocene deglacial dates from Eureka Sound and Nansen Sound, Ellesmere and Axel Heiberg islands. "ES" = Eureka Sound, "NS" = Nansen Sound. Sources: Ó Cofaigh (this volume); Hodgson *et al.* (1991); Hein and Mudie (1991); Bell (1996); Bednarski (1995; 1998).

of Eureka Sound, or (2) that older samples were not collected or preserved in the southern part of the channel. Given that outer Nansen Sound would probably have been located close to the northern margin of any extensive ice cover over the Queen Elizabeth Islands during the Last Glacial Maximum, whereas southern Eureka Sound would have been more in the interior (cf. Blake 1970; Bednarski 1998; Dyke *in press* a and b), earlier deglaciation of Nansen Sound is likely. Therefore deglaciation of Eureka Sound commenced $\leq 10,600$ BP [12,420 (12,110) 11,610 cal BP] and the channel was ice-free by 9030 ± 70 BP [9930 (9810) 9540 cal BP]. It is possible that the driving mechanism for ice retreat through the sound was eustatic sea level rise between ~ 9.5 - 10.2 ka ^{14}C BP and 11 - 11.5 ka cal BP (Fairbanks 1989; Bard *et al.* 1990; Blanchon and Shaw 1995), coupled to an abrupt increase in temperature commencing ~ 10 - 10.2 ka ^{14}C BP (Alley *et al.* 1993; Meese *et al.* 1994; Kapsner *et al.* 1995; Lowe and Walker 1997).

2.3.4 Implications

Significance of landscape zonation in fiords

On western Ellesmere and Axel Heiberg islands many authors have noted a contrast between prominent glacial landform/sediment assemblages found in the inner parts of many fiords, and a sparsity or absence of such features from the outer fiords (Hodgson 1985; England 1987, 1990; Lemmen *et al.* 1994; Bell 1996; Ó Cofaigh Chapter 3, this volume). The significance of this landscape zonation has been the subject of much debate, with most discussion centring around whether the sparsity of deglacial landform/sediment assemblages in outer fiords implies a restricted late Wisconsinan ice cover (*e.g.*, England 1987, Bell 1996), or alternatively reflects a more extensive cold-based ice-cover, which inhibited the formation of glacial landforms and preserved pre-existing weathered terrain (*e.g.*, Sugden and Watts 1977; Hughes 1987).

A third alternative to explain this landscape zonation is that rapid deglaciation, as indicated by glacial geomorphic and radiocarbon dating evidence in several fiords in southern Eureka Sound (cf. Ó Cofaigh Chapter 3, this volume), may have occurred *regionally* across western Ellesmere and Axel Heiberg islands. Rapid radial retreat of ice by calving in the larger fiords and inter-island channels (Lemmen *et al.* 1994; Funder and Hansen 1996; Ó Cofaigh

Chapter 3, this volume; Bednarski 1998; England *in press*) would have promoted extensional flow and thinned the ice profile, facilitating extensive crevassing and meltwater drainage, which could have inhibited formation of deglacial landforms and sediments until ice-margins stabilised on-land. Extensive deglacial landform/sediment assemblages at many fiord heads in the region are inferred to record this stillstand (cf. Hodgson 1985; Ó Cofaigh Chapter 3, this volume).

Several workers have proposed that this regional, fiord head belt of glacial landforms and sediments marks a climatically-driven change in the style of early Holocene deglacial sedimentation, associated with a transient switch in the basal thermal regime of trunk glaciers from cold-based to warm (*e.g.*, Lemmen 1990; Stewart 1991). This was largely based on the interpretation of a restricted late Wisconsinan ice cover, characterised by limited expansion of cold-based glaciers. However, dispersal trains and associated ice-moulded bedrock of late Wisconsinan age in southern Eureka Sound demonstrate that some trunk glaciers were warm-based throughout much of their length, and associated early Holocene grounding-line fans and morainal banks indicate that they remained so during deglaciation. Together with glacial geomorphic evidence for spatial variation in basal thermal regime between retreating trunk glaciers (Ó Cofaigh Chapter 3, this volume), this argues against any climatically-driven regional switch to warm-based thermal conditions during the early Holocene (Ó Cofaigh *et al.* submitted).

Late Wisconsinan glaciation of northern Eureka Sound

Late Wisconsinan granite-carrying ice exiting Bay Fiord, advanced northwards along Eureka Sound towards Nansen Sound (see above). Recent work from the latter location (Bednarski 1998) reports stratigraphic and chronologic evidence of only one glacial cycle there, which is assigned to the late Wisconsinan/early Holocene. During that interval, Nansen Sound was infilled by northward-flowing ice emanating from Eureka Sound (tributary to Nansen Sound). Such a reconstruction requires extensive ice in northern Eureka Sound during the last glaciation (Bednarski 1998) and is consistent with northward-flowing, late Wisconsinan ice in southern Eureka Sound (this study).

Along northern Eureka Sound, glacial geomorphological and geological evidence (including the northward component of the granite dispersal train mapped in southern Eureka Sound during this study) demonstrates pervasive glaciation of this area at some time in the past (Bell 1992). This evidence has been assigned to two episodes of regional glaciation, dating late Tertiary/early Quaternary and early-mid Quaternary respectively (Bell 1992). This interpretation is based predominantly on amino acid ratios (alloisoleucine to isoleucine) on shell fragments from surface tills, and on the interpretation of high elevation (160-170 m asl) outwash deposits as raised marine shorelines (Holocene marine limit is ≤ 150 m asl; Bell 1996). The question to be addressed here is does this evidence categorically negate extensive late Wisconsinan glaciation in northern Eureka Sound?

Amino acid ratios obtained on glacially-transported shell fragments (commonly surface collections) from surficial till, were argued as demonstrating that two populations of mutually exclusive ratios existed along northern Eureka Sound with respect to till location (Bell 1992). These were named Group I (total ratios of 0.089-0.185) and Group II (total ratios of 0.047-0.086; although shells with total ratios as low as 0.045 are also included, Bell 1992, Table C.2). A third group (Group III) was identified which contained "mixed" populations (total ratios of 0.041-0.09). The occurrence of tills containing ice-transported shells with discrete amino acid ratios (Groups I and II) was inferred to be consistent with at least two regional glaciations (Bell 1992).

However, ratios were not obtained on shell fragments from tills in stratigraphic section, and thus the chronologic subdivision of tills into discrete glaciations lacks a *stratigraphic* basis. Furthermore, many ratios were obtained from surface samples, and the duration of exposure of these samples is unknown. Surface shells can yield higher D/L ratios than samples of the same age which have been buried >1 m for most of their history due to the different thermal histories since deposition (Miller and Brigham-Grette 1989). Thus the ratios of some of these samples may be maximum estimates, and so correlation with ratios obtained from buried samples may not necessarily be meaningful. The thermal history of all samples is further complicated by the fact they were transported and covered for an unknown length of time by warm-based ice which was at the pressure melting point and thus much warmer than the current mean annual air temperature in the area (-20°C). As a result, samples

may have been subjected to significant oscillations in temperature throughout their thermal history which could have affected their epimerisation rate and resulting ratios.

Outwash interpreted as raised marine shorelines in northern Eureka Sound lacks associated fine-grained raised marine sediments with *in-situ* macrofauna, and thus is undated. The highest categorically raised marine shorelines in this area (as deduced from their association with included *in-situ* raised marine fauna) date early Holocene. It is therefore possible that these outwash deposits are glaciofluvial kames or glaciolacustrine shorelines and do not record pre-Holocene high relative sea levels. Deglaciation of a regional ice cover along northern Eureka Sound would therefore be recorded by raised marine sediments of early Holocene age, implying that the area was inundated by late Wisconsinan glaciation.

Thus the validity of both the subdivision of glaciations based on amino acid ratios and of pre-Holocene raised marine "shorelines" is regarded as equivocal, and it is concluded that the evidence from northern Eureka Sound does not preclude extensive late Wisconsinan glaciation there. Such an interpretation is regionally consistent with reconstructions for areas immediately to the south (this study) and northwest (Bednarski 1998).

Origin of Eureka Sound and its tributaries

It has long been proposed that the fiords and inter-island channels of the Canadian Arctic represent a Tertiary dendritic drainage system which was subsequently overdeepened by glacial erosion (*e.g.*, Fortier and Morley, 1956; Hattersley-Smith 1969; Sugden 1978). In the Eureka Sound region, evidence for Tertiary fluvial drainage exists in the form of high-level (up to 600 m asl) plateau fluvial deposits (Fyles in Jeness 1962; Fyles 1989; Hodgson *et al.* 1991; Bell 1992). The interpretation of glacial erosion was inferred from bathymetric evidence for features such as overdeepened channels, hanging valleys, sills and U-shaped valleys (Horn 1963; Marlowe 1968; Hattersley-Smith 1969). However, based upon studies in the Greely Fiord/Nansen Sound fiord system, Ellesmere Island, England (1987) challenged this interpretation, arguing that the minimal evidence above sea level for a trunk glacier, together with a restricted late Wisconsinan ice-cover which was presumably cold-based and therefore non-erosive for much of its duration (based on analogy with modern glaciers in the region), refuted a glacial erosional origin for this fiord. He proposed that the fiords and inter-island

channels resulted from Tertiary block-faulting (cf. Kerr 1980), and that any pervasive glaciation in the Canadian High Arctic pre-dated this faulting. This hypothesis was discussed by Trettin (1991b) who argued that it conflicted with structural geological evidence, and concluded that there was no viable alternative to the original explanation for formation of the fiords and inter-island channels by Tertiary fluvial incision and glacial erosion.

Late Wisconsinan shelly till along Bay Fiord and the east coast of southern Eureka Sound demonstrates that these fiords must pre-date the late-Wisconsinan. Bell (1992) similarly concluded from shelly till along northern Eureka Sound that the channel existed prior to the earliest glaciation responsible for till deposition, assigned by him to the late Tertiary/early Quaternary (but see above). On northwestern Ellesmere Island, Bednarski (1995) reports stratigraphic evidence for several glaciations, consisting of multiple tills and outwash in section. Shells or shell fragments from these deposits provided discrete radiocarbon dates and amino acid ratios, supporting the stratigraphic basis for multiple glaciations. The implication of these data is that irrespective of the age of the shelly tills along Eureka and Nansen sounds, these fiords and their tributaries existed as some form of marine channels *prior* to the earliest glaciation(s) which deposited the shelly till. The presence of *in-situ* marine macrofauna of Late Pliocene age on northwestern Ellesmere Island (Fyles *et al.* 1998) indicates that the fiords and inter-island channels in this region must be at least that old.

Glacial geological evidence for inundation of a pre-existing Eureka Sound/Nansen Sound fiord system (this paper; Bell 1992; Bednarski 1995, 1998) removes a principal tenet on which the block-faulting hypothesis was based, namely the absence of geologic evidence for trunk ice in these channels. The lack of structural geological evidence for block-faulting (Trettin 1991) also argues against this explanation. Regionally, the presence of overdeepened elongate depressions along the floors of many channels, their frequently undulating longitudinal profiles and steep-sides (Horn 1963; Marlowe 1968; Hattersley-Smith 1969; Praeg 1989), in conjunction with ice-moulded and striated bedrock throughout many fiords (*e.g.*, Blake 1977, 1993; Bednarski 1998; Ó Cofaigh 1997, Chapters 2 and 3, this volume), demonstrates erosional modification of the channels and fiords during glacial inundation. The process or processes responsible for their *initial* formation cannot be resolved at present, and their morphology prior to glaciation is also unknown. However, the lack of structural

geological evidence for block-faulting (Trettin 1991b) suggests a non-structural origin for the inter-island channels and fiords on western Ellesmere Island. The original hypothesis of fluvial incision and subsequent glacial erosion (the latter categorically occurred) therefore remains viable.

Late Wisconsinan glaciation of the western Arctic Archipelago

During the Last Glacial Maximum, regional granite-carrying ice flowing across northern Svendsen and southern Raanes peninsulas, probably coalesced with southerly-flowing trunk ice exiting Eureka Sound (see above, Section 2.3.2)(Fig. 2.9). Such coalescent ice would have flowed southwestwards towards Norwegian Bay. Several workers (*e.g.*, St.-Onge 1965; Balkwill *et al.*, 1974) have documented granite erratics on Amund Ringnes and Ellef Ringnes islands in the western Arctic. These erratics have been ascribed to either an early Quaternary northward advance of Laurentide ice from the mainland (Hodgson 1989), or to an ice advance from the eastern and southeastern parts of the Arctic Archipelago (Craig and Fyles 1960; St.-Onge 1965). If the granite erratics on the Ringnes Islands were deposited by Laurentide ice advancing northwards across the archipelago, this ice would presumably have crossed Bathurst Island, as well as Grinnell Peninsula on northwestern Devon Island. With the exception of one shield erratic close to marine limit on Ile Vanier (off western Bathurst Island), recent fieldwork in these locations (Bednarski 1996; Dyke *in press a*) does not report shield erratics above marine limit.

This raises the possibility that during the late Wisconsinan, granite-carrying Ellesmere Island ice from southern Eureka Sound advanced into Norwegian Bay and extended westwards across the Ringnes Islands. Dyke (*in press a*) has documented ice-flow directional indicators of late Wisconsinan age on northern Grinnell Peninsula which demonstrate northerly flow. If Ellesmere Island ice had extended into Norwegian Bay, it would likely have coalesced with this northerly flowing Devon Island ice and been deflected northwestwards across the Ringnes islands. Northwesterly ice-flow directional indicators along the east coast of Amund Ringnes Island (Balkwill *et al.*, 1974) may reflect streaming of this ice through Massey Sound between Amund Ringnes and Axel Heiberg islands. The validity of this

hypothesis awaits more detailed fieldwork in Norwegian Bay, and surface-exposure dating of granite erratics and ice-moulded bedrock on the Ringnes Islands.

2.4 REFERENCES

- Aitken, A.E. and Bell, T.J. (1998). Holocene glacimarine sedimentation and macrofossil palaeoecology in the Canadian High Arctic: environmental controls. *Marine Geology*, **145**, 151-171.
- Alley, R.B., Meese, D.A., Shuman, C.A., Gow, A.J., Taylor, K.C., Grootes, P.M., White, J.W.C., Ram, M., Waddington, E.D., Mayewski, P.A. and Zielinski, G.A. (1993). Abrupt increase in Greenland snow accumulation at the end of the Younger Dryas event. *Nature*, **362**, 527-529.
- Andrews, J.T. (1970). *A geomorphic study of postglacial uplift with particular reference to Arctic Canada*. Institute of British Geographers, London, England, Special Publication No. 2, 156p.
- Balkwill, H.R., Roy, K.J., Hopkins, W.S. and Sliter, W.V. (1974). Glacial features and pingos, Amund Ringnes Island, Arctic Archipelago. *Canadian Journal of Earth Sciences*, **11**, 1319-1325.
- Bard, E., Hamelin, B. and Fairbanks, R.G. (1990). U-Th ages obtained by mass spectrometry in corals from Barbados: sea level during the past 130,000 years. *Nature*, **346**, 456-458.
- Bednarski, J. (1986). Late Quaternary glacial and sea-level events, Clements Markham Inlet, northern Ellesmere Island, Arctic Canada. *Canadian Journal of Earth Sciences*, **23**, 1343-1355.
- Bednarski, J. (1995). Glacial advances and stratigraphy in Otto Fiord and adjacent areas, Ellesmere Island, Northwest Territories. *Canadian Journal of Earth Sciences*, **32**, 52-64.
- Bednarski, J. (1996). Surficial geology and sea level history of Bathurst Island, Northwest Territories. In: *Current Research Part B, Geological Survey of Canada, Paper 96-B*, 61-66.
- Bednarski, J. (1998). Quaternary history of Axel Heiberg Island bordering Nansen Sound, Northwest Territories, emphasising the last glacial maximum. *Canadian Journal of Earth Sciences*, **35**, 520-533.

- Bell, T. (1992). *Glacial and sea level history of western Fosheim Peninsula, Ellesmere Island, Arctic Canada*. Unpublished PhD thesis, University of Alberta, Edmonton, 172pp.
- Bell, T. (1996). Late Quaternary glacial and sea level history of Fosheim Peninsula, Ellesmere Island, Canadian High Arctic. *Canadian Journal of Earth Sciences*, **33**, 1075-1086.
- Blake, W.R., Jr. (1970). Studies of glacial history in arctic Canada. I. Pumice, radiocarbon dates, and differential postglacial uplift in the eastern Queen Elizabeth Islands. *Canadian Journal of Earth Sciences*, **7**, 634-664.
- Blake, W., Jr. (1972). Climatic implications of radiocarbon-dated driftwood in the Queen Elizabeth Islands, Arctic Canada. In: Vasari, Y., Hyvärinen, H. and Hicks, S. (eds.), *Climatic Changes in Arctic Areas during the Past Ten-Thousand Years*. Acta Universitatis Ouluensis, Series A. Scientifiae Rerum Naturalium, No. 3, Geologica No. 1, 77-104.
- Blake, W.R., Jr. (1977). Glacial sculpture along the east-central coast of Ellesmere Island, Arctic Archipelago. *Geological Survey of Canada Paper 77-1C*, 107-115.
- Blake, W.R., Jr. (1992a). Holocene emergence at Cape Herschel, east central Ellesmere Island, Arctic Canada: implications for ice sheet configuration. *Canadian Journal of Earth Sciences*, **29**, 1958-1980.
- Blake, W.R., Jr. (1992b). Shell-bearing till along Smith Sound, Ellesmere Island - Greenland: age and significance. *Sverigies Geologiska Undersökning*, **81**, 51-58.
- Blake, W.R., Jr. (1993). Holocene emergence along the Ellesmere Island coasts of northernmost Baffin Bay. *Norsk Geologisk Tidsskrift*, **73**, 147-160.
- Blake, W.R., Jr., Boucherle, M.M., Fredskild, B., Janssens, J.A. and Smol, J.P. (1992). The geomorphological setting, glacial history and Holocene development of "Kap Inglefield Sø" North-West Greenland. *Meddelelser om Grønland, Geoscience*, **27**, 41p.
- Blake, W.R. Jr., Jackson, H.R. and Currie, C.G. (1996). Seafloor evidence for glaciation, northernmost Baffin Bay. *Bulletin of the Geological Society of Denmark*, **43**, 157-168.

- Blanchon, P. and Shaw, J. (1995). Reef-drowning events during the last deglaciation: evidence for catastrophic sea-level rise and ice-sheet collapse. *Geology*, **23**, 4-8.
- Boesch, H. (1963). Notes on the geomorphological history. In: *Preliminary report 1961-1962*. McGill University, Montréal, Axel Heiberg Island Research Reports, 163-168.
- Bradley, R.S. (1985). *Quaternary Paleoclimatology: methods of paleoclimatic reconstruction*. Chapman and Hall, London, 472pp.
- Craig, B.G. and Fyles, J.G. (1960). *Pleistocene geology of Arctic Canada*. Geological Survey of Canada, Paper 60-10, 21p.
- De Freitas, T.A. (1990). Implications of glacial striae on Hans Island, between Greenland and Ellesmere Island (Nares Strait). *Journal of Glaciology*, **36**, 129-130.
- Department of Fisheries and Oceans (1979). Eureka Sound and southern approaches including Baumann Fiord. Canadian Hydrographic Service, Chart 7940, scale 1: 3,00 000.
- Dyck, W. and Fyles, J.G. (1964). Geological Survey of Canada radiocarbon dates III. *Radiocarbon*, **6**, 167-181.
- Dyck, W., Fyles, J.G. and Blake, W., Jr. (1965). Geological Survey of Canada radiocarbon dates IV. *Radiocarbon*, **7**, 24-46.
- Dyke, A. S. (*in press*, a). The last glacial maximum and deglaciation of Devon Island: Support for an Innuitian Ice Sheet. *Quaternary Science Reviews*.
- Dyke, A. S. (*in press*, b). Holocene delevelling of Devon Island, Arctic Canada: Implications for ice sheet geometry and crustal response. *Canadian Journal of Earth Science*.
- England, J. (1976). Late Quaternary glaciation of the eastern Queen Elizabeth Islands, Northwest Territories, Canada: alternative models. *Quaternary Research*, **6**, 185-202.
- England, J. (1978). The glacial geology of northeastern Ellesmere Island, NWT, Canada. *Canadian Journal of Earth Sciences*, **15**, 603-617.
- England, J. (1983). Isostatic adjustments in a full glacial sea. *Canadian Journal of Earth Sciences*, **20**, 895-917.
- England, J. (1987). Glaciation and the evolution of the Canadian high arctic landscape. *Geology*, **15**, 419-424.

- England, J. (1990). The late Quaternary history of Greely Fiord and its tributaries, west-central Ellesmere Island. *Canadian Journal of Earth Sciences*, **27**, 255-270.
- England, J. (1992). Postglacial emergence in the Canadian High Arctic: integrating glacioisostasy, eustasy and late deglaciation. *Canadian Journal of Earth Sciences*, **29**, 984-999.
- England, J. (1996). Glacier dynamics and paleoclimatic change during the last glaciation of eastern Ellesmere Island, Canada. *Canadian Journal of Earth Sciences*, **33**, 779-799.
- England, J. (1997). Unusual rates and patterns of Holocene emergence, Ellesmere Island, Arctic Canada. *Journal of the Geological Society*, London, **154**, 781-792.
- England, J. (1998). Support for the Innuitian Ice Sheet in the Canadian High Arctic during the Last Glacial Maximum. *Journal of Quaternary Science*, **13**, 275-280.
- England, J. (*in press*). Coalescent Greenland and Innuitian ice during the Last Glacial Maximum: revising the Quaternary of the Canadian High Arctic. *Quaternary Science Reviews*.
- England, J. and Bradley, R.S. (1978). Past glacial activity in the Canadian High Arctic. *Science*, **200**, 265-270.
- England, J., Bradley, R.S. and Stuckenrath, R. (1981). Multiple glaciations and marine transgressions, western Kennedy Channel, Northwest Territories, Canada. *Boreas*, **10**, 71-89.
- Evans, D.J.A. (1990). The last glaciation and relative sea history of northwest Ellesmere Island, Canadian High Arctic. *Journal of Quaternary Science*, **5**, 67-82.
- Fairbanks, R. G. (1989). A 17,000 year glacio-eustatic sea level record: influence of glacial melting rates on the Younger Dryas event and deep ocean circulation. *Nature*, **342**, 637-642.
- Farrand, W.F. and Gadsby, R.T. (1962). Isobases on the Wisconsin marine limit in Canada. *Geographical Bulletin*, **17**, 5-22.
- Funder, S. and Hansen, L. (1996). The Greenland ice sheet - a model for its culmination and decay during and after the last glacial maximum. *Bulletin of the Geological Society of Denmark*, **42**, 137-152.

- Fyles, J.G. (1962). In: Jenness, S.E. (ed.), *Field Work, 1961; Geological Survey of Canada Information Circular No.5*, 4-6.
- Fyles, J.G. (1965). Surficial geology, western Queen Elizabeth Islands. In: *Report of Activities, Field 1964. Geological Survey of Canada Paper 65-1*, 3-5.
- Fyles, J.G. (1989). High terrace sediments, probably of Neogene age, west-central Ellesmere Island, Northwest Territories. In: *Current Research, Part D, Geological Survey of Canada, Paper 89-1D*, 101-104.
- Fyles, J.G., McNeil, D.H., Matthews, J.V., Jr., Barendregt, R.W., Marincovich, L., Jr., Brouwers, E., Bednarski, J., Brigham-Grette, J.M., Ovenden, L.O., Baker, J. and Irving, E. (1998). *Geology of Hvitland beds (late Pliocene), White Point Lowland, Ellesmere Island, Northwest Territories*. Geological Survey of Canada Bulletin 512, 35p.
- Hattersley-Smith, G. (1969). Glacial features of Tanquary Fiord and adjoining areas of northern Ellesmere Island, NWT. *Journal of Glaciology*, **8**, 23-50.
- Hättestrand C. and Stroeven, A.P. (1996). Field evidence for wet-based ice-sheet erosion from the south-central Queen Elizabeth Islands, Northwest Territories, Canada. *Arctic and Alpine Research*, **28**, 466-474.
- Hein, F.J. and Mudie, P.J. (1991). Glacial-marine sedimentation, Canadian polar margin, north of Axel Heiberg Island. *Géographie Physique et Quaternaire*, **45**, 213-227.
- Hodgson, D.A. (1973). Landscape and late-glacial history, head of Vendom Fiord, Ellesmere Island. In: *Report of Activities, Part B, Geological Survey of Canada Paper 73-1B*, 129-136.
- Hodgson, D.A. (1979). *Surficial material, south-central Ellesmere Island, NWT*. Geological Survey of Canada Open File 635.
- Hodgson, D.A. (1982). *Surficial materials and geomorphological processes, western Sverdrup and adjacent islands, District of Franklin*. Geological Survey of Canada, Paper 81-9, 37p.
- Hodgson, D.A. (1985). The last glaciation of west-central Ellesmere island, Arctic Canada. *Canadian Journal of Earth Sciences*, **22**, 347-368.

- Hodgson, D.A. (1989). Quaternary geology of the Queen Elizabeth Islands. In: Fulton, R.J. (ed.), *Quaternary Geology of Canada and Greenland*. Geological Survey of Canada, Geology of Canada, no. 1, 441-477.
- Hodgson, D.A. (1990). Were erratics moved by glaciers or icebergs to Prince Patrick Island, western Arctic Archipelago, Northwest Territories? In: *Current Research, Part D, Geological Survey of Canada, Paper 90-1D*, 67-70.
- Hodgson, D.A., St-Onge, D.A. and Edlund, S.A. (1991). Surficial materials of Hot Weather Creek basin, Ellesmere Island, Northwest Territories. In: *Current Research, Part E, Geological Survey of Canada Paper 91-1E*, 157-163.
- Horn, D.R. (1963). *Marine geology, Peary Channel, District of Franklin*. Geological Survey of Canada, Paper 63-11, 33p.
- Hughes, T. (1987). Ice dynamics and deglaciation models when ice sheets collapsed. In: Ruddiman, W.F. and Wright, H.E. Jr., (eds.), *North America and adjacent oceans during the last deglaciation*. Boulder, Colorado, Geological Society of America, The Geology of North America, v.K-3, pp. 183-220
- Hughes, B.A. and Hughes, T.J. (1994). Transgressions: rethinking Beringian glaciation. *Palaeogeography, Palaeoclimatology, Palaeoecology*, **110**, 275-294.
- Kapsner, W.R., Alley, R.B., Shuman, C.A., Anandakrishnan, S. and Grootes, P.M. (1995). Dominant influence of atmospheric circulation on snow accumulation in Greenland over the past 18,000 years. *Nature*, **373**, 52-54.
- Kerr, J.W. (1980). *Structural framework of the Lancaster Aulucogen, Arctic Canada*. Geological Survey of Canada Bulletin, 319, 24p.
- Koerner, F. M. (1989). Queen Elizabeth Islands glaciers. In *Quaternary Geology of Canada and Greenland*. Edited by R.J. Fulton. Geological Survey of Canada, Geology of Canada, Vol.1, pp. 464-473.
- Koerner, F.M., Fisher, D.A. and Patterson, W.S.B. (1987). Wisconsinan and pre-Wisconsinan ice thickness on Ellesmere Island, Canada: inferences from ice cores. *Canadian Journal of Earth Sciences*, **24**, 296-301.
- Lemmen, D.S. (1989). The last glaciation of Marvin Peninsula, northern Ellesmere Island, High Arctic, Canada. *Canadian Journal of Earth Sciences*, **26**, 2578-2590.

- Lemmen, D.S. (1990). Glaciomarine sedimentation in Disraeli Fiord, High Arctic Canada. *Marine Geology*, **94**, 9-22.
- Lemmen, D.S. and England, J. (1992). Multiple glaciations and sea level changes, northern Ellesmere Island, high arctic Canada. *Boreas*, **21**, 137-152.
- Lemmen, D.S., Aitken, A.E. and Gilbert, R. (1994). Early Holocene deglaciation of Expedition and Strand fiords, Canadian High Arctic. *Canadian Journal of Earth Sciences*, **31**, 943-958.
- Lowdon, J.A. and Blake, W. Jr. (1968). Geological Survey of Canada radiocarbon dates VII. *Radiocarbon*, **10**, 207-245.
- Lowdon, J.A. and Blake, W. Jr. (1978). *Geological Survey of Canada radiocarbon dates XVIII*. Geological Survey of Canada, Paper 78-7, 20p.
- Lowe, J.J. and Walker, M.J.C. (1997). *Reconstructing Quaternary Environments*. Second edition, Longman, 446p.
- Marlowe, J.I. (1968). Sedimentology of the Prince Gustaf Adolf Sea area, District of Franklin. *Geological Survey of Canada, Paper 66-29*, 83p.
- Meese, D.A., Gow, A.J., Grootes, P., Mayewski, P.A., Ram, M., Stuiver, M., Taylor, K.C., Waddington, E.D. and Zielinski, G.A. (1994). The accumulation record from the GISP2 core as an indicator of climate change throughout the Holocene. *Science*, **266**, 1680-1682.
- Miller, G.H. and Brigham-Grette, J.B. (1989). Amino acid geochronology: resolution and precision in carbonate fossils. *Quaternary International*, **1**, 111-128.
- Ó Cofaigh, C. (1997). Glaciation and sea level change, Raanes Peninsula, western Ellesmere Island, Arctic Canada. *Quaternary Newsletter*, **82**, 40-41.
- Ó Cofaigh, C., Lemmen, D.S., Evans, D.J.A., and Bednarski, J. (*submitted*). Glacial landform/sediment assemblages in the Canadian High Arctic: implications for controls of basal thermal regime. *Annals of Glaciology*.
- Phillips, F.M. (1995). Cosmogenic Chlorine-36 accumulation: a method for dating Quaternary landforms. In: Rutter, N.W. and Catto, N.R. (eds.), *Dating Methods of Quaternary Deposits*, Geotext 2, Geological Association of Canada, 61-66.

- Praeg, D. (1989). Geomorphic and geologic evidence for a fluvial/glacial origin of submarine troughs in southern Norwegian Bay, Canadian Arctic Archipelago. *18th Annual Arctic Workshop, Program with Abstracts*, Department of Geography, University of Lethbridge, Alberta, (abstract).
- Reeh, N. (1984). Reconstruction of the glacial ice covers and Greenland by three-dimensional, perfectly plastic ice-sheet modelling. *Annals of Glaciology*, **5**, 115-121.
- Schei, P. (1904). Preliminary account of the geological investigations made during the second Norwegian Polar Expedition in the Fram, 1898-1902. In Sverdrup, O. (ed.) *New Land*, Volume 2. Longhams, Green and Company, London, 455-466.
- St. Onge, D. (1965). *La geomorphologie de l'Île Ellef Ringnes Territoires du Nord-Ouest, Canada*. Geographical Branch, Paper 38, 58p.
- Stewart, T.G. (1991). Glacial marine sedimentation from tidewater glaciers in the Canadian High Arctic. In: Anderson, J.B. and Ashley, G.M. (eds.), *Glacial Marine Sedimentation; Paleoclimatic Significance*. Geological Society of America Special Paper 261, pp. 95-105.
- Stuiver, M. and Reimer, P.J. (1993). Extended ^{14}C data base and revised CALIB 3.0 ^{14}C age calibration program. *Radiocarbon*, **35**, 215-230.
- Sugden, D.E. (1978) Glacial erosion by the Laurentide Ice Sheet. *Journal of Glaciology*, **20**, 367-391.
- Sugden, D.E. and Watts, S.H. (1977). Tors, felsenmeer, and glaciation in northern Cumberland Peninsula, Baffin Island. *Canadian Journal of Earth Sciences*, **14**: 2817-2823.
- Tozer, E.T. (1963). Troid Fiord. In: Fortier, Y.O., Blackadar, R.G., Glenister, B.F., Greiner, H.R., McLaren, D.J., McMillan, N.J., Norris, A.W., Roots, E.F., Souther, J.G., Thorsteinsson, R. and Tozer, E.T., *Geology of the north-central part of the Arctic Archipelago, Northwest Territories (Operation Franklin)*, Geological Survey of Canada Memoir 320, 370.
- Trettin, H. P. (1991a). *Geology of the Inuitian Orogen and Arctic Platform of Canada and Greenland*. Geological Survey of Canada, Geology of Canada, No.3, 569p.

- Trettin, H.P. (1991b). Middle and late Tertiary tectonic and physiographic developments. In Trettin, H.P. (ed.), *Geology of the Innuatian Orogen and Arctic platform of Canada and Greenland*. Geological Survey of Canada, Geology of Canada, No. 3, 493-496.
- Troelsen, J.C. (1952). Geological investigations in Ellesmere Island. *Arctic*, 5, 199-210.
- Tushingham, A. M. (1991). On the extent and thickness of the Innuitian Ice-Sheet: a postglacial-adjustment approach. *Canadian Journal of Earth Sciences*, 28, 231-239.
- Zreda, M., England, J., Phillips, F. and Elmore, D. (1994). The timing and retreat of the Greenland Ice-Sheet from Nares Strait based on chlorine-36 buildup dating. *American Geophysical Union, Fall Meeting, San Francisco, California*, 221, (abstract).
- Zreda, M., England, J., Phillips, F., Elmore, D. and Sharma, P. (*in press*). Age of glaciation of Nares Strait by the Greenland ice sheet. *Nature*.

CHAPTER THREE

Geomorphic and sedimentary signatures of early Holocene deglaciation in High Arctic fiords, Ellesmere Island: implications for thermal regime and ice dynamics during deglaciation

3.1 INTRODUCTION

Deglaciation of temperate ice-masses in glacioisostatically-depressed marine basins and fiords commonly produces sedimentologically diverse lithofacies recording changes in both relative sea level and proximity of the ice margin. In ice-proximal settings, rain-out, sediment gravity flow and till deposition can occur in close spatial and temporal proximity, producing stacked sequences of sand, gravel, mud, and diamict (Powell and Molnia 1989; Hein and Syvitski 1992; Lønne 1995; McCabe and Haynes 1996).

A major control on deglacial sedimentation by temperate tidewater glaciers is the rate of glacier retreat, which in turn is controlled by both climatic, and non-climatic (*e.g.*, water depth) factors. Eustasy and isostasy are the principal controls on water depth, but for an individual fiord, topography/bathymetry can become critical for relative water depth and thus glacier dynamics (cf. England 1992; Lemmen *et al.* 1994), and can control the amount, type and location of deglacial sediments in a fiord (Crossen 1991; Seramur *et al.* 1997). Thick sequences are produced at locations where retreat is punctuated by temporary ice-marginal stillstands. Stillstands occur preferentially where fiords are characterised by irregular side wall and bottom relief which result in a constriction of fiord width and reduction in water depth. Such constrictions serve as pinning points for the retreating ice-margin and the loci of subsequent depocentres (Crossen 1991; Hunter *et al.* 1996; Seramur *et al.* 1997). In their absence, ice retreat by calving may be rapid (Hughes 1987; Meier and Post 1987), and the deglacial sedimentary signature may be sparse or absent.

In the Canadian High Arctic, sedimentological studies of emergent glaciomarine deposits have been rare (*e.g.*, Bednarski 1988; Stewart 1991; Aitken and Bell 1998), as have attempts to integrate glacial sedimentology, geomorphology and fiord topography/bathymetry with past glacier dynamics (Lemmen *et al.* 1994). This paper presents results of an integrated study of glacial geomorphology, sedimentology, marine limit elevations and radiocarbon

dating from two High Arctic fiords (Starfish Bay and Blind Fiord) on southwestern Ellesmere Island (Figs. 3.1 and 3.2). These fiords exhibit marked contrasts in early Holocene deglacial landform/sediment associations. The purpose of this paper is to highlight the roles of fiord topography and basal thermal regime in controlling early Holocene deglacial ice dynamics and sedimentation, and to discuss implications for debates concerning the extent of the last glaciation in the Canadian High Arctic.

Starfish Bay and Blind Fiord are located on Svendsen Peninsula and Raanes Peninsula, respectively, southwestern Ellesmere Island (Figs. 3.1 and 3.2). Both fiords are cut in north northeast striking limestones, sandstones and shales of Ordovician, Carboniferous and Triassic age (Trettin 1991). Uplands reach >1000 m asl and are dissected by steep fiords and valleys, aligned both parallel to bedrock structure (Blind Fiord) and cross-cutting it (Starfish Bay). Present-day glaciers are limited to small, upland ice-caps (Fig. 3.2).

3.2 STARFISH BAY

Fresh striae recording westerly ice-flow, and roches moutonnées with plucked westerly faces and smoothed and striated easterly faces, occur on carbonate bedrock throughout the fiord (Fig. 3.3). Till with granite erratics commonly overlies this bedrock. The source of these erratics lies 60 km to the east under the Prince of Wales Icefield (Trettin 1991)(Figs. 3.1 and 3.2). The granites and ice-flow directional indicators demonstrate that trunk ice flowed westwards and exited the fiord mouth, where a southwestwards shift in the orientation of striae and roches moutonnées indicates coalescence with trunk ice in Trold Fiord (Fig. 3.3). Southwesterly oriented striae immediately west of the mouth of Trold Fiord, demonstrate that this coalescent ice then flowed into Baumann Fiord.

Deglacial landform/sediment associations, marine limit elevations and radiocarbon dates are discussed below for three sectors, A, B, C, which refer to the outer, central, and inner fiord, respectively (Fig. 3.3). All radiocarbon dates discussed are listed in Table B.1 (see Appendix B).

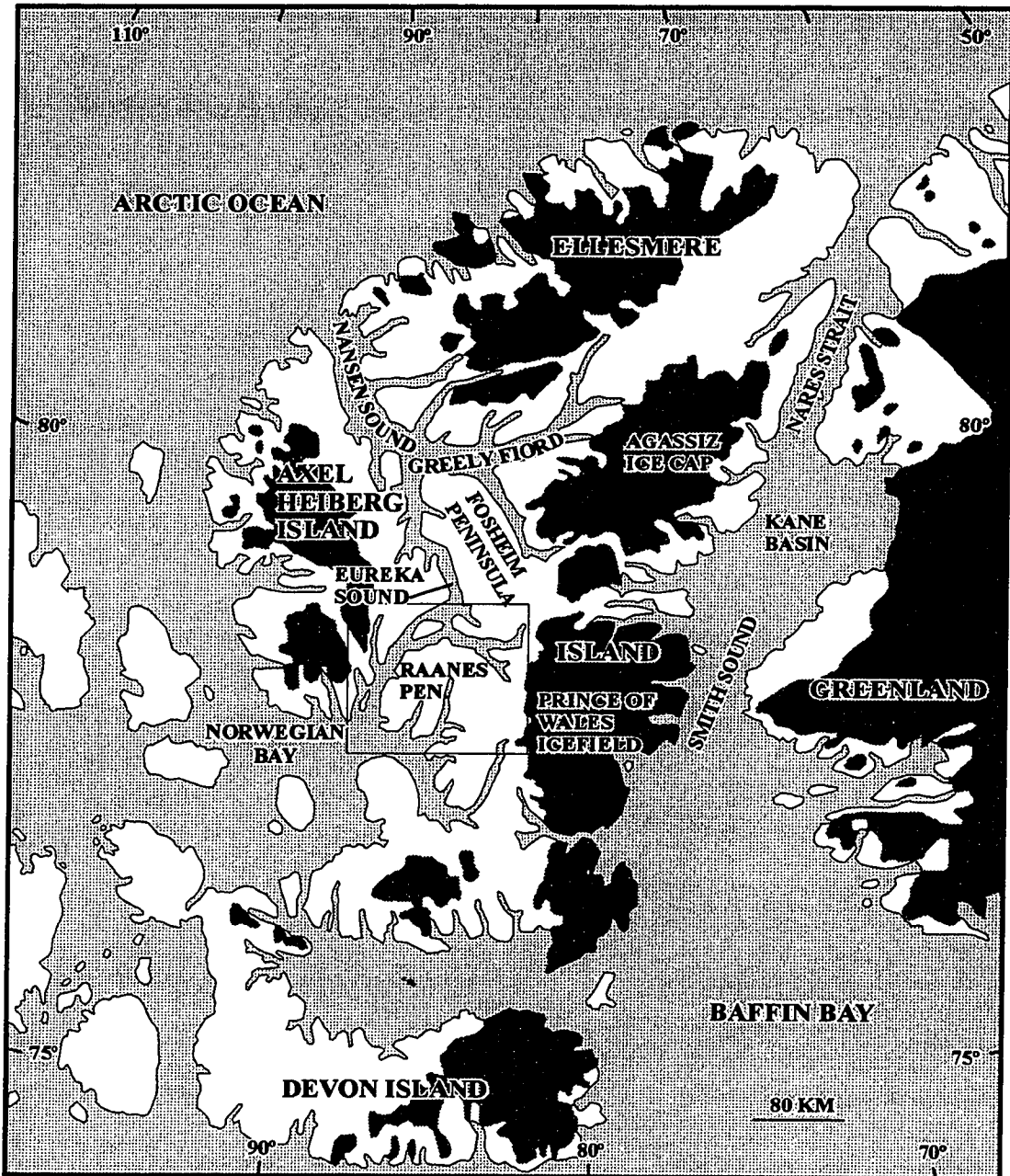


Figure 3.1: Eastern Queen Elizabeth Islands and northwest Greenland showing location of the study area (box) and contemporary ice cover (dark shading).

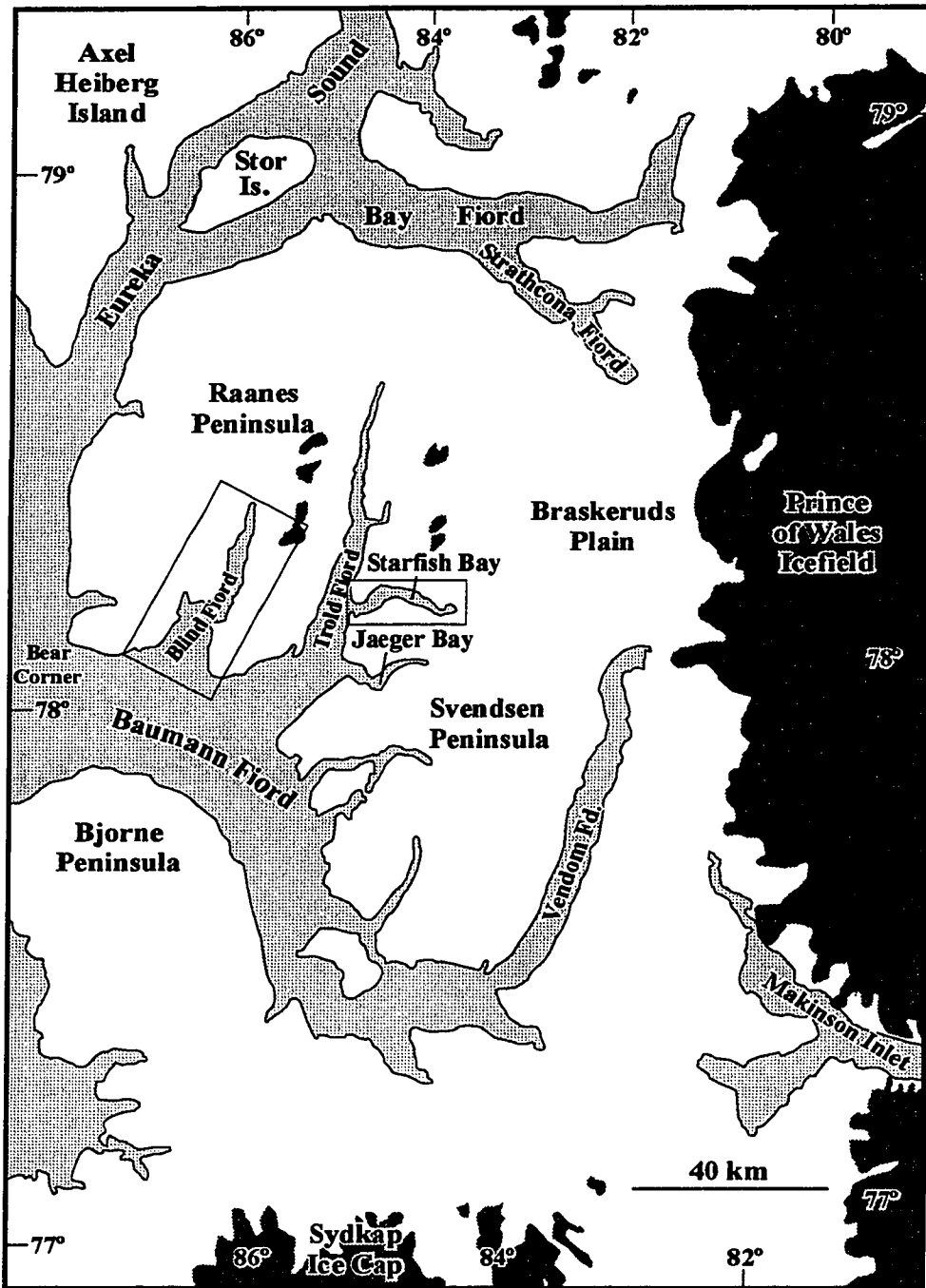
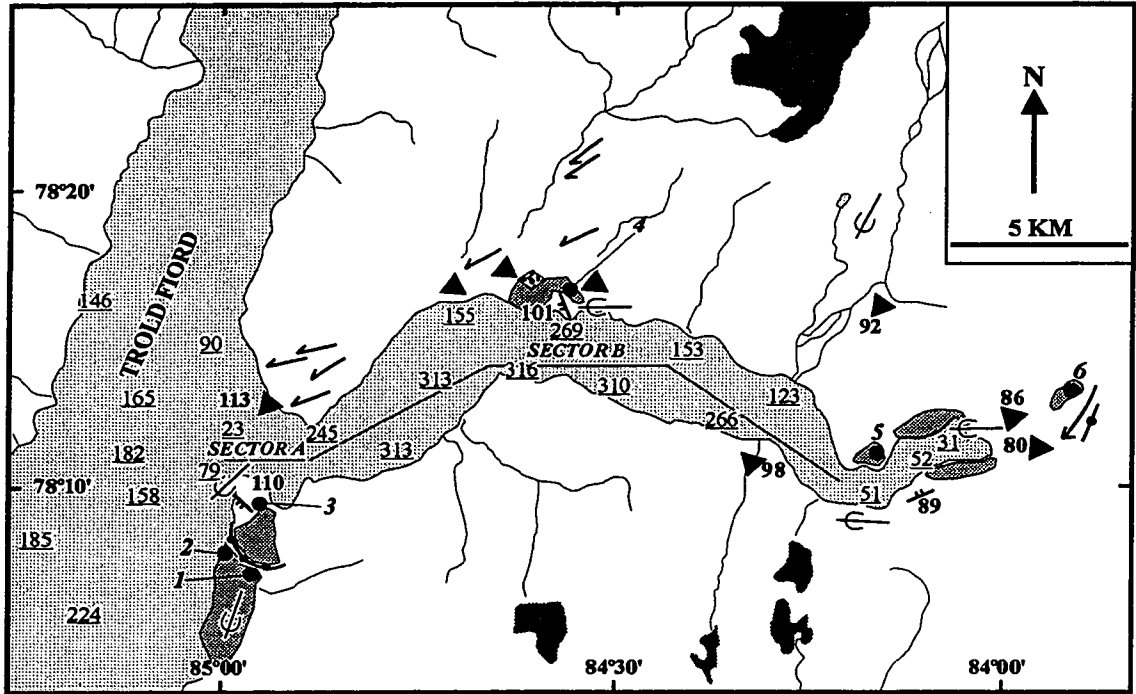


Figure 3.2: Southwestern Ellesmere Island and the study area.



- | | | | |
|-----|------------------------------|-----|--------------------------------|
| | Glaciers | | Mound of glaciomarine outwash |
| 313 | Contemporary water depth (m) | | Raised marine muds |
| | Lateral meltwater channel | 92 | Marine limit elevation (m asl) |
| | Proglacial meltwater channel | | delta |
| | Striae/ice moulded bedrock | | washing limit |
| | Moraine/morainal bank | 5 ● | ¹⁴ C dated samples |

Figure 3.3: Starfish Bay showing sector A, B, C boundaries referred to in the text, deglacial landform-sediment associations, marine limit elevations, and radiocarbon date locations as described in Table I. Charted water depths are from Department of Fisheries and Oceans (1979).

3.2.1 Sector A

Geomorphology and sedimentary sequences

A resistant carbonate bedrock ridge in outer Starfish Bay causes an abrupt deflection in fiord orientation to the southwest and a constriction in fiord width (Fig. 3.3). Immediately south of the fiord mouth this bedrock ridge is heavily ice-moulded, and a prominent arcuate ridge of fine-grained sediments, interpreted as a morainal bank (see below), is inset between it and uplands 2 km to the east (Figs. 3.3 and 3.4). Roches moutonnées and striae occur southwards along Troid Fiord from the mouth of Starfish Bay to Jaeger Bay, and record south-southwesterly ice-flow by coalescent Starfish Bay/Troid Fiord ice (Fig. 3.3). A veneer of massive diamict containing granite erratics directly overlies this striated bedrock, both above and below marine limit, and is interpreted as till. Raised marine silt blankets this till.

An east/west oriented section, 12 m high by 120 m long, was logged along the south side of the arcuate ridge (S_1 on Fig. 3.4) and two major lithofacies, comprising stacked, alternating units, were identified (Fig. 3.5). The first lithofacies (~20-30% of logged section), consists of horizontally laminated, sand/silt couplets with isolated pebble-sized dropstones (Figs. 3.5 and 3.6a) and occasional fragile, paired valves of *Portlandia arctica*. It is laterally continuous across section, and commonly has a broadly lenticular to channelled geometry. Individual sand/silt couplets vary in thickness from 0.8-3 cm. Sand laminae range from 0.2-1.5 cm thick, whereas the silt component of the couplets is thicker, 0.3-3 cm. Sand laminae are fine to very fine with sharp bases. They are normally graded, fining upwards into massive silt.

The second major lithofacies (~70-80% of logged section) consists of massive diamict with dispersed clasts in a sandy silt matrix (Fig. 3.5). Clasts are subangular to rounded and many are striated and faceted. Typically, individual diamict beds are internally massive. However, locally, diamicts contain laterally discontinuous lines of pebbles and cobbles, one clast thick (Fig. 3.6c), undeformed stringers of fine sand (0.5-1.5 cm thick by ≤ 50 cm wide in section, maximum 250 cm in width), and occasional lenticular pebbly gravel interbeds (up to 180 cm wide in section and 20-100 cm thick) with erosional to deformed boundaries (Fig. 3.6d). Gravel interbeds are clast to matrix-supported, poorly-sorted, ungraded and unstratified. Westwards, across the section, bedding within the diamict increases. Individual beds are 5-40 cm thick and frequently have a channelled geometry in section (Fig. 3.6c).

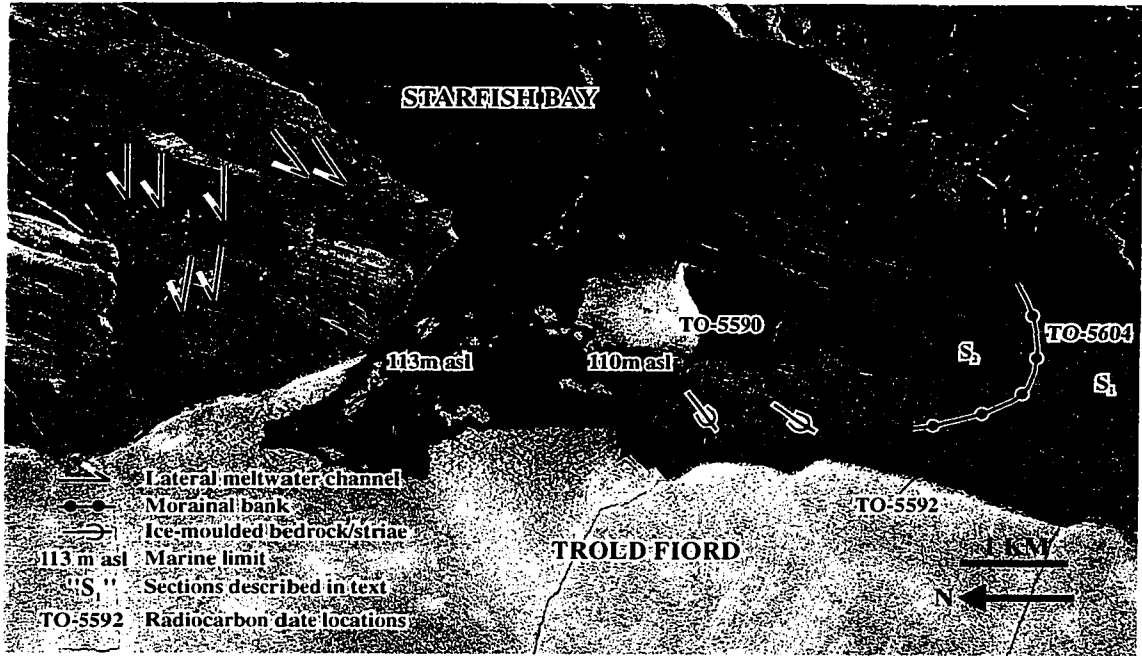


Figure 3.4: Starfish Bay, sector A, showing major glacial landforms and marine limit elevations. National Air Photo Library A16987-116, 1960

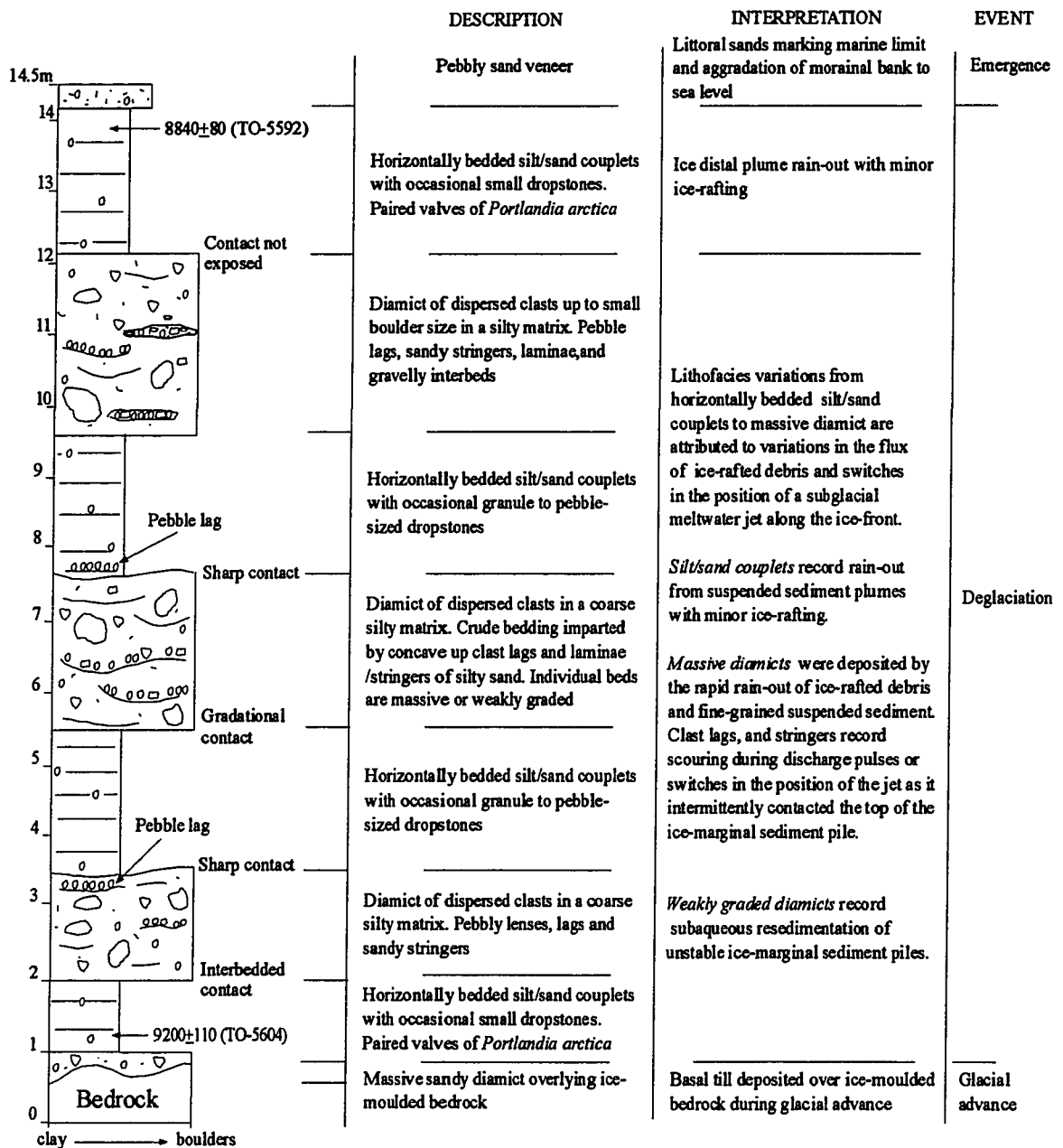


Figure 3.5: Composite log from south side of morainal bank, Starfish Bay, Sector A, section S₁.

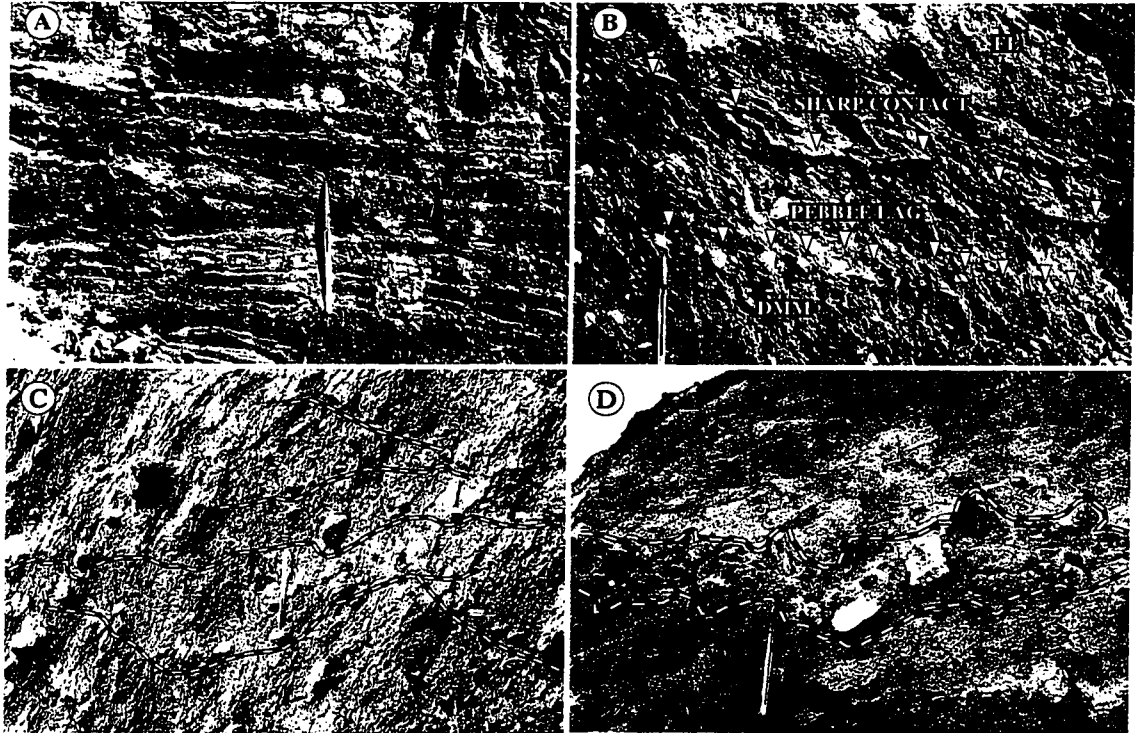


Figure 3.6: Lithofacies exposed on south side of morainal bank, Starfish Bay, sector A, section S₁, (see Figure 3.4 for section location). Pen = 15 cm in length. **A.** Horizontally bedded sand/silt couplets from lower part of morainal bank. **B.** Contact between lower massive matrix-supported diamict facies ("DMM") and overlying laminated fines ("FL"). Note pebble lag and sharp contact which defines lenticular-channelled geometry of the FL unit. **C.** Diamict of subrounded-subangular clasts in a silty matrix. Scoured surfaces (outlined) are defined by clast lags which demarcate lenticular-channelled beds of massive diamict. **D.** Gravel interbed within massive diamict facies. Note lenticular geometry, deformed erosional contact with diamict, and chaotic internal structure.

Bedding is defined by prominent pebble-cobble lags (Fig. 3.6c), and thin parting planes, in places marked by silty sand laminae (0.1-0.2 cm thick). Individual beds are predominantly massive, but occasionally exhibit weakly developed normal or inverse coarse-tail grading, sometimes with large clasts at bed tops. A bivalve of *P. arctica*, still attached at the hinge, was recovered from the diamict facies.

A 3.5 m high section consisting of two main units, occurs on the north side of the arcuate ridge (site S₂ on Fig. 3.4). The lower 2 m is composed of medium and coarse sand beds which dip gently west southwest. Coarser sand infills broad, shallow scours (70 cm wide, 8 cm deep). Internally, the sand is typically massive or exhibits diffuse normal grading. The silty clay from the upper unit has penetrated and deformed the top 50 cm of the sand. Penetrative structures are up to 45-50 cm deep by 130 cm wide, and have sharp contacts with surrounding sand. The upper unit consists of 50 cm of deformed silty clay and fine sand with occasional large cobbles. Discontinuous, pebble lines and elongate sand lenses (5-18 cm thick) within the upper unit dip north northeast at 10-30°.

Interpretation

The alternating sand/silt couplets are similar to subaqueous outwash described from both modern, temperate, tidewater glaciomarine environments (Mackiewicz *et al.* 1984; Cowan and Powell 1990), and the early Holocene glaciomarine record of the High Arctic (Lemmen 1990; Stewart 1991). The sand component of the couplets indicates an ice-proximal formation, with couplets forming by variable sediment fluxes from suspended turbid plumes (Mackiewicz *et al.* 1984). Silt infills broad channels cut into massive diamict facies. Channel cutting and subsequent infilling are inferred to result from switches in the position of a meltwater jet emanating from a subglacial conduit at the ice-margin. Channels were eroded when the jet was in direct contact with the sea floor (Powell 1990). Overlying silts record a change to a depositional regime, and this likely reflects a lateral shift in the axis of the jet, or a minor recession of the ice-margin. Alternatively, channels could have been eroded by turbidity currents moving downslope into deeper water. However, throughout the section, the sedimentology of the overlying silt is not indicative of deposition by mass flow (cf. Eyles 1987; Walker 1992), but rather points to a genesis by plume rain-out. Thus, the simplest

interpretation is that channel erosion and silt deposition were connected, and involved changes in the position of a meltwater jet as it migrated across rapidly aggrading, ice-marginal sediment.

Interbedded or gradational contacts between silt and overlying diamict demonstrate that sedimentation of both lithofacies was continuous, without a major hiatus. Features diagnostic of a basal till origin for the diamict facies (cf. Dreimanis 1989), or of glaciotectonic deformation (cf. Benn and Evans 1996), are absent, and underlying laminated silt is undeformed (Fig. 3.6a). The massive structure, interbedded or gradational contacts with subaqueous outwash, and increased percentage of pebbles and cobbles relative to underlying silt, suggest diamict formation predominantly by the rain-out of iceberg-rafted debris combined with suspension settling of fines (Powell 1984; Eyles and Lagoë 1990; Dowdeswell *et al.* 1994; Cowan *et al.* 1997).

Local concave-up clast lines within diamict facies are inferred to record localised scour, associated with impingement of a meltwater jet on the substrate (Fig. 3.6b). Scours suggest switches in the central axis of the jet across the ice-front, rather than its cessation, during diamict formation. The scours may record surges in the jet produced by discharge fluctuations or clearance of episodic tunnel blockages (Powell 1990), or, alternatively, could imply a more proximal location relative to the efflux, perhaps due to minor ice-marginal oscillations. Gravel interbeds within diamicts are interpreted as localised zones of scour and fill, which formed when waning flows from a subglacial efflux, probably in the form of a plane jet, intermittently contacted the sea floor in the zone of flow establishment (Powell 1990). This interpretation is compatible with their frequently lenticular geometry, locally erosional contacts, coarse texture and massive internal structure, which suggest rapid deposition from hyperconcentrated flows. The greater frequency of bedding within diamict facies westwards across section is inferred to represent increased meltwater pulses across the top of the sediment pile and/or a more proximal location relative to the subglacial efflux, and hence increased scouring. Sandy stringers record intermittent deposition by traction currents or plumes.

Weakly graded diamicts originated from partially turbulent, subaqueous mass flows (Postma 1986; Eyles 1987), which would be expected in an ice-proximal setting, where rapid

sedimentation from suspension would produce unstable deposits close to a subglacial efflux. It is unlikely, however, that the massive diamicts originated by subaqueous mass flow, as they lack many diagnostic features (*e.g.*, flow noses, soft-sediment clasts derived from underlying laminated silt, projecting clasts from bed tops, grading, and lower contacts that are gradational or interbedded rather than sharp to locally erosive as is common in debris flows) (*cf.* Middleton and Hampton 1976; Lowe 1982; Eyles 1987). The former explanation of massive diamict genesis predominantly by rain-out is therefore preferred.

On the north side of the arcuate ridge (site S₂ on Fig. 3.4), the massive or normally graded structure, shallow scours, and low-angle crossbedding of the lowermost sand point to a turbidite origin (Eyles 1987; Walker 1992). Penetrative deformation of the top of the sand by overlying silty clay, pebble lines, and elongate sand lenses (dipping at 10-30° in the upper unit), may reflect glacial overriding of the sequence from the northeast, during which sand and gravel were attenuated by subglacial shear, and silty clay was loaded into underlying sand by overriding ice (Benn and Evans 1996). This interpretation is compatible with the west southwest dips in the lowermost sand, which indicate an ice-margin to the east northeast.

The arcuate morphology of the ridge, its location inset between an ice-moulded bedrock high and the fiord wall, its stratigraphic context overlying ice-moulded bedrock and till, and its internal structure consisting, proximally, of glaciotectionised sediments and, distally, of ice-rafted debris and subaqueous outwash, indicate that it marks the former grounding line of the Starfish Bay glacier which was temporarily pinned at the fiord mouth during deglaciation. These morphological and sedimentological characteristics are compatible with an origin as a glaciomarine morainal bank (*cf.* Powell 1981; Powell and Molnia 1989; Eyles and McCabe 1989). Sedimentologically, this morainal bank is distinct from grounding line deposits described previously in the High Arctic (Stewart 1991), on account of the abundance of iceberg-rafted, massive diamict facies.

Marine limit and radiocarbon chronology

Marine limit is recorded by washing limits around ice-moulded bedrock immediately north of the morainal bank at 110 m asl, and kame deltas on the north side of the fiord mouth at 113

m asl (Figs. 3.4 and 3.7)³. Several radiocarbon dates constrain deglaciation and bracket formation of the morainal bank. Paired valves of *P. arctica* from laminated silt near the base of the bank (41 m asl) dated 9200±110 BP [10150 (9940) 9690 cal BP⁴](TO-5604; Site 1, Fig. 3.3 and Table B.1), whereas paired valves of the same species from the crest at 71 m asl dated 8840±80 BP [9810 (9510) 9380 cal BP](TO-5592; Site 2, Fig. 3.3 and Table B.1). Finally, a *Hiatella arctica* fragment at 102 m asl from the surface of northern end of the ice-moulded bedrock ridge, dated 7470±70 BP [8130 (7950) 7800 cal BP](TO-5590; Site 3, Figs. 3.3, 3.4 and Table B.1). These dates indicate morainal bank formation in ~400 years, commencing 9200±110 BP [10150 (9940) 9690 cal BP], and that ice had vacated the site by ≤8840±80 BP [9810 (9510) 9380 cal BP]. Deglaciation of the mouth of Trold Fiord therefore occurred prior to 9.2 ka BP.

3.2.2 Sector B

Geomorphology

This sector of Starfish Bay is ~18 km long and includes most of the fiord (Fig. 3.3) ranging in width from 3.25 to 2.25 km. Local constrictions and changes in fiord orientation are produced by protruding bedrock ridges. For much of its length, Sector B is characterised by an absence of deglacial landforms and sediments. However, thick, deglacial silt, overlying ice-moulded bedrock and till, occurs in the lee (down-ice) side of an ice-moulded bedrock knoll along the central north shore. A large, flat-topped gravel mound occurs northwest of this knoll at 91 m asl. Several deltas, ranging in elevation from 69-89 m asl, are located at the mouths of meltwater channels in the vicinity of the knoll, and record retreat of tributary glaciers (Fig. 3.3).

³ Altimeter readings accurate to ± 2 m. Corrected for changes in pressure and temperature. Marine limit elevations from deltas relate to the elevation of the delta lip; *i.e.*, the break of slope between the highest terrace surface and foreslope.

⁴ All ¹⁴C dates were calibrated using CALIB 3.0 (Stuiver and Reimer 1993). Calibrated dates are reported to 2 standard deviations.

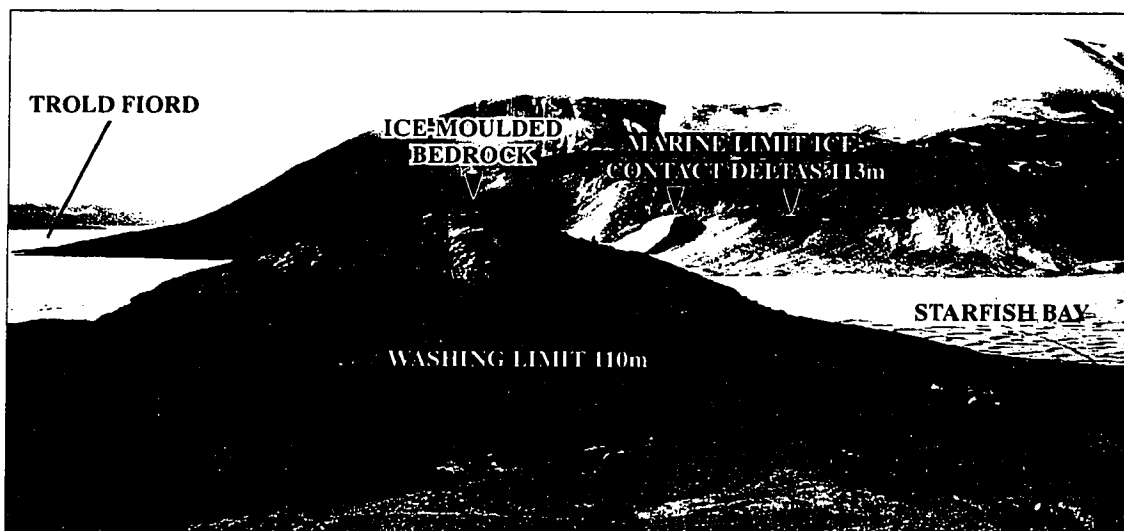


Figure 3.7: Starfish Bay, sector A, showing marine limit elevations, ice-moulded bedrock and ice-contact deltas. View looking north across the mouth of Starfish Bay.

Marine limit and radiocarbon chronology

Marine limit along the north side of central Starfish Bay is marked by a washing limit at 101 m asl which trims the west side of the ice-moulded bedrock knoll. A surface sample of *H. arctica* and *Mya truncata* valves collected from glaciomarine silt at 78 m asl on the north side of the knoll dated 7740±90 BP [8410 (8230) 8000 cal BP](GSC-6037; Site 4, Fig. 3.3 and Table B.1). This provides a minimum date for deglaciation and establishment of the 101 m asl marine limit.

Interpretation

Rapid ice retreat from the morainal bank in Sector A through the outer part of Sector B is suggested by an absence of deglacial landforms and sediments, and water depths of >300 m (cf. Lemmen *et al.* 1994). However, the large accumulation of sediment in the lee of the bedrock knoll farther up-fiord, suggests that it acted as a pinning point, which temporarily halted ice retreat. Alternatively, this sediment could have been deposited by meltwater from tributary glaciers immediately to the north. The elevation of the flat-topped gravel mound (91 m asl) is lower than local marine limit (101 m asl) immediately up-fiord (Fig. 3.3), and this suggests that the mound was deposited by later meltwater from tributary ice. The bedrock knoll was ice-free by >7.7 ka BP (probably >8.7 ka BP, see below). East of the knoll, deep water, the wide fiord, and a lack of deglacial landforms and sediments, point to rapid retreat towards the inner fiord.

3.2.3 Sector C

Geomorphology and sedimentology

This sector comprises the inner 4 km of the fiord and the area east (inland) of the fiord head. Fiord width narrows from ~1.4 km in the outer part of the sector to 0.8 km at the fiord head. Immediately east of the fiord head, the valley is constricted by ice-moulded bedrock abutted by marine limit deltas at 86 m asl, and, farther to the east, at 80 m asl (Fig. 3.3). Thick, dissected glaciomarine silt extends westward from these deltas. At the fiord head, an 11 m high section oriented northwestwards through the silt exposes two main units. The lower 6 m is composed of massive diamict with striated clasts in a coarse silty matrix. The diamict

directly overlies ice-moulded bedrock and is interpreted as a basal till. It is overlain by ~5 m of stratified silt with numerous dropstones, stringers and starved ripple trains of fine sand, channelled interbeds of normally graded pebbly gravel, and thin (≤ 5 cm) interbeds of massive pebbly sand. Laterally across section, the silt becomes more distinctly stratified, changing to couplets of fine silty sand and silt with occasional dropstones. Sand laminae (≤ 1 cm thick) are normally graded with sharp lower, and gradational upper contacts with overlying silt. The silt component is thicker ($\leq 2-3$ cm) and massive.

Marine limit and radiocarbon chronology

Marine limit on the south side of the inner fiord, ~2 km west of the fiord head, is 89 m asl, but falls progressively from 86 to 80 m asl to the east (Fig. 3.3). Hodgson (1985) reported a date of 8710 ± 120 BP [9730 (9420) 9060 cal BP](GSC-2719; Site 5, Fig. 3.3 and Table B.1) on a sample of *P. arctica* at 68 m asl, 3 km west of the fiord head. This sample was from the lower 50 cm of glaciomarine rhythmites overlying till and ice-moulded bedrock. Hodgson inferred that this date provided an approximate age for the fiord head deltas. A valve of *H. arctica* from raised marine silt at 71 m asl, immediately *up-fiord* from both these deltas, dated 7240 ± 80 BP [7910 (7730) 7570 cal BP](TO-5596; Site 6, Fig. 3.3, Table B.1), and provides a minimum age for deglaciation of the fiord head.

Interpretation

Fiord head deltas and glaciomarine silt record ice-marginal stabilisation due to decreasing water depth and the presence of constricting bedrock highs. Horizontally-stratified silt is interpreted as having formed ice-proximally, by suspension sedimentation from turbid plumes (cf. Mackiewicz *et al.* 1984; Cowan and Powell 1990), with occasional traction current activity and ice-rafting. Interbeds of normally graded gravel and massive pebbly sand are turbidites, based on their internal structure and erosional contacts (Walker 1992). The sequence of silt overlain by a marine limit delta (86 m asl), indicates ice-marginal subaqueous sedimentation, with aggradation of the sediment pile to former sea level and development of an ice-contact delta (cf. Powell 1990).

Radiocarbon dates indicate rapid retreat of trunk ice from the fiord mouth (8840±80 BP)[9810 (9510) 9380 cal BP](TO-5592) to the inner fiord (8710±120 BP)[9730 (9420) 9060 cal BP](GSC-2719), a distance of ~18 km in 90 years based on the calibrated dates (0.2 km/year; cf. Meier and Post 1987, Table 2). However, the standard errors of these dates overlap and thus deglaciation of Starfish Bay may have been catastrophic. Fiord head deglaciation and delta formation were complete by at least 7240±80 BP [7910 (7730) 7570 cal BP](TO-5596). Starfish Bay, therefore, was characterised by a two-step pattern of deglaciation, whereby initial rapid retreat through the outer and mid-fiord was succeeded by stabilisation in the inner fiord between ≤ 8.7 ka BP (9.4 ka cal BP) and >7.2 ka BP (7.7 ka cal BP).

3.3 BLIND FIORD

Fresh, fiord-parallel striae and grooves in carbonate bedrock along the east side of the inner fiord, indicate that trunk ice moved generally southwards in Blind Fiord. Presentation of the glacial geomorphology, marine limit elevations and radiocarbon dates is divided into three sectors, A, B, and C, which correspond to the outer, central and inner fiord, respectively (Fig. 3.8). Radiocarbon dates are listed in Table B.1.

3.3.1 Sector A

Geomorphology

This sector ranges in width from ~12 km at the fiord mouth to 3 km farther up-fiord. Deglacial landforms and sediments recording the retreat of trunk ice were not observed. Dykes and local gabbro erratics on shale/siltstone uplands west of the fiord mouth are commonly shattered or grussified, and dykes occasionally form small tors. It is noteworthy, however, that relatively unweathered gabbro erratics also occur throughout the area on upland surfaces above marine limit. Shelly diamict, containing rare striated erratics, including granite, forms a patchy veneer above marine limit and is interpreted as till (Fig. 3.8). Immediately west of the fiord mouth, dissected mounds of parallel-laminated, silty sand containing occasional dropstones, paired valves of *Macoma calcarea*, *Astarte borealis*, *H. Arctica* and *Clinocardium ciliatum* and redeposited organics capped by regressive beach

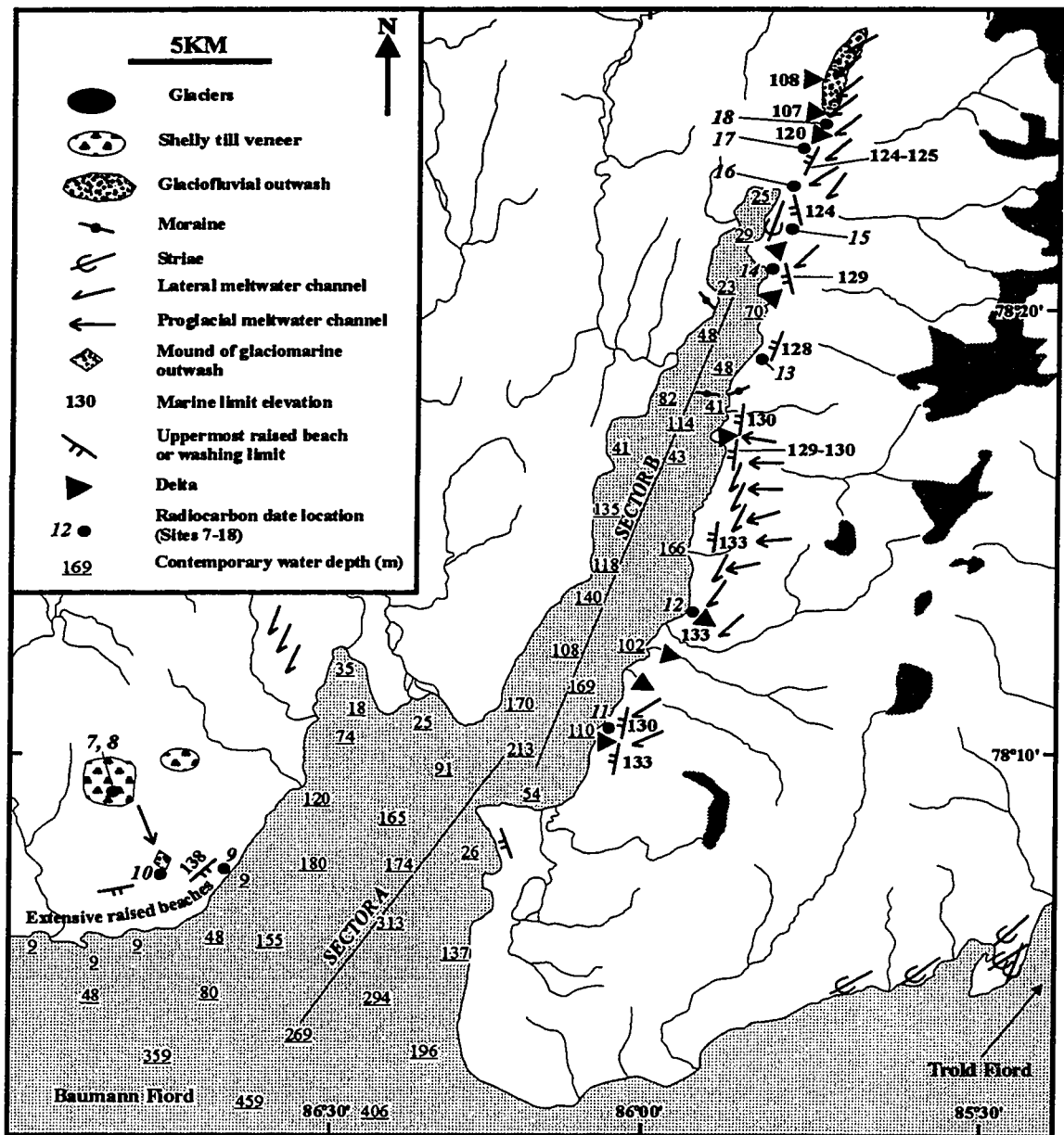


Figure 3.8: Blind Fiord showing sectors A, B, and C boundaries referred to in the text, deglacial landform-sediment associations, marine limit elevations, and radiocarbon date locations as described in Table 1. Charted water depths are from Department of Fisheries and Oceans (1979).

gravels, are preserved at 60-73 m asl, at the mouth of a proglacial meltwater channel. The laminae are predominantly massive and ungraded, and the deposits are interpreted as dissected remnants of raised marine, deltaic bottomset beds.

Marine limit and radiocarbon chronology

Two individual shell fragments from the shelly till described above dated 36,910±410 BP (TO-5600) and 36,160±430 BP (TO-5615, Sites 7 and 8, Fig. 3.8 and Table B.1). These are probably minimum ages, given the possibility of contamination by modern carbon (Bradley 1985). Well developed raised beaches west of the fiord mouth mark local marine limit at 138 m asl (Fig. 3.8). A fragment of *M. truncata* collected from a beach surface at 128 m asl dated 8590±70 BP [9460 (9330) 9060 cal BP](TO-5862; Site 9, Fig. 3.8 and Table B.1), and provides a minimum age for marine limit. A single valve of *M. calcarea* from horizontally-laminated sand west of the fiord mouth dated 8160±70 BP [8960 (8700) 8500 cal BP](TO-5610; Site 10, Fig. 3.8 and Table B.1).

3.3.2 Sector B

Geomorphology

For almost 15 km northwards through this sector, the fiord maintains a uniform width of 3-4 km and its side-walls are unbroken by protruding bedrock ridges. In the final 4.5 km of Sector B, fiord width decreases to 1.8-2.5 km. Lateral meltwater channels incised during the retreat of trunk ice (into shale/siltstone in the outer two thirds of the sector, and limestone in the inner third) are common along the east side of central Blind Fiord (Figs. 3.8 and 3.9), and become increasingly prominent up-fiord. Typically, channels are nested and shallow and, based on air photo examination, appear to have lower gradients than channels in Sector C. Channels are graded to raised beaches, gravelly benches and poorly-developed deltas marking local marine limit. Fine-grained glaciomarine sediment is absent. Above marine limit, bedrock is highly weathered, and local sandstone erratics are shattered and grussified.

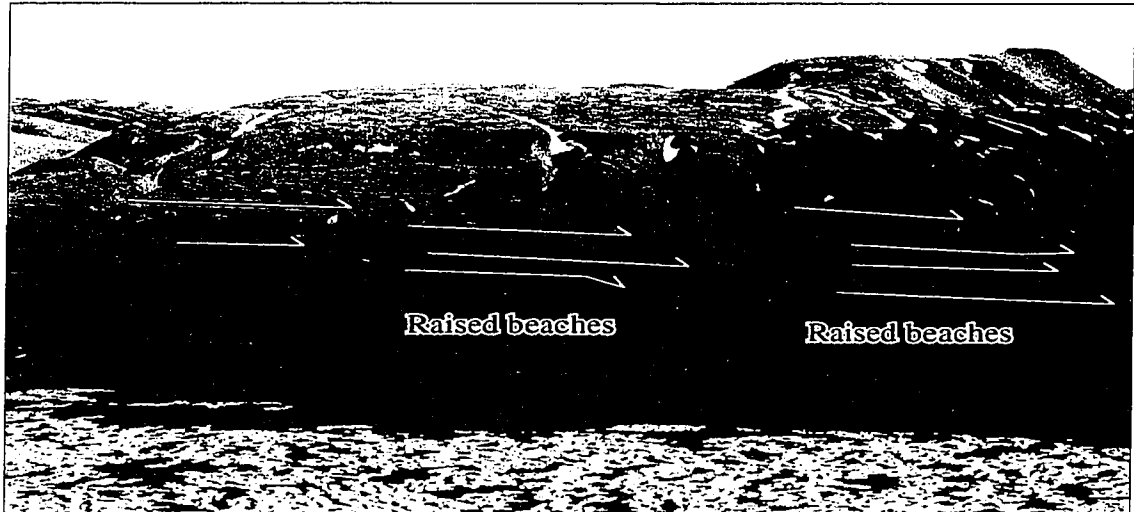


Figure 3.9: Nested, low gradient lateral meltwater channels along the east side of central Blind Fiord (sector B). Channels are cross-cut by deep, tributary ice, proglacial meltwater channels.

Marine limit and radiocarbon chronology

Marine limit is ~133 m asl for 9 km throughout Sector B, and gradually descends up-fiord to ~128 m asl over the next 10 km (Fig. 3.8). Three dates constrain the timing of deglaciation from the outer part of this sector (Fig. 3.8 and Table 1). A fragment of *M. truncata* from the surface of a raised beach at 127 m asl dated 8510±80 BP [9400 (9220) 8970 cal BP](TO-5612; Site 11, Fig. 3.8 and Table B.1). Beaches extend upslope to a bench at 133 m asl marking local marine limit. Up-fiord, a sample of *H. arctica* and *M. truncata* valves from a beach at 119 m asl dated 8550±80 BP [9420 (9250) 9000 cal BP](GSC-6047; Site 12, Fig. 3.8 and Table B.1). Here, beaches extend to 124 m asl, terminating below crudely flat-topped, gravel mounds at the mouth of a lateral meltwater channel. The mounds are interpreted as small deltas marking marine limit at 133 m asl. Finally, a fragment of *H. arctica* collected from a raised beach at 122 m asl (at the northern end of the sector) dated 8670 ± 190 BP [9850 (9390) 8930 cal BP](TO-5598; Site 13, Fig. 3.8 and Table B.1). Local marine limit is marked by a beach at 128 m asl.

3.2.3 Sector C

Geomorphology

Fiord width decreases in this sector from ~2 km to 1 km at the fiord head. Lateral meltwater channels are ubiquitous throughout the inner fiord and north of the fiord head. Typically, channels are well developed and are nested along the fiord side (Figs. 3.8 and 3.10). North of the fiord head, coarse glaciofluvial outwash emanates from the mouths of well developed lateral meltwater channels (Figs. 3.8 and 3.10). The surface of this gravel outwash is disrupted and irregular, with numerous depressions, elongate furrows, and small 1-2 m high gravel mounds, inferred to record the melt-out of buried ice. Throughout Sector C, there is a conspicuous lack of fine-grained, raised glaciomarine sediment.

Marine limit and radiocarbon chronology

Marine limit decreases from 129 m asl in the southern part of this sector to ~107 m asl ~5 km inland from the fiord head (Fig. 3.8). Five radiocarbon dates provide minimum age estimates for deglaciation and establishment of local marine limit (Fig. 3.8 and Table B.1). A fragment



Figure 3.10: Blind Fiord, sector C, showing major glacial landforms and marine limit elevations. Note well-developed, steep, nested lateral meltwater channels. National Air Photo Library A16605-9, 1959.

of *H. arctica* collected from a raised beach at 123 m asl (in the southern part of the sector) dated 8310±80 BP [9210 (8950) 8630 cal BP](TO-5608; Site 14, Fig. 3.8 and Table B.1). Local marine limit is marked by a gravel bench at 129 m asl. At the fiord head, two dates provide minimum ages for marine limit at 124 m asl. A sample dominated by *M. truncata* from a beach at 86 m asl dated 7990±140 BP [8920 (8460) 8190 cal BP](GSC-5924; Site 15, Fig. 3.8 and Table B.1). A second sample of *H. arctica* and *M. truncata* at 107 m asl was collected from coarse glaciomarine outwash 1 km to the north. This sample dated 8220±100 BP [9100 (8830) 8470 cal BP](GSC-6054; Site 16, Fig. 3.8 and Table B.1). Two km up-fiord, a fragment of *H. arctica* from a raised beach at 109 m asl dated 7090±70 BP [7760 (7580) 7440 cal BP](TO-5863; Site 17, Fig. 3.8 and Table B.1). Marine limit here is marked by a beach at 124-125 m asl. A final sample dominated by *H. arctica* and *M. truncata* was collected at 95 m asl on the foreslope of a 120 m delta and dated 8090±110 BP [8950 (8560) 8370 cal BP](GSC-5896; Site 18, Fig. 3.8 and Table B.1).

Interpretation

Calibrated radiocarbon dates indicate that trunk ice retreated from the fiord mouth [9460 (9330) 9060 cal BP; TO-5862] to the southern part of Sector C [9210 (8950) 8630 cal BP; TO-5608], a distance of 32 km, in 380 years (0.1 km/year). However, the standard errors of these dates overlap and hence this retreat may have been catastrophic (cf. Starfish Bay). Glacial geomorphological evidence also supports rapid early Holocene retreat in Blind Fiord (see below).

Lateral meltwater channels are widespread in Sectors B and C, and together with the absence of fine-grained subaqueous outwash above sea level throughout the fiord, this suggests that trunk ice was predominantly cold-based during retreat (Dyke 1993). In this regard, it is noteworthy that subaqueous outwash and extensive accumulations of fine-grained glaciomarine sediments (cf. Starfish Bay) were not observed from the fiord head northwards, even though deglacial landform/sediment associations are completely exposed above sea level throughout this area. The rapid deglaciation recorded by radiocarbon dates was likely achieved by calving (cf. Hughes 1987; Meier and Post 1987). In Sector B, channels are nested and shallow, with gentle longitudinal gradients, marine limit deltas are poorly developed and

fine-grained glaciomarine sediments are absent. This geomorphology may reflect a combination of rapid deglaciation with a predominantly cold-based thermal regime. Calving would have triggered increased extensional flow resulting in a lowering of the surface profile of trunk ice, the production of shallow, stepped lateral meltwater channels with low gradients, and, in association with a cold-based thermal regime, a low rate of sediment supply.

Well developed lateral meltwater channels and associated extensive outwash in Sector C demonstrate the increased stability of the ice-margin and greater availability of meltwater when trunk ice reached the inner fiord. Radiocarbon dates indicate that retreat through the southern 6 km of this sector was rapid as far as the 120 m asl delta. However, north of this delta, the abrupt drop in marine limit to 107 m asl, in association with the extensive sedimentary infill and well developed channels, suggest subsequent slower retreat.

The absence of deglacial landforms associated with retreat of trunk ice in Sector A contrasts with Sectors B and C. This contrast cannot be explained by differences in bedrock lithology, because lateral meltwater channels are absent from shale/siltstone bedrock in Sector A, but are present on these lithologies in Sector B. One interpretation therefore could be that outer Blind Fiord lay beyond the last ice limit. However, direct evidence for glaciation of the outer fiord exists in the form of shelly till. Even though radiocarbon dates from this till are interpreted as minimum ages (see above), they do not negate a last glaciation age for the till. It is noteworthy that the till is incised by Holocene marine limit and that pre-Holocene shorelines, indicative of the retreat of ice pre-dating the last glaciation, are absent. Thus evidence for only one glacial cycle, recorded by till and overlying marine sediments, is preserved here. The simplest interpretation is that retreat occurred during the Holocene, and therefore, that the outer fiord was covered by ice during the last glaciation.

The lack of deglacial landforms in Sector A may simply record the interplay of fiord topography, deglaciation by calving and basal thermal regime. The wide and deep outer fiord would have promoted rapid retreat by calving and extensive crevassing. This would have facilitated evacuation of supraglacial and lateral meltwater, and so prevented channel formation. If the ice was cold-based, pre-existing weathered terrain such as tors and grussified erratics could be preserved (cf. Dyke 1993). Channels in Sector B record an increased availability of meltwater for channel formation probably associated with a reduction in

crevassing due to the narrower fiord, but their shallow depths and low gradients reflect rapid deglaciation. Slow retreat through Sector C resulted in decreased crevassing and a greater supply of supraglacial and lateral meltwater for erosion and deposition.

Thus in terms of the fiord as a whole, there is a crude continuum in the morphology of lateral meltwater channels, from a *lack* of channels in Sector A, to shallow channels with gentle gradients in Sector B, to steeper, well developed channels and extensive outwash in Sector C. It is inferred that this continuum results from variation in the rate of glacier retreat, coupled with an increasing availability of meltwater and reduction in crevassing concurrent with deglaciation.

The dominance of lateral meltwater channels and absence of subaqueous outwash and fine-grained glaciomarine sediment (which contrasts with Starfish Bay) is interpreted above as indicating that the retreating trunk glacier in Blind Fiord was predominantly cold-based. Alternatively, it might be argued that the trunk glacier was in fact warm-based or polythermal, and the deglacial geomorphology merely reflects a more poorly-developed subglacial drainage system than that which characterised Starfish Bay. However, this explanation is deemed unlikely on the account of the apparent absence of *any* subaqueous outwash or fine-grained glaciomarine deposits above sea level throughout Blind Fiord, particularly north of the fiord head where the complete deglacial record is exposed. The former explanation of a predominantly cold-based glacier is therefore preferred.

3.4 DISCUSSION

3.4.1 Controls on Early-Holocene Deglacial Sedimentation and Ice-retreat

Fiord Topography

Early Holocene deglaciation in Blind Fiord and Starfish Bay was characterised by a two-step retreat pattern, initially rapid through Sectors A and B, and then slower in Sector C. This variation is linked here to fiord bathymetry, in particular the presence or absence of pinning points. Initial deglaciation of southern Eureka Sound prior to 9200±110 BP [10150 (9940) 9690 cal BP] may have been driven by eustatic sea level rise (Fairbanks 1989; Chappell and Polach 1991; Blanchon and Shaw 1995), coupled to an abrupt early Holocene (~10-10.2 ka BP) increase in temperature (Alley *et al* 1993; Meese *et al.* 1994; Kapsner *et*

al. 1995; Lowe and Walker 1997). In Blind Fiord, a lack of pinning points and deep water in Sectors A and B, would have facilitated calving and allowed rapid retreat to continue as far as the inner fiord, where retreat then slowed due to the narrower fiord and shallower water. These also allowed correspondingly greater sedimentation in Sector C than farther down-fiord.

Similarly, in Starfish Bay, rapid retreat through the outer and mid-fiord was facilitated by deep water and relatively large fiord widths. This rapid retreat was punctuated by brief stillstands and ice-marginal glaciomarine sedimentation at fiord-side topographic irregularities which acted as pinning points (cf. Eyles and McCabe 1989; Merrit *et al.* 1995; Seramur *et al.* 1997). The narrower and shallower inner fiord, in conjunction with bedrock highs immediately east of the fiord head, allowed stabilisation of the ice-margin and glaciomarine deposition. Water depth is approximately similar in both Starfish Bay and Blind Fiord, so its effect on calving would likely also have been similar in the two fiords (cf. Meier and Post 1987; Pelto and Warren 1991). Therefore, the brief stillstands inferred from deglacial landform/sediment associations in Starfish Bay, in contrast to Blind Fiord, were likely the result of a narrower, and more irregular fiord. This topographical effect may have been augmented by a higher flow rate of ice in Starfish Bay on account of a warm-based thermal regime (see below), and also perhaps, a thicker trunk glacier. These would have helped offset calving losses and enhanced the ability of the retreating glacier to utilise pinning points.

Basal Thermal Regime

Discrete glaciomarine sediments throughout Starfish Bay are similar to lithofacies described from both modern and Quaternary, temperate and Arctic glaciomarine environments (*e.g.*, Powell and Molnia 1989; Stewart 1991; Hein and Syvitski 1992; McCabe and Haynes 1996), and illustrate the important role of meltwater discharge from subglacial conduits. The presence of numerous striated and glacially faceted clasts within massive diamict facies demonstrates their basal derivation and transport, and also points to warm-based thermal conditions. These deposits demonstrate that the retreating Starfish Bay glacier had significant basal debris and a well developed subglacial drainage system, and thus was characterised by a warm-based thermal regime.

Thermal regime exerted an equally strong control on the formation of deglacial landform/sediment associations in Blind Fiord. Although glacier retreat in Sector C was slow and characterised by greater sedimentation than in the outer sectors, the lack of fine-grained subaqueous outwash is striking. This, in association with the abundance of lateral meltwater channels, provides strong support that trunk ice lacked a well developed subglacial drainage system and was predominantly cold-based during deglaciation.

Therefore, trunk glaciers in Starfish Bay and Blind Fiord are inferred to have had different basal thermal regimes during early Holocene deglaciation. This contrast in thermal regime may reflect the different sources of trunk glaciers in both fiords (with respect to ice thickness and spatial extent of accumulation area). Directional ice-flow indicators show that Blind Fiord was fed from Raanes Peninsula, while Starfish Bay was fed by flow from an expanded Prince of Wales Icefield (Fig. 3.2). The latter source was both more extensive and possibly thicker than that on Raanes Peninsula. Convergent flow of a large volume of ice into Starfish Bay, which is narrower throughout than Blind Fiord, would have resulted in enhanced internal deformation and strain heating. This would have promoted higher flow rates and facilitated frictional heating and basal sliding, leading to the development of a warm-based thermal regime.

By contrast, ice-flow in Blind Fiord originated from a more restricted source area. Rapid deglaciation by calving could have induced increased extensional flow, with overall thinning of the trunk glacier, particularly in the lower part of the ablation zone. This increased extensional flow to feed calving at the terminus may have resulted in the rapid advection of colder ice from up-flowline towards the margins in the fiord (cf. Blatter and Haeberli 1984), thereby facilitating frozen bed conditions, and overwhelming the warming effect caused by convergent flow. Thinning of the glacier would also diminish internal deformation as well as reduce insulation of the bed from colder surface temperatures.

3.4.2 Implications

1) This study indicates that early Holocene deglaciation of High Arctic fiords was characterised by variation in basal thermal regime, even in adjacent fiords.

2) In fiord settings, it is possible to reconstruct past deglacial thermal regime through studies of glacial sedimentology and geomorphology. It is proposed that retreat of cold-based glaciers will be characterised by formation of lateral meltwater channels (cf. Dyke 1993) and a lack of fine-grained subaqueous outwash, in contrast to warm-based conditions where deposition of subaqueous outwash lithofacies will accompany slow retreat (cf. Stewart 1991).

3) During the last glaciation of the region, trunk glaciers in Blind Fiord and Troid Fiord extended beyond their fiord mouths into Baumann Fiord (see above). Deglaciation involved a two-step retreat for both fiords, which consisted of initial rapid break-up $>9200 \pm 110$ BP [10150 (9940) 9690 cal BP], preceding slower retreat as ice-margins became terrestrially-based in the inner fiords (cf. Dyke 1984; Lemmen *et al.* 1994; Funder and Hansen 1996; England *in press*).

A common feature of many fiords in the northern Queen Elizabeth Islands is the juxtaposition of a prominent belt of glaciogenic landforms and sediments in the inner fiord, with a sparsity or absence of such features from the outer fiord or adjacent higher peaks which often exhibit a correspondingly greater degree of weathering (*e.g.*, England 1987; 1990; Lemmen *et al.* 1994; Bell 1996). Similar morphological contrasts have been documented in previously glaciated regions elsewhere (*e.g.*, Dyke 1979; Nesje *et al.* 1994; McCarroll *et al.* 1996). Interpretations of this landscape zonation have frequently been polarised between those who argue that the outer areas were beyond the limit of the last glaciation and therefore underwent a greater duration of weathering (*e.g.*, Pheasant and Andrews 1973; England 1987, 1996; Ballantyne 1997), and those who argue that they reflect cold-based thermal conditions beneath a more extensive ice-cover, which inhibited the formation of glacial landforms and deposits and preserved pre-existing weathered terrain (*e.g.*, Sugden and Watts 1977; Hughes 1987; Kleman 1994; Rea *et al.* 1996).

In Blind Fiord, however, the lack of deglacial landforms and sediments in Sector A is inferred to reflect rapid deglaciation through the wide outer fiord. It is proposed that this model of two-step deglaciation is applicable to other fiords in the Queen Elizabeth Islands which have previously been interpreted in terms of a restricted last glaciation. The combined effects of eustatic sea level rise >9.2 ka BP (9.8 cal BP) and an abrupt increase in early Holocene temperature may have triggered destabilisation and rapid break-up of the marine-

based component of ice in many fiords and inter-island channels by calving (cf. Funder and Hansen 1996; Forman *et al.* 1996; England *in press*). This would have resulted in increased extensional flow and thinning, leading to greater crevassing, with drainage of supraglacial and marginal meltwater. Meltwater evacuation, in combination with rapid radial retreat, would have inhibited formation of deglacial landforms and sediments until terrestrial stabilisation. The belt of glaciogenic landforms at the heads of many fiords in the region likely records this stabilisation. Hodgson (1985) was the first to suggest that the fiord heads “drift-belt” on western Ellesmere Island could record a prominent ice-marginal stillstand during the retreat of a regional ice-sheet (his “Model A”).

This model of initial rapid deglaciation is supported by recent work on the post 18 ka BP migration of marine molluscs (Dyke *et al.* 1996), which shows a rise in the number of 9 ka vs. 10 ka radiocarbon dates for the northern Queen Elizabeth Islands and implies that the major inter-island channels and fiords were rapidly opened during this interval (cf. Blake 1972). The larger fiords and inter-island channels (*e.g.*, Greely Fiord, Nansen Sound, Eureka Sound, Baumann Fiord, Makinson Inlet) would have been particularly susceptible to such initial rapid deglaciation on account of their frequently cliffed sides and deep water which would have been accentuated by the combined effects of glacioisostatic loading and eustatic sea level rise.

3.5 REFERENCES

- Aitken, A.E. and Bell, T.J. (1998). Holocene glacimarine sedimentation and macrofossil palaeoecology in the Canadian High Arctic: environmental controls. *Marine Geology*, **145**, 151-171.
- Alley, R.B., Meese, D.A., Shuman, C.A., Gow, A.J., Taylor, K.C., Grootes, P.M., White, J.W.C., Ram, M., Waddington, E.D., Mayewski, P.A. and Zielinski, G.A. (1993). Abrupt increase in Greenland snow accumulation at the end of the Younger Dryas event. *Nature*, **362**, 527-529.
- Ballantyne, C.K. (1997). Periglacial trimlines in the Scottish Highlands. *Quaternary International*, **38/39**, 119-136.
- Bednarski, J. (1988). The geomorphology of glaciomarine sediments in a high arctic fiord. *Géographie physique et Quaternaire*, **42**, 65-74.
- Bell, T. (1996). Late Quaternary glacial and sea level history of Fosheim Peninsula, Ellesmere Island, Canadian High Arctic. *Canadian Journal of Earth Sciences*, **33**, 1075-1086.
- Benn, D.I. and Evans, D.J.A. (1996). The interpretation and classification of subglacially-deformed materials. *Quaternary Science Reviews*, **15**, 23-52.
- Blake, W., Jr. (1972). Climatic implications of radiocarbon-dated driftwood in the Queen Elizabeth Islands, Arctic Canada. In: Vasari, Y., Hyvärinen, H. and Hicks, S. (eds.), *Climatic Changes in Arctic Areas during the Past Ten-Thousand Years*. Acta Universitatis Ouluensis, Series A. Scientifiae Rerum Naturalium, No. 3, Geologica No. 1, 77-104.
- Blanchon, P. and Shaw, J. (1995). Reef-drowning events during the last deglaciation: evidence for catastrophic sea-level rise and ice-sheet collapse. *Geology*, **23**, 4-8.
- Blatter, H. and Haeberli, W. (1984). Modelling temperature distribution in alpine glaciers. *Annals of Glaciology*, **5**, 18-22.
- Bradley, R.S. (1985). *Quaternary Paleoclimatology: methods of paleoclimatic reconstruction*. Chapman and Hall, London.
- Chappell, J. and Polach, H. (1991). Post-glacial sea-level rise from a coral record at Huon Peninsula, Papua New Guinea. *Nature*, **349**, 147-149.

- Cowan, E.A. and Powell, R.D. (1990). Suspended sediment transport and deposition of cyclically interlaminated sediment in a temperate glacial fiord, Alaska, U.S.A. In: Dowdeswell, J.A. and Scourse, J.D. (eds.), *Glacimarine Environments: Processes and Sediments*. Geological Society of London Special Publication No. 53, pp.75-89.
- Cowan, E.A., Cai, J., Powell, R.D., Clark, J.D. and Pitcher, J.N. (1997). Temperate glacimarine varves: an example from Disenchantment Bay, southern Alaska. *Journal of Sedimentary Research*, **67**, 536-549.
- Crossen, K.J. (1991). Structural control of deposition by Pleistocene tidewater glaciers, Gulf of Maine. In: Anderson, J.B. and Ashley, G.M. (eds.), *Glacial Marine Sedimentation; Paleoclimatic Significance*. Geological Society of America Special Paper 261, pp. 127-135.
- Department of Fisheries and Oceans (1979). Eureka Sound and southern approaches including Baumann Fiord. Canadian Hydrographic Service, Chart 7940, scale 1: 3,00000.
- Dowdeswell, J.A., Whittington, R.J. and Marienfeld, R. (1994). The origin of massive diamicton facies by iceberg rafting and scouring, Scorsby Sund, East Greenland. *Sedimentology*, **41**, 21-35.
- Dreimanis, A. (1988). Tills: their genetic terminology and classification. In: Goldthwaite, R.P. and Matsch C.L. (eds.), *Genetic Classification of Glacigenic Deposits*. Balkema, Rotterdam, pp. 17-84.
- Dyke, A.S. (1979). Glacial and sea level history of southwestern Cumberland Peninsula, Baffin Island, N.W.T., Canada. *Arctic and Alpine Research*, **11**, 179-202.
- Dyke, A.S. (1984). *Quaternary geology of Boothia Peninsula and northern District of Keewatin, central Canadian Arctic*. Geological Survey of Canada, Memoir 407.
- Dyke, A.S. (1993). Landscapes of cold-centred Late Wisconsinan ice caps, Arctic Canada. *Progress in Physical Geography*, **17**, 223-247.
- Dyke, A.S., Dale, J.E. and McNeely, R.N. (1996). Marine molluscs as indicators of environmental change in glaciated North America and Greenland during the last 18,000 years. *Géographie physique et Quaternaire*, **50**, 125-184.

- England, J. (1987). Glaciation and the evolution of Canadian high arctic landscape. *Geology*, **15**, 419-424.
- England, J. (1990). The late-Quaternary history of Greely Fiord and its tributaries, west-central Ellesmere Island. *Canadian Journal of Earth Sciences*, **27**, 255-270.
- England, J. (1992). Postglacial emergence in the Canadian High Arctic: integrating glacioisostasy, eustasy, and late deglaciation. *Canadian Journal of Earth Sciences*, **29**, 984-999.
- England, J. (1996). Glacier dynamics and paleoclimatic change during the last glaciation of eastern Ellesmere Island, Canada. *Canadian Journal of Earth Sciences*, **33**, 779-799.
- England, J. (*in press*). Coalescent Greenland and Innuitian ice during the Last Glacial Maximum: revising the Quaternary of the Canadian High Arctic. *Quaternary Science Reviews*.
- Eyles, C.H. and Lagoe, M.B. (1990). Sedimentation patterns and facies geometries on a temperate glacially-influenced continental shelf: the Yakataga Formation, Middleton Island, Alaska. In: Dowdeswell, J.A. and Scourse, J.D. (eds.), *Glacimarine Environments: Processes and Sediments*. Geological Society of London Special Publication No. 53, pp. 363-386.
- Eyles, N. (1987). Late Pleistocene debris flow deposits in large glacial lakes in British Columbia and Alaska. *Sedimentary Geology*, **53**, 33-71.
- Eyles, N. and McCabe, A.M. (1989). The late Devensian (<22,000 BP) Irish Sea basin: the sedimentary record of a collapsed ice sheet margin. *Quaternary Science Reviews*, **8**, 307-351.
- Fairbanks, R. G. (1989). A 17,000 year glacio-eustatic sea level record: influence of glacial melting rates on the Younger Dryas event and deep ocean circulation. *Nature*, **342**, 637-642.
- Forman, S.L., Lubinski, D., Miller, G.H., Matishov, G.G., Korsun, S., Snyder, J., Herlihy, F., Weihe, R., and Myslivets, V. 1996. Postglacial emergence of western Franz Josef Land, Russia, and retreat of the Barents Sea Ice Sheet. *Quaternary Science Reviews*, **15**, 77-90.

- Funder, S. and Hansen, L. (1996). The Greenland ice sheet - a model for its culmination and decay during and after the last glacial maximum. *Bulletin of the Geological Society of Denmark*, **42**, 137-152.
- Hein, F. J. and Syvitski, J. P. M. (1992). Sedimentary environments and facies in an arctic basin, Itirbilung Fiord, Baffin Island, Canada. *Sedimentary Geology*, **81**, 17-45.
- Hodgson, D.A. (1985). The last glaciation of west-central Ellesmere Island, Arctic Archipelago, Canada. *Canadian Journal of Earth Sciences*, **22**, 347-368.
- Hughes, T. (1987). Ice dynamics and deglaciation models when ice sheets collapsed. In: Ruddiman, W.F. and Wright, H.E. Jr., (eds.), *North America and adjacent oceans during the last deglaciation*. Boulder, Colorado, Geological Society of America, The Geology of North America, v.K-3, pp. 183-220
- Hunter, L.E., Powell, R.D. and Smith, G.W. (1996). Facies architecture and grounding-line fan processes of morainal banks during the deglaciation of coastal Maine. *Geological Society of America Bulletin*, **108**, 1022-1038.
- Kapsner, W.R., Alley, R.B., Shuman, C.A., Anandakrishnan, S. and Grootes, P.M. (1995). Dominant influence of atmospheric circulation on snow accumulation in Greenland over the past 18,000 years. *Nature*, **373**, 52-54.
- Kleman, J. (1994). Preservation of landforms under ice sheets and ice caps. *Geomorphology*, **9**, 19-32.
- Lemmen, D.S. (1990). Glaciomarine sedimentation in Disraeli Fiord, High Arctic Canada. *Marine Geology*, **94**, 9-22.
- Lemmen, D.S., Aitken, A.E. and Gilbert, R.G. (1994). Early Holocene deglaciation of Expedition and Strand fiords, Canadian High Arctic. *Canadian Journal of Earth Sciences*, **31**, 943-958.
- Lønne, I. (1995). Sedimentary facies and depositional architecture of ice-contact glaciomarine systems. *Sedimentary Geology*, **98**, 13-43.
- Lowe, D.R. (1982). Sediment gravity flows. II. Depositional models with special reference to the deposits of high-density turbidity currents. *Journal of Sedimentary Petrology*, **52**, 279-297.

- Lowe, J.J. and Walker, M.J.C. (1997). *Reconstructing Quaternary Environments*. Second edition, Longman, 446p.
- Mackiewicz, N.E., Powell, R.D., Carlson, P.R. and Molnia, B.F. (1984). Interlaminated ice-proximal glaciomarine sediments in Muir Inlet, Alaska. *Marine Geology*, **57**, 113-147.
- McCabe, A.M. and Haynes, J.R. (1996). A late Pleistocene intertidal boulder pavement from an isostatically emergent coast, Dundalk Bay, eastern Ireland. *Earth Surface Processes and Landforms*, **21**, 555-572.
- McCarroll, D., Ballantyne, C.K., Nesje, A. and Dahl, S. O. (1996). Nunataks of the last ice sheet in northwest Scotland, *Boreas*, **24**, 305-323.
- Meese, D.A., Gow, A.J., Grootes, P., Mayewski, P.A., Ram, M., Stuiver, M., Taylor, K.C., Waddington, E.D. and Zielinski, G.A. (1994). The accumulation record from the GISP2 core as an indicator of climate change throughout the Holocene. *Science*, **266**, 1680-1682.
- Meier, M.F. and Post, A. (1987). Fast tidewater glaciers. *Journal of Geophysical Research*, **92**, 9051-9058.
- Merritt, J.W., Auton, C.A. and Firth, C.R. (1995). Ice-proximal glaciomarine sedimentation and sea level change in the Inverness area, Scotland: a review of the deglaciation of a major ice stream of the British late Devensian Ice Sheet. *Quaternary Science Reviews*, **14**, 289-329.
- Middleton, G.V. and Hampton, M.A. (1976). Subaqueous sediment transport and deposition by sediment gravity flows. In: Stanley D.J. and Swift, D.J.P. (eds.), *Marine Sediment Transport and Environmental Management*. Wiley, New York, pp. 197-218.
- Nesje, A., McCarroll, D. and Dahl, S.O. (1994). Degree of rock surface weathering as an indicator of ice sheet thickness along an east-west transect across southern Norway. *Journal of Quaternary Science*, **9**, 337-347.
- Pelto, M.S. and Warren, C. (1991). Relationship between tidewater calving velocity and water depth at the calving front. *Annals of Glaciology*, **15**, 115-118.
- Pheasant, D.R. and Andrews, J.T. (1973). Wisconsin glacial chronology and relative sea level movements, Narpaing Fiord Broughton Island area, eastern Baffin Island, N.W.T. *Canadian Journal of Earth Sciences*, **10**, 1621-1641.

- Postma, G. (1986). Classification for sediment gravity flow deposits based on flow conditions during sedimentation. *Geology*, **14**, 291-294.
- Powell, R.D. (1981). A model for sedimentation by tidewater glaciers. *Annals of Glaciology*, **2**, 129-134.
- Powell, R.D. (1984). Glacimarine processes and inductive lithofacies modelling of ice shelf and tidewater glacier sediments based on Quaternary examples. *Marine Geology*, **57**, 1-52.
- Powell, R.D. (1990). Glacimarine processes at grounding-line fans and their growth to ice-contact deltas. In: Dowdeswell, J.A. and Scourse, J.D. (eds.), *Glacimarine Environments: Processes and Sediments*. Geological Society of London Special Publication No. 53, pp. 53-73.
- Powell, R.D. and Molnia, B.F. (1989). Glacimarine sedimentary processes, facies and morphology of the south-southeast Alaska shelf and fiords. *Marine Geology*, **85**, 359-390.
- Rea, B.R., Whalley, W.B., Rainey, M.M. and Gordon, J.E. (1996). Blockfields, old or new? Evidence and implications from some plateaus in northern Norway. *Geomorphology*, **15**, 109-121.
- Seramur, K. C., Powell, R.D. and Carlson, P. R. (1997). Evaluation of conditions along the grounding line of temperate marine glaciers: an example from Muir Inlet, Glacier Bay, Alaska. *Marine Geology*, **140**, 307-327.
- Stewart, T.G. (1991). Glacial marine sedimentation from tidewater glaciers in the Canadian High Arctic. In: Anderson, J.B. and Ashley, G.M. (eds.), *Glacial Marine Sedimentation; Paleoclimatic Significance*. Geological Society of America Special Paper 261, pp. 95-105.
- Stuiver, M. and Reimer, P.J. (1993). Extended ¹⁴C data base and revised CALIB 3.0 ¹⁴C age calibration program. *Radiocarbon*, **35**, 215-230.
- Sugden, D.E. and Watts, S.H. (1977). Tors, felsenmeer, and glaciation in northern Cumberland Peninsula, Baffin Island. *Canadian Journal of Earth Sciences*, **14**, 2817-2823.

- Trettin, H. P. (1991). *Geology of the Innuitian Orogen and Arctic Platform of Canada and Greenland*. Geological Survey of Canada, Geology of Canada, No.3, 569p.
- Walker, R.G. (1992). Turbidites and submarine fans. In: Walker, R.G. and James, N.P. (eds.), *Facies Models: Response to Sea Level Change*. Geological Association of Canada, pp. 239-263.

CHAPTER FOUR

Holocene emergence and shoreline delevelling, southern Eureka Sound, High Arctic Canada

4.1 INTRODUCTION

This paper presents the postglacial relative sea level history of southern Eureka Sound, High Arctic Canada (Figs. 4.1 and 4.2), focussing on initial emergence, pattern of shoreline delevelling and implications for former glacier loading. Blake (1970) first proposed the existence of the *Innuitian Ice Sheet* in the Canadian High Arctic during the late Wisconsinan on the basis of the pattern of differential postglacial rebound since 5 ka BP. He demonstrated that shorelines of this age in the Queen Elizabeth Islands were highest (>25 m asl) throughout a broad northeast/southwest oriented corridor extending from northern Eureka Sound to Bathurst Island. He proposed that this emergence reflected a regional ice sheet over the Queen Elizabeth Islands during the Last Glacial Maximum whose centre corresponded to the zone of greatest emergence (cf. Walcott 1972; Tushingham 1991). In contrast, a markedly different reconstruction, advocating a restricted late Wisconsinan glaciation for the same region, was proposed by England (1976a and b) on the basis of glacial geologic data from northeastern Ellesmere Island and an alternative interpretation of the postglacial emergence. These contrasting reconstructions broadly defined the ensuing debate concerning the extent of the Last Glacial Maximum in the Queen Elizabeth Islands (e.g., Blake, 1992a and b, 1993; Blake *et al.* 1992; de Freitas 1990; Tushingham 1991; England 1987, 1990, 1996, England *et al.* 1991; Lemmen 1989; Bell 1996).

Previous work on the postglacial emergence history of northern Eureka Sound and Greely Fiord has reported evidence for a period of stable relative sea level at marine limit (England 1992). This is similar to sea level curves from northeastern and eastern Ellesmere Island which show either an interval of sea level arrest subsequent to marine limit formation (England 1983), or slow (1-2 m/century) initial emergence (England 1997). These curves contrast markedly with those reported from elsewhere on Ellesmere and Axel Heiberg Islands (Blake 1975, 1992a; Hodgson *et al.* 1991; Lemmen *et al.* 1994; Bednarski 1995) which indicate continuous rapid unloading (4.5-7 m/century), and are thus similar to curves from

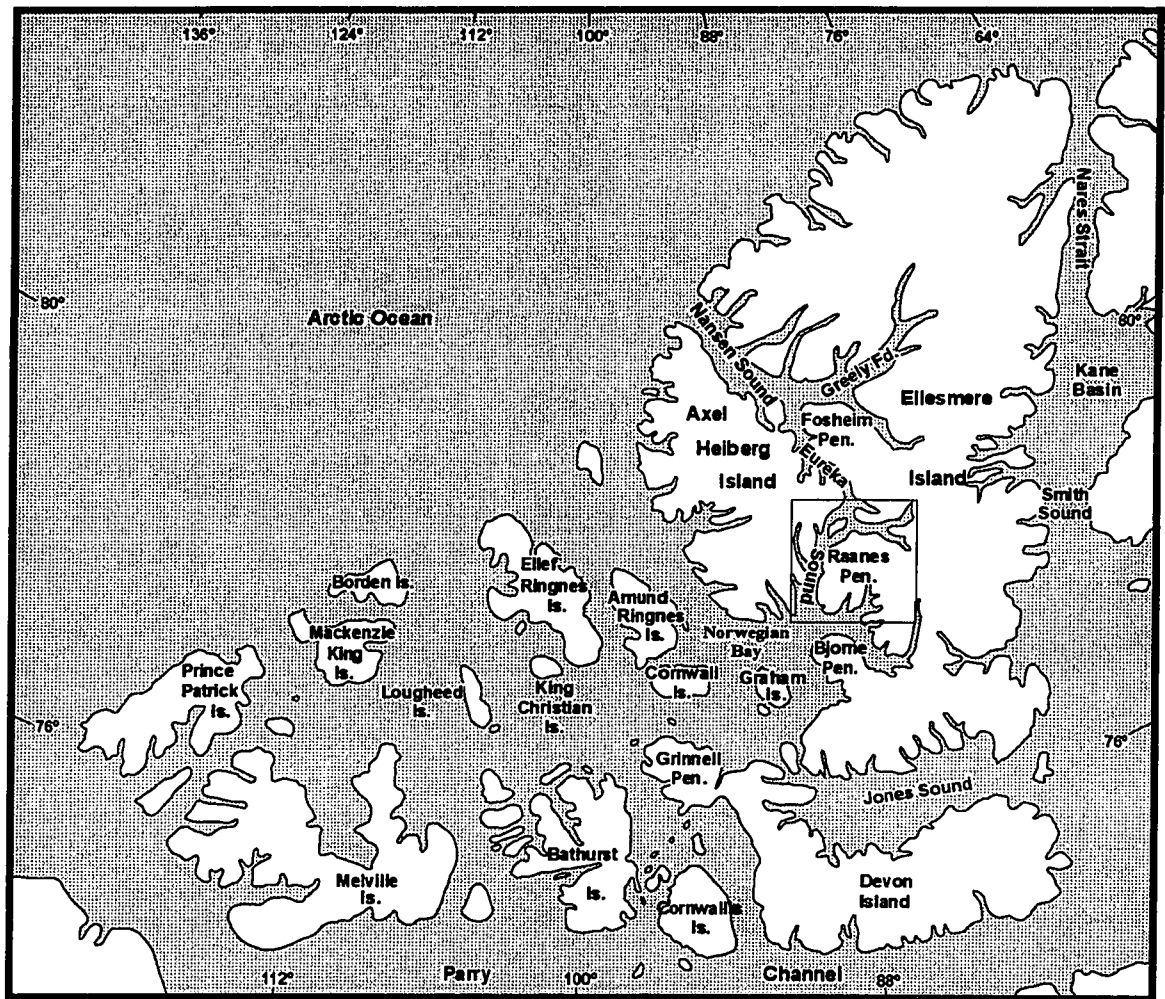


Figure 4.1: Queen Elizabeth Islands, Canada, and location of study area.

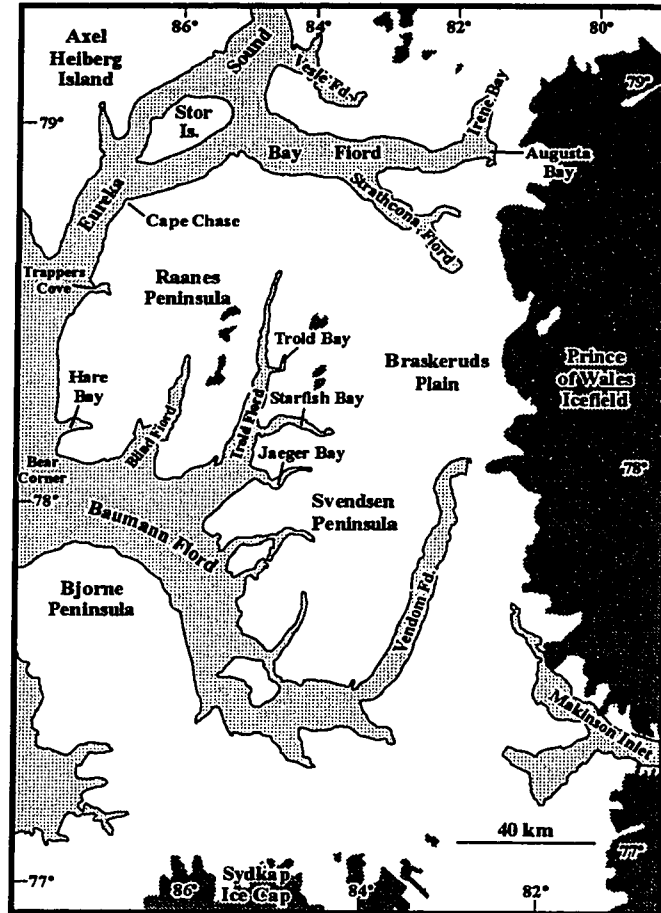


Figure 4.2: Southern Eureka Sound showing contemporary ice cover (dark shading) and location of placenames referred to in text.

areas of the Canadian Arctic which were formerly covered by the *Laurentide Ice Sheet* (Andrews 1970; Dyke 1984; Dyke *et al.* 1991).

Isobases drawn by England (1992, 1997) on the 8 ka shoreline in Greely Fiord, west-central Ellesmere Island, exhibit a narrow plunging ridge of maximum emergence, essentially parallel to the regional geological structure. This contrasted with the broad cells of uplift documented elsewhere in Arctic Canada which record postglacial unloading following removal of the *Laurentide Ice Sheet* (cf. Andrews 1970; Dyke 1984), and as result, a possible neotectonic contribution to Holocene emergence was proposed for western Ellesmere Island (England 1992, 1997). Both the slow rate of initial emergence and apparently anomalous isobase pattern in the form of the steeply-plunging ridge, coupled to independent glacial geological evidence suggesting a restricted Last Glacial Maximum, were interpreted as being incompatible with a late Wisconsinan *Innuitian Ice Sheet* (England 1983, 1992, 1997; Bell 1996). However, more recent glacial geologic fieldwork validates an extensive late Wisconsinan glacial cover for at least the alpine sector of the Queen Elizabeth Islands and areas of the central Arctic (Hättestrand and Stroeven 1996; Bednarski 1998; England 1998, *in press*; Dyke *in press a*; Ó Cofaigh Chapter 2, this volume; see also Funder and Hansen 1996). Integration of this new glacial geologic evidence with the associated postglacial relative sea level histories of these areas has only commenced (Dyke *in press b*; England and Ó Cofaigh 1998).

Glacial geologic and chronologic evidence indicates that late Wisconsinan glaciation in southern Eureka Sound was characterised by an extensive ice cover (Ó Cofaigh Chapter 2, this volume). This paper presents the postglacial relative sea history associated with removal of that ice load, and provides new data on the magnitude, timing and pattern of postglacial emergence. It has three principal objectives: (1) to reconstruct initial postglacial emergence at several sites where the best chronological control is available; (2) to reconstruct the pattern of shoreline delevelling in southern Eureka Sound from isobases drawn on the 8.5 ka shoreline, and to link this data with previously published work to the north and south (England 1976b, 1992; Bell 1996; Dyke *in press a* and *b*; and (3) to assess implications for former ice sheet loading in the region.

4.2 STUDY AREA

Eureka Sound is the inter-island channel, 300 km long and 10-28 km wide, which separates Ellesmere and Axel Heiberg islands. Raanes Peninsula and Bay Fiord border central and southern Eureka Sound, respectively, along its east side (Figs. 4.1 and 4.2). Geologically, the study area is dominated by north-northeast striking sedimentary lithologies, although igneous intrusives outcrop locally (Trettin 1991). The geological structure imparts a distinctive topographic grain to the region, forming ridges and valleys. Uplands of >1000 m asl are dissected by steep-sided, glacially-eroded fiords and valleys aligned both parallel to bedrock structure (*e.g.*, Blind Fiord) and cross-cutting it (*e.g.*, Bay Fiord). Contemporary glaciers are limited to small, upland ice-caps, although the region is bordered immediately to the east by the Prince of Wales Icefield (Fig. 4.2).

4.3 LATE WISCONSINAN GLACIATION OF SOUTHERN EUREKA SOUND

During the late Wisconsinan, southern Eureka Sound supported extensive glaciation, consisting of expanded ice-caps which were coalescent along the length of the channel. Ice-divides were located along the highlands of central Ellesmere and Axel Heiberg islands, from which ice flowed east and west into Eureka Sound, with development of preferential flow along the axes of major fiords (Ó Cofaigh, Chapter 2, this volume). Raanes Peninsula supported a local ice-dome. Once in Eureka Sound, trunk ice flowed north towards Nansen Sound (*cf.* Fyles *in* Jenness 1965; Bell 1992; Bednarski 1998) and south towards Norwegian Bay (Ó Cofaigh, Chapter 2, this volume). Deglaciation of southern Eureka Sound commenced $\geq 9200 \pm 110$ BP [10150 (9940) 9690 cal BP⁵] and was characterised by initial break-up of ice in the channel with subsequent retreat east and west to the former ice-divides. Thus marine limit throughout the study area is time-transgressive and records sequential entry of the sea with ice retreat.

⁵ All ¹⁴C dates were calibrated using CALIB 3.0 (Stuiver and Reimer 1993). Calibrated dates are reported to 2 standard deviations.

4.4 METHODOLOGY

4.4.1 Surveying technique and definition of marine limit

The elevation of raised marine features above present sea level was determined in the field using a Wallace and Tiernan micro-altimeter (accuracy ± 2 m). Readings were corrected for fluctuations in atmospheric pressure and site specific temperature. High tide level was used as the reference datum for sea level. Radiocarbon dates on marine shells and driftwood provide chronological control on the establishment of marine limit and subsequent emergence.

Marine limit is the maximum elevation attained by the sea along a glacioisostatically depressed coastline. Its elevation at a site reflects both distance from the former edge of the ice sheet (which is a measure of the ice thickness over the site), date of deglaciation and eustatic sea level rise (Andrews 1970). Throughout the study area, marine limit was determined on the basis of the following criteria: (1) The highest raised marine delta or beach; (2) The lowest altitude of undisturbed till or felsenmeer (washing limits). Washing limits are commonly marked by a notch cut in the till with a well sorted sediment veneer below, or by an abrupt textural transition between poorly sorted till/felsenmeer, and well sorted washed sediment below; (3) The highest elevation at which well preserved marine shells were found. The latter provides a minimum estimate on marine limit.

4.5 MARINE LIMIT: ELEVATION AND PATTERN

The highest marine limit observed in the study area occurs on the north coast of Stor Island at $>145 - \leq 151$ m asl (Fig. 4.3). Marine limits of >140 m asl also occur along the south coast of Raanes Peninsula between Eureka Sound and Troid Fiord (Fig. 4.3). Fiords on southern Raanes Peninsula and northwestern Svendsen Peninsula (Blind Fiord, Troid Fiord, Starfish Bay, Jaeger Bay) all exhibit a progressive decline in marine limit from mouth to head. For example, in Troid Fiord, marine limit falls from 143 m asl at the mouth to 98 m asl at the head, whereas in Starfish and Jaeger bays marine limit decreases from 113 m and 106 m asl, respectively, to 80-92 m asl at the heads.

Along Eureka Sound, north of Hare Bay, marine limit is recorded by deltas at the mouths of several valleys. In inner Trapper's Cove, ice-contact deltas grade to relative sea levels at 118-120 m asl (Fig. 4.3). This contrasts with the outer cove and Eureka Sound coast,

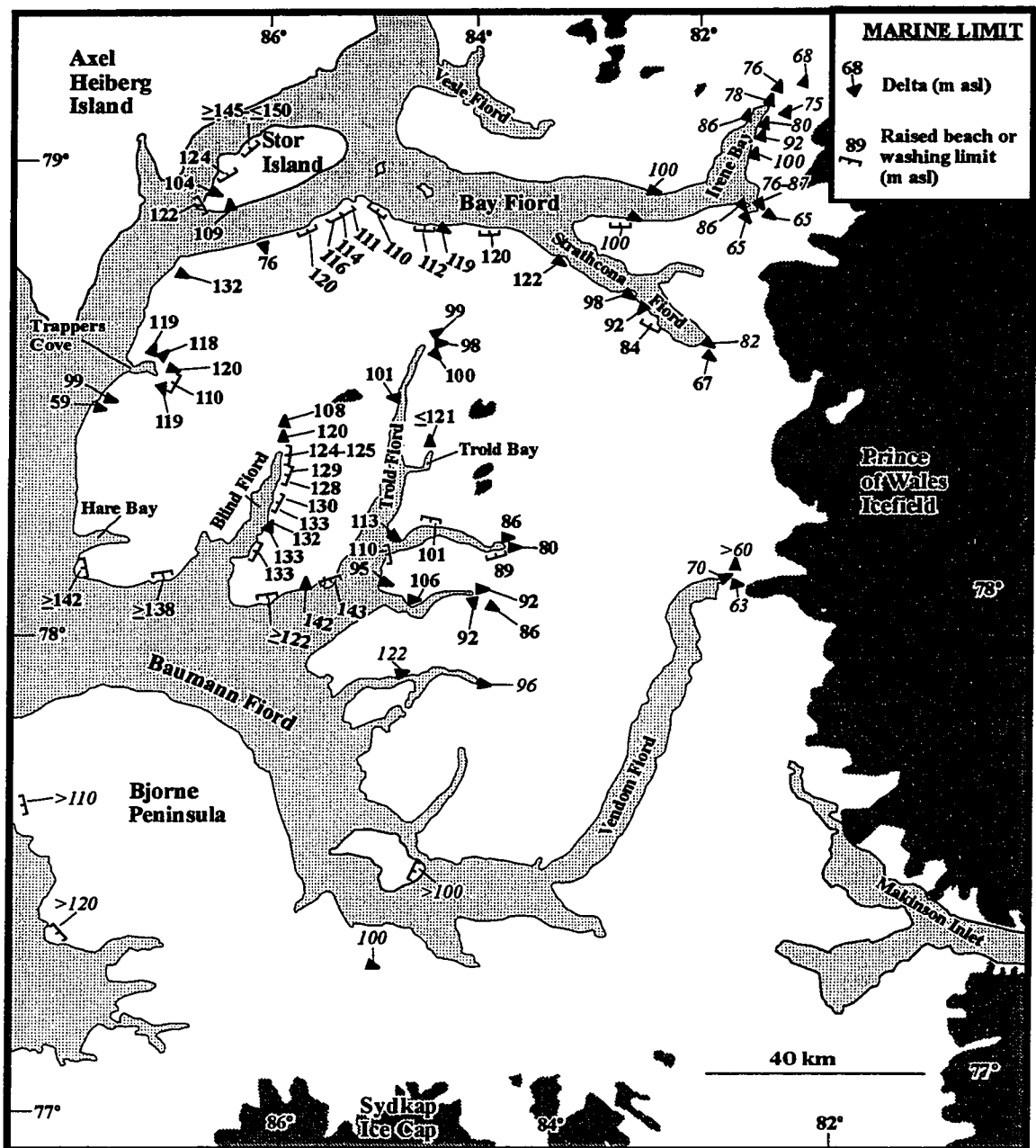


Figure 4.3: Marine limit elevations (m asl) marked by the uppermost delta, washing limit or raised beach, southern Eureka Sound. Italicised marine limit elevations are from Hodgson (1985).

where marine limit is defined by poorly-preserved raised beaches at 83 m asl (minimum), and deltas immediately to the south at 99 m asl (Fig. 4.3). The north coast of Raanes Peninsula along Eureka Sound and Bay Fiord is characterised by variable marine limit elevations which range from 76 to 120 m asl in Eureka Sound and central Bay Fiord respectively, before falling progressively to 65-87 m asl at the heads of Strathcona Fiord and Irene Bay (Fig. 4.3). Regionally therefore, marine limit exhibits an overall decrease in elevation eastwards from Eureka Sound to the fiord heads. However, this decrease is variable over short distances, a pattern inferred to reflect the metachronous age of marine limit occasioned by ice retreat.

4.6 RELATIVE SEA LEVEL CURVES

Emergence data from the study area are presented for three sites (Fig. 4.4). At each site, the elevation and age of radiocarbon dated samples and their associated relative sea levels are given. Figure 4.5 shows the relative sea level curves for the three sites. All radiocarbon dates (including calibrated ages, reported as "cal BP") are listed in Table C.1 (see Appendix C).

4.6.1 Blind Fiord

At the mouth of Blind Fiord, marine limit is defined by the uppermost raised beach at 138 m asl. A fragment of *Mya truncata* collected from a beach surface at 128 m asl provided an Accelerator Mass Spectrometry (AMS) date of 8590±70 BP [9460 (9330) 9060 cal BP](TO-5862; Site 1, Fig. 4.4 and Table C.1), and provides a minimum age estimate on the 138 m marine limit. In the central fiord marine limit falls to 133 m asl and two samples provide minimum dates on its formation. A surface fragment of *M. truncata* from a raised beach at 127 m asl dated 8510±80 BP [9400 (9220) 8970 cal BP](TO-5612; Site 2, Fig. 4.4 and Table C.1). Immediately up-fiord, whole valves and fragments of *Hiatella arctica* and *M. truncata* from a raised beach at 119 m asl dated 8550±80 BP [9420 (9250) 9000 cal BP](GSC-6047; Site 3, Fig. 4.4 and Table C.1). Both dates provide minimum age estimates for the 133 m asl marine limit. The standard errors of these three dates overlap and thus indicate rapid formation of marine limit through the outer and central fiord. The dates also indicate that at least 5 m of unloading occurred in <100 (¹⁴C and calendar years) years based on the samples relating to their respective marine limits (138 m and 133 m). If the samples are related to their

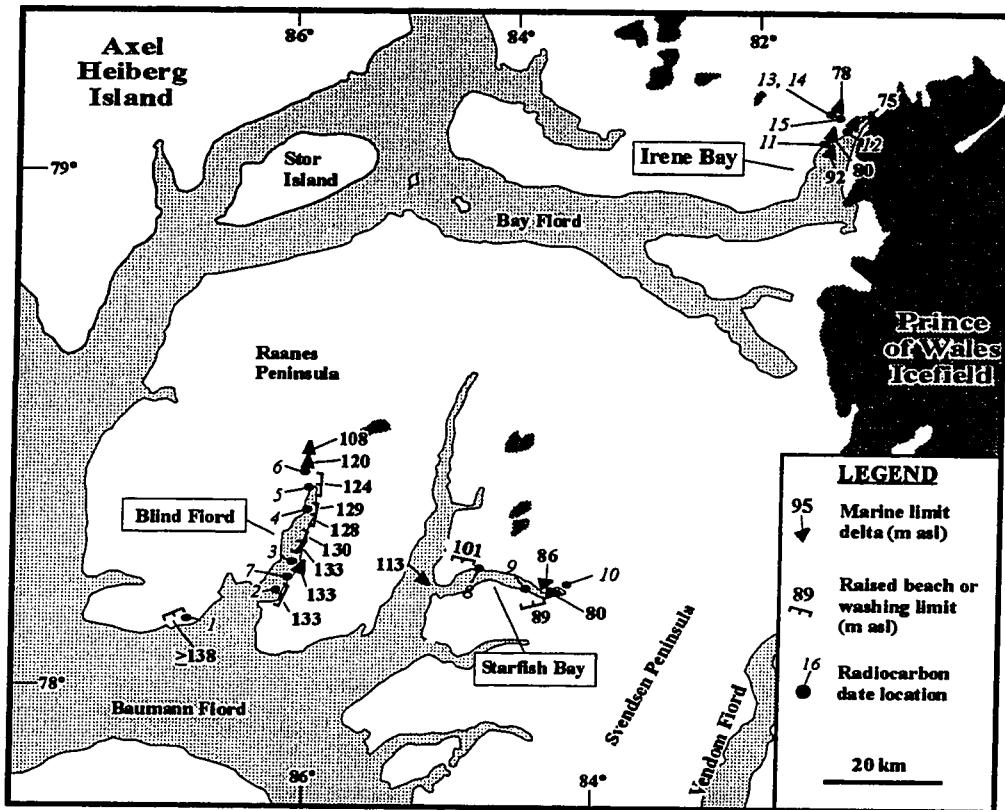


Figure 4.4: Marine limit landforms, elevations (m asl) and location of radiocarbon dates in Starfish Bay, Blind Fiord, and Irene Bay as discussed in text (Section 4.5). Corresponding site numbers of radiocarbon dates are listed in Table C.1.

(A) BLIND FIORD

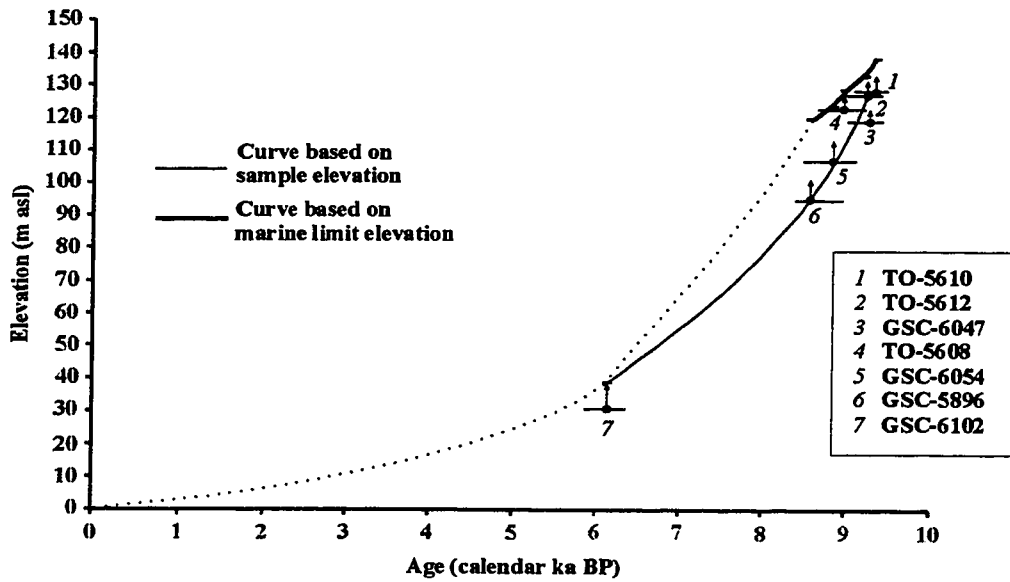
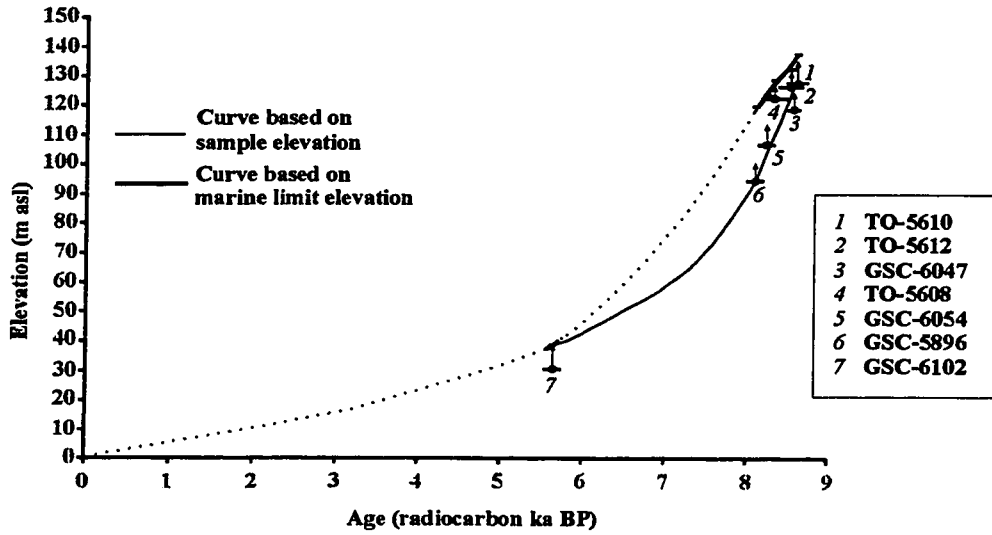


Figure 4.5: Emergence curves (radiocarbon and calendar years) from Ellesmere Island side of southern Eureka Sound. (A) Blind Fiord. (B) Starfish Bay (head). (C) Irene Bay. Dashed parts of curves are approximate. Site numbers of control points refer to Table C.1.

(B) STARFISH BAY (head)

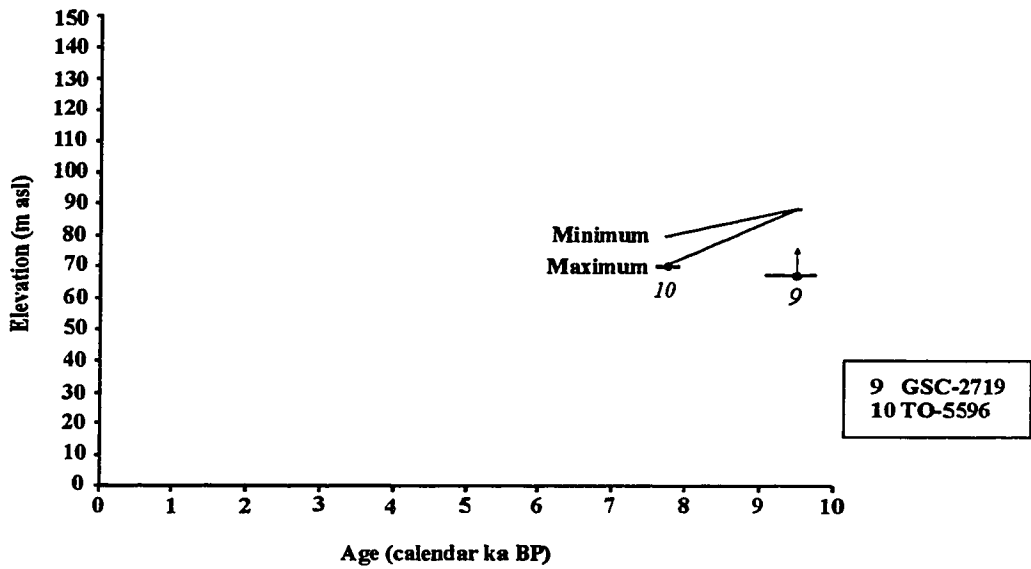
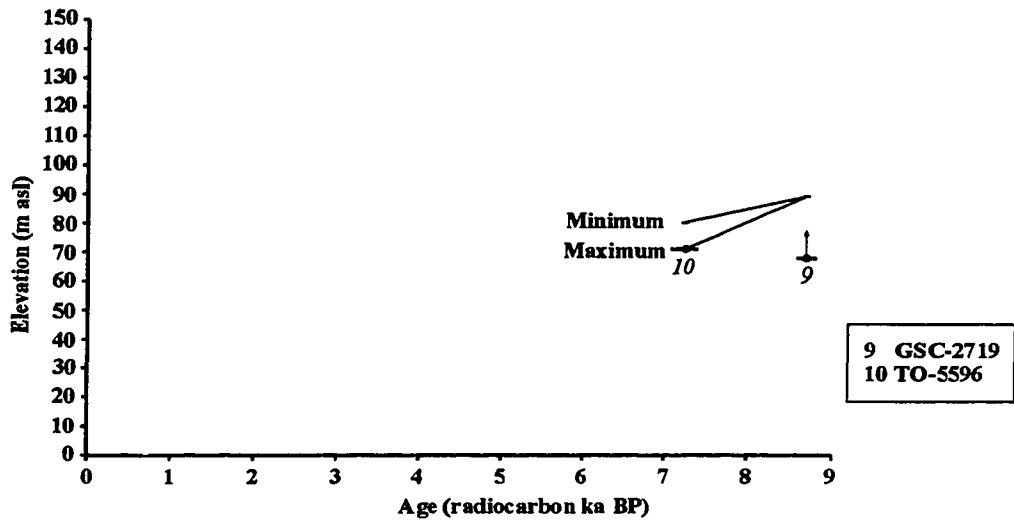


Figure 4.5 continued

(C) IRENE BAY

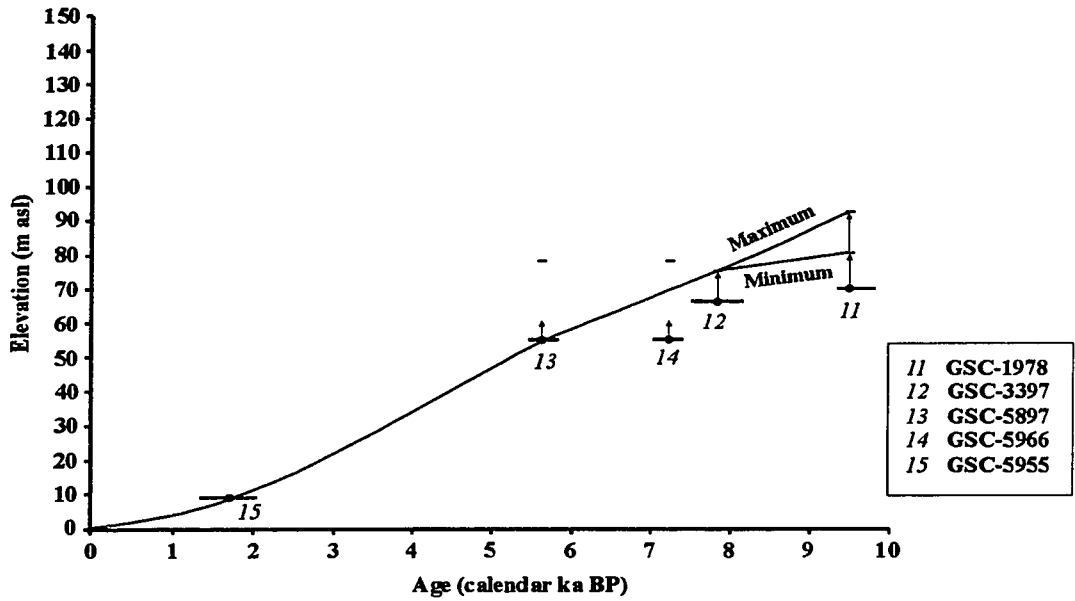
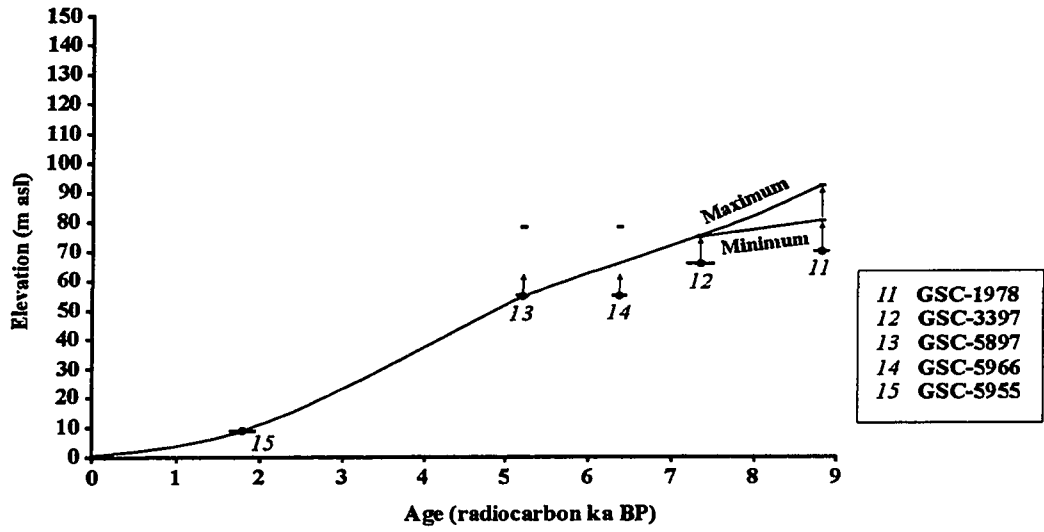


Figure 4.5: continued

elevations, then emergence could be as much as 9 m in <100 years (sample elevations at 128 and 119 m asl). Although both GSC-6047 and TO-5612 yielded similar ages for the 133 m marine limit in central Blind Fiord, the former is a bulk date, and thus likely contains a mixture of different aged shells. If this sample is excluded from the reconstruction and the emergence rate based on the two AMS dates (TO-5610 and TO-5612), initial emergence is still 5 m in <100 years.

Control on subsequent unloading in Blind Fiord is provided by four dates. In the inner fiord, marine limit is defined by a gravel berm at 129 m asl (Fig. 4.4). A surface fragment of *H. arctica* from a raised beach at 123 m asl dated 8310±80 BP [9210 (8950) 8630 cal BP](TO-5608; Site 4, Fig. 4.4 and Table C.1) and provides a minimum age estimate on the 129 m marine limit. North of the fiord head, whole valves and fragments of *H. arctica* and *M. truncata* from 107 m asl dated 8220±100 BP [9100 (8830) 8470 cal BP](GSC-6054; Site 5, Fig. 4.4 and Table C.1), which is also a minimum date on local marine limit at 124 m asl. Up-fiord of this site, a marine limit delta at 120 m asl occurs at the mouth of a lateral meltwater channel. Single valves and fragments dominated by *M. truncata* collected at 95 m asl on the delta foreslope gave a radiocarbon date of 8090±110 BP [8950 (8560) 8370 cal BP](GSC-5896; Site 6, Fig. 4.4 and Table C.1), which is a minimum age for the 120 m marine limit. Finally, paired valves of *Astarte borealis* and *H. arctica* from 31 m asl in silt immediately underlying a tributary delta at 39 m asl in the central fiord dated 5640±110 [6360 (6140) 5870 cal BP](GSC-6102; Site 7, Fig. 4.4 and Table C.1). It is important to note that although sites at the fiord head are separated from sites in the outer fiord by a distance of ~38 km, the fiord *parallels* the regional isobases at 8.5 ka BP (see Fig. 4.6 below), and hence differential postglacial rebound due to variations in ice thickness does not play a significant role at this site. The relative sea level curve for Blind Fiord (Fig. 4.5A) demonstrates continuous emergence from 8.6 ka BP to present. Initial emergence was rapid (5 m in <100 years).

4.6.2 Starfish Bay

Deglaciation of Starfish Bay followed the retreat of ice from outer Trold Fiord. At the mouth of the bay, ice-contact deltas occur at 113 m asl (Fig. 4.3) and mark a stillstand during retreat

of trunk ice. Marine limit drops to 101 m asl along the north shore of the bay where it is defined by a prominent washing limit. A surface sample consisting of whole valves of *H. arctica* and *M. truncata* collected from glaciomarine silt at 78 m asl dated 7740±90 BP [8410 (8230) 8000 cal BP](GSC-6037; Site 8, Fig. 4.4 and Table C.1). This represents a minimum age for deglaciation and establishment of marine limit.

Marine limit in the inner fiord is marked by a bench cut in till at 89 m asl (Fig. 4.4). At the fiord head, well-developed deltas fronted by extensive glaciomarine silt occur at 86 and 80 m asl (Fig. 4.4). These deposits mark a prominent stillstand of the trunk glacier during deglaciation. A sample of *P. arctica* collected from silt at 68 m asl, 3 km west of the fiord head, dated 8710±120 BP [9730 (9420) 9060 cal BP](GSC-2719; Site 9, Fig. 4.4 and Table C.1)(Hodgson 1985). Hodgson inferred that this date provided an approximate age for the fiord head deltas. However, because the sample site occurs 3 km west of the deltas, the validity of this inferred relationship is uncertain, and the date could alternatively relate to the 89 m bench along the inner fiord. A final sample consisting of a single valve of *H. arctica*, was collected from silt at 71 m asl east (inland) of these deltas. This dated 7240±80 BP [7910 (7730) 7570 cal BP](TO-5596; Site 10, Fig. 4.4, Table C.1) and provides a minimum age for deglaciation and formation of the fiord head deltas.

Therefore, at the fiord head between 8710±120 BP [9730 (9420) 9060 cal BP] and 7240±80 BP [7910 (7730) 7570 cal BP], sea level could have fallen by as little as 9 m, based on the assumption that the 8.7 ka BP (9.4 ka cal BP) date relates to the 89 m marine limit in the inner fiord, and the 7.2 ka BP (7.7 ka cal BP) date relates to a relative sea level at 80 m asl (Fig. 4.5B, “minimum”). This is equivalent to an emergence rate of only 0.5 m/century (based on the calibrated ages). If the 7.2 ka BP (7.7 ka cal BP) date is related to its sample elevation of 71 m asl, then emergence increases to 18 m (1 m/century)(Fig. 4.5B, “maximum”). Higher shorelines (>89 m asl) were not observed in the inner fiord or at the fiord head.

4.6.3 Irene Bay

Prominent marine limit deltas and thick raised marine silt record ice-marginal stabilisation and deposition at the fiord head during deglaciation. Hodgson (1985) reported several

radiocarbon dates from this site and these are discussed below. Ice-contact deltas on the south side of inner Irene Bay are graded to relative sea levels of 80 and 92 m asl (Figs. 4.3 and 4.4). Whole valves of *P. arctica* were collected at 70-74 m asl from glaciomarine rhythmites capped by the 80 m delta. This sample dated 8820±90 BP [9810 (9490) 9340 cal BP](GSC-1978; Site 11, Fig. 4.4 and Table C.1). Immediately east of this site, ice-contact deltas with thick pro-delta silt grade to 75 m asl. Whole valves of *H. arctica* and *M. truncata* from 66-70 m asl in this silt dated 7340±170 BP [8170 (7830) 7500 cal BP](GSC-3397; Site 12, Fig. 4.4 and Table C.1) and provide a minimum age for the 75 m delta. These ages indicate ~5 m of emergence between 8.8 ka BP (9.4 ka cal BP) and 7.3 ka BP (7.8 ka cal BP), equivalent to an emergence rate of only 0.3 m/century, based on the calibrated ages (Fig. 4.5C, "minimum"). If the standard errors of the dates are considered, the 8.8 ka BP (9.4 ka cal BP) date related to the 92 m delta (the highest marine limit in this part of the fiord) and the 7.3 ka BP (7.8 ka cal BP) date related to a sea level at 70 m asl (the sample elevation), this results in a maximum initial emergence rate of 2 m/century (Fig. 4.5C, "maximum").

Immediately up-fiord from the 8.8 ka BP site, a marine limit delta is graded to a former relative sea level at 78 m asl. A sample of paired valves of *A. borealis* and *H. arctica* collected by A. Podor from bedded sand on the delta foreslope at 55 m asl dated 5200±70 BP [5840 (5620) 5460 cal BP](GSC-5897; Site 13, Fig. 4.4 and Table C.1). This provides a minimum age estimate on delta formation. Thus sea level at 5.2 ka BP (5.6 ka cal BP) must have been at least as high as 55 m asl (Fig. 4.5D). This indicates that between 7.3 ka BP (7.8 ka cal BP) and 5.2 ka BP (5.6 ka cal BP) a *maximum* of 20 m of emergence occurred, equivalent to ~1 m/century based on the calibrated ages. A second sample consisting of a piece of driftwood was recovered from 55 m asl in a raised beach which off-laps the same delta. This dated 6360±100 BP [7400 (7230) 7010 cal BP](GSC-5966; Site 14, Fig. 4.4 and Table C.1). Given the presence of GSC-5897 from the same elevation and location which dated >1000 years younger, this driftwood date is considered to be a maximum age on the 55 m sea level.

A second driftwood sample recovered from 9 m asl in a raised beach at the fiord head dated 1790±160 [2050 (1710) 1340 cal BP](GSC-5955; Site 15, Fig. 4.4 and Table C.1). This sample is shown on Fig. 4C as relating to a relative sea level at its elevation, resulting

in a slight inflection in the lower part of the emergence curve. Alternatively, the date could relate to a relative sea level above the sample elevation (*i.e.*, the date is a maximum age for the 9 m sea level; cf. driftwood sample GSC-5966 above) in which case the inflection in the curve would be less pronounced.

4.7 POSTGLACIAL ISOBASES 8.5 KA BP

Regionally, across western Ellesmere and Axel Heiberg islands, many Holocene dates of 8500 ± 150 BP [9490 (9200) 8720 cal BP] are available. In southern Eureka Sound, more dates exist for this interval than any other, and hence it was selected for assessing differential emergence in the study area. These dates form the control points for the isobase reconstruction presented in Fig. 4.6 which integrates new shoreline and radiocarbon data from southern Eureka Sound with previously published information from northwestern Ellesmere Island (Bednarski 1995), northern Eureka Sound (England 1992; Bell 1996), western Axel Heiberg Island (Lemmen *et al.* 1994) and Norwegian Bay (Hodgson 1985; Hodgson in McNeely 1989; Dyke *in press* a and b). This isobase reconstruction (Fig. 4.6) will likely be refined with additional radiocarbon and relative sea level data, particularly from Norwegian Bay.

Isobases drawn on the 8.5 ka shoreline exhibit a westward and eastward rise towards Eureka Sound, and define a closed cell of highest emergence oriented crudely north/south along the axis of the channel. At its northern end, the ridge extends northeastwards into Greely Fiord with closure of the 120 m and 130 m isobases (cf. England 1992). The 8.5 ka shoreline falls to ≤ 110 m asl in central Hare Fiord (Fig. 4.6)(Bednarski 1995), and therefore the higher values must run to the south of this. At the southern end, the 130 m isobase extends at least as far south as the mouth of Blind Fiord/Bear Corner, and may extend further south onto Bjorne Peninsula and the entrance to Norwegian Bay. Further southwest, on the north coast of Grinnell Peninsula, Devon Island, the 8.5 ka shoreline is < 130 m asl (Dyke *in press* a and b). This demonstrates that the 130 m isobase closes to the northwest, and supports the above interpretation of closure in the vicinity of northern Bjorne Peninsula. It also indicates that the 120 m isobase either closes in Norwegian Bay in the vicinity of Graham and eastern Cornwall islands, or continues southwestwards onto Grinnell Peninsula.

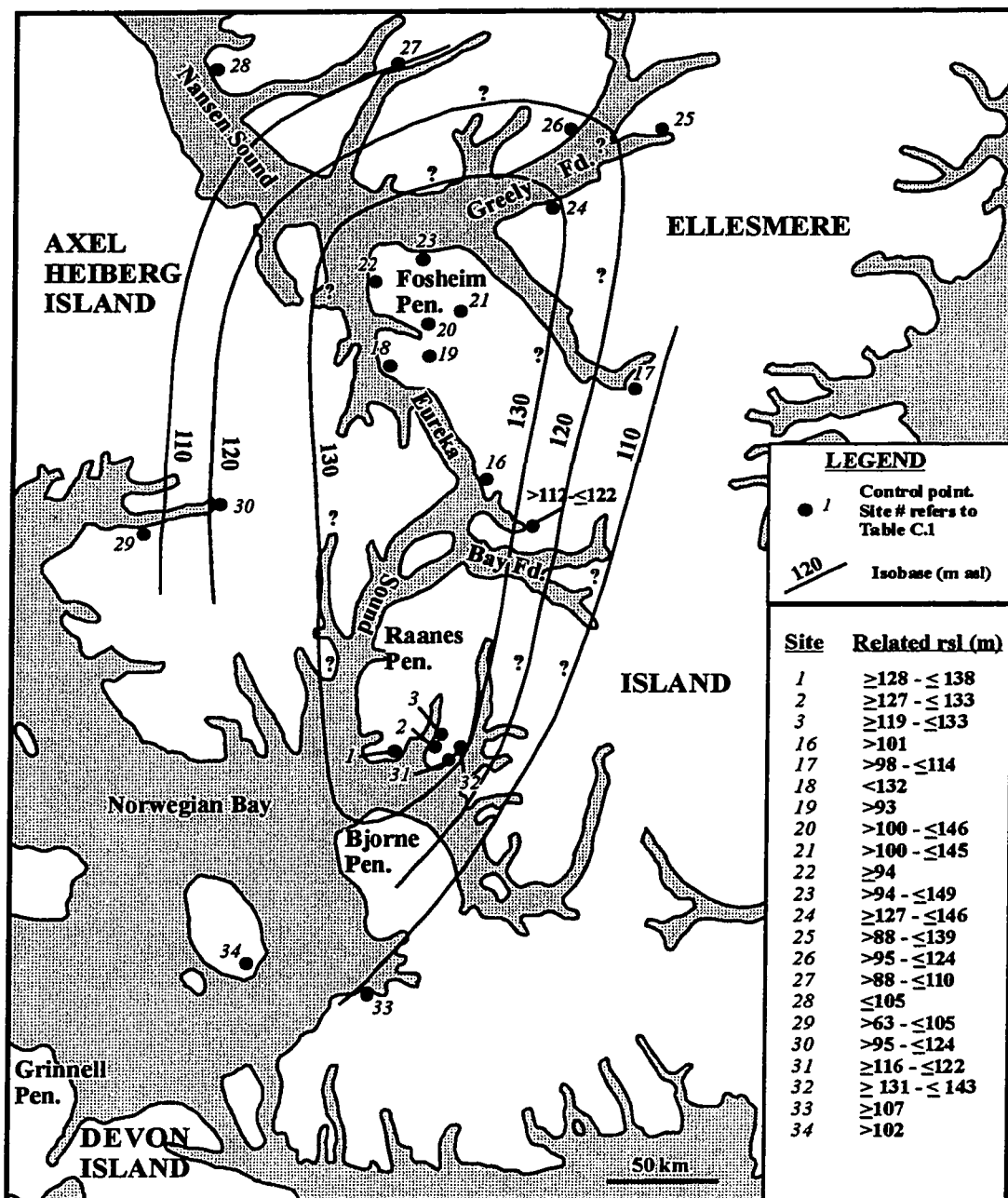


Figure 4.6: Postglacial isobases (provisional) drawn on the 8.5 ka BP shoreline in greater Eureka Sound. The reconstruction utilises radiocarbon dates from previous Quaternary studies in this region (Hodgson 1985; England 1992; Bednarski 1995, 1998; Bell 1996) and builds upon isobases drawn previously for northern Eureka Sound (England 1992, 1997; Bell 1996). Italicised site numbers refer to Table C.1. Control point without site numbers (" ≥ 112 m - ≤ 122 m") is based on a personal communication from J. England (1998).

Currently, this cannot be resolved given the lack of emergence data from much of Norwegian Bay, and hence the 120 and 110 m isobases are left open to the south.

4.8 DISCUSSION

4.8.1 Initial postglacial emergence

Marked contrasts in initial postglacial emergence are recorded in the study area. In Blind Fiord, initial unloading was rapid and characterised by rates of ≥ 5 m/century (cf. Blake 1975, 1992a; Lemmen *et al.* 1994). At this site, relative sea level exhibits a continuous fall since deglaciation and marine limit formation (cf. Type A curve of Quinlan and Beaumont 1981, and Zone 1 of Clark *et al.* 1978). The emergence history is thus broadly similar to that from other areas of eastern Arctic Canada formerly covered by the *Laurentide Ice Sheet*. Postglacial rebound in such areas typically exhibits continuous emergence since deglaciation with initial unloading of 7-30 m/century gradually decreasing to present (Andrews 1970; Dyke 1984, 1993, Dyke *et al.* 1991). The relative sea level history of Blind Fiord is therefore compatible with glacial geological evidence which indicates an extensive late Wisconsinan glaciation in southern Eureka Sound (Ó Cofaigh Chapters 2 and 3, this volume).

However, the Blind Fiord curve contrasts with those from Irene and Starfish bays, where initial emergence rates of ≤ 1 m/century are recorded. It is important to note that the timing of initial emergence at all three sites is similar. Slow initial emergence in Irene and Starfish bays commenced at 8.8 and 8.7 ka BP respectively (~ 9.4 ka cal BP), and extended to at least 7.3 ka BP (7.8 ka cal BP) and 7.2 ka BP (7.7 ka cal BP). However, in Blind Fiord, emergence during this *same* interval (~ 8.6 -8.0 ka BP; 9.3-8.5 ka cal BP) was characterised by rates of ≥ 5 m/century.

Sea level curves similar to those from Irene and Starfish bays have been presented for several other areas on Ellesmere Island (England 1983, 1992, 1997). For example, in Greely Fiord, England (1992) documented a period of relative sea level stability at marine limit from 8.8 to 7.8 ka (^{14}C) BP, after which emergence proceeded slowly (2 m/century) until 7.2 ka BP when it increased to 13 m/century. He attributed this arrest in sea level after marine limit formation to a balance between glacioisostatic unloading and eustatic sea level rise. The lack of initial rapid unloading at these sites was considered to be compatible with a limited late

Wisconsinan glacial cover as inferred from independent glacial geologic evidence (England 1978; 1990, 1996).

Emergence curves showing a period of relative sea level stability at marine limit have also been presented from the area of the former *Barents Sea Ice Sheet* (Forman 1990, Forman *et al.* 1996, 1997), and this stability is also attributed to a balance between glacioisostasy and eustasy. These sites are inferred to have sustained a thinner glacial load than at the former ice sheet centre over the northern and western Barents Sea where Type A (Quinlan and Beaumont 1981) sea level curves are reported (see Forman 1990). It should be noted, however, that ice thicknesses over the sites which exhibit slow initial unloading may have been on the order of ≤ 1500 m (Forman *et al.* 1995, 1996).

Thus the slow initial emergence recorded in Irene and Starfish bays may not necessarily be incompatible with an extensive ice cover over these sites during the late Wisconsinan. Minimum estimates of ice thickness in southern Eureka Sound based on glacial geological evidence are ~ 1200 m (Ó Cofaigh Chapter 2, this volume), and maximum estimates obtained from glaciological modelling are 1500 m or 2000 m (Reeh 1984). The three emergence curves would therefore imply marked spatial variations in the form and rate of initial emergence between sites in close proximity; Blind Fiord and inner Starfish Bay are < 45 km apart. Slow initial emergence at the fiord heads of Irene and Starfish bays might therefore reflect a major ice-marginal stillstand during retreat, as marked by the "drift belt" (Hodgson 1985; Ó Cofaigh Chapter 3, this volume), which locally restrained rebound at both fiord heads.

However, such marked variations in initial emergence may be problematic due to the proximity in timing of deglaciation and marine limit formation between the three sites, which would presumably have resulted in integration of the associated unloading over a wide area (Walcott 1970; Andrews 1970). Given the inter-site similarities in the timing of deglaciation and onset of unloading, the slow emergence documented by the Irene and Starfish bay curves cannot be explained as representing the later part of the local emergence history following an earlier phase of rapid unloading.

Obviously, the legitimacy of slow initial emergence in Starfish and Irene bays is dependent upon the validity of two fiord head dates of 8.8 and 8.7 ka BP on *P. arctica* which

are associated with relative sea levels of 80-92 m asl. This reconstruction would be invalid if the samples relate to higher relative sea levels not observed in the field, or if the true ages of the original samples were actually younger than the reported ages. No evidence was found at either fiord head for higher shorelines above the surveyed marine limit which is well defined by raised deltas and wave-cut benches. With respect to the latter point, Forman and Polyak (1997) have demonstrated from radiocarbon dating of pre-bomb *P. arctica* that this species can have marine reservoir values as high as 764 years, possibly reflecting either incorporation of old carbon from the surrounding deposits and porewater, or from freshwater inputs by streams or glacial meltwater. Currently the reservoir effect of *P. arctica* in Eureka Sound is unknown. However, a variable reservoir effect for this genus, possibly as high as 700-800 years, could imply that some dates on this species may be too old. Resolution of this issue through analysis of pre-bomb *P. arctica* from the Canadian High Arctic and comparison of their ages with other shell species is currently in progress (J. England *personal communication* 1998).

4.8.2 Postglacial Isobases

Isobases drawn on the 8.5 ka shoreline demonstrate an elongate ridge of emergence, oriented crudely parallel with the axis of Eureka Sound, extending from Greely Fiord in the north to the entrance to Norwegian Bay in the south. This extends previous reconstructions of postglacial shoreline delevelling in the region (Blake 1970; England 1976b, 1992, 1997; Bell 1996), and is significant in that it demonstrates: (a) that the highest emergence values form a cell over the length of Eureka Sound; and (b) that this highest cell does not appear to extend southwestwards across Norwegian Bay to Grinnell Peninsula on Devon Island (cf. Blake 1970), but rather closes in the vicinity of the entrance to Norwegian Bay.

Along the Eureka Sound/Nansen Sound fiord system, glacial geologic and chronologic evidence indicates extensive late Wisconsinan glaciation, which inundated fiords and inter-island channels (Ó Cofaigh Chapter 2, this volume; Bednarski 1998). A similar reconstruction, advocating extensive ice during the Last Glacial Maximum, has also recently been presented for Devon Island and Norwegian Bay (Hättestrand and Stroeven 1996; Dyke *in press* a and b). This glacial geological evidence negates an explanation of this isobase pattern in terms of

overlapping peripheral depressions from separate ice masses on Ellesmere and Axel Heiberg islands. The pattern of shoreline delevelling recorded by the isobases is inferred to be the result of a glacioisostatic response to the unloading which accompanied early Holocene deglaciation (cf. Blake 1970; England and Ó Cofaigh 1998). This supports earlier reconstructions of maximum late Wisconsinan loading along Eureka Sound/Nansen Sound (e.g., Blake 1970; Walcott 1972).

Modelling of an *Innuitian Ice Sheet* over the Canadian High Arctic during the Last Glacial Maximum (Reeh 1984) results in *maximum* ice thicknesses of 1500 and 2000 m being located *west* of the main ice-divide, in the vicinity of Fosheim Peninsula/Eureka Sound. In contrast, ice at the modelled main ice-divide, which is located along the highland rim of eastern Ellesmere Island, is $\sim \geq 700 - \leq 1000$ m thick (Reeh 1984)(current thickness $\sim 500-800$ m, Koerner 1989). Koerner *et al.* (1987) also propose that the ice divide over the Agassiz Ice Cap during the Wisconsinan was only 200 m thicker than today. Glacial geological data from Eureka Sound indicate a *minimum* ice thickness of ~ 1200 m in the channel during the Last Glacial Maximum (Ó Cofaigh Chapter 2, this volume). This suggests that the 8.5 ka BP isobase pattern which shows maximum unloading along Eureka Sound reflects the thickest ice load being located there during the Last Glacial Maximum (cf. Blake 1970). Closure of the highest values to the southwest points to the presence of a saddle connecting the Eureka Sound loading centre to that proposed in the western part of Norwegian Bay (Hättestrand and Stroeven 1996; Dyke *in press* a and b).

4.9 REFERENCES

- Andrews, J.T. (1970). *A geomorphic study of postglacial uplift with particular reference to Arctic Canada*. Institute of British Geographers, London, England, Special Publication No. 2, 156p.
- Bednarski, J. (1995). Glacial advances and stratigraphy in Otto Fiord and adjacent areas, Ellesmere Island, Northwest Territories. *Canadian Journal of Earth Sciences*, **32**, 52-64.
- Bednarski, J. (1998). Quaternary history of Axel Heiberg Island bordering Nansen Sound, Northwest Territories, emphasising the last glacial maximum. *Canadian Journal of Earth Sciences*, **35**, 520-533.
- Bell, T. (1992). *Glacial and sea level history of western Fosheim Peninsula, Ellesmere Island, Arctic Canada*. Unpublished PhD thesis, University of Alberta, Edmonton, 172pp.
- Bell, T. (1996). Late Quaternary glacial and sea level history of Fosheim Peninsula, Ellesmere Island, Canadian High Arctic. *Canadian Journal of Earth Sciences*, **33**, 1075-1086.
- Blake, W.R., Jr. (1970). Studies of glacial history in arctic Canada. I. Pumice, radiocarbon dates, and differential postglacial uplift in the eastern Queen Elizabeth Islands. *Canadian Journal of Earth Sciences*, **7**, 634-664.
- Blake, W.R., Jr. (1975). Radiocarbon age determinations and postglacial emergence at Cape Storm, southern Ellesmere Island, Arctic Canada. *Geografiska Annaler*, **57A**, 1-71.
- Blake, W.R., Jr. (1992a). Holocene emergence at Cape Herschel, east central Ellesmere Island, Arctic Canada: implications for ice sheet configuration. *Canadian Journal of Earth Sciences*, **29**, 1958-1980.
- Blake, W.R., Jr. (1992b). Shell-bearing till along Smith Sound, Ellesmere Island - Greenland: age and significance. *Sverigies Geologiska Undersökning*, **81**, 51-58.
- Blake, W.R., Jr. (1993). Holocene emergence along the Ellesmere Island coasts of northernmost Baffin Bay. *Norsk Geologisk Tidsskrift*, **73**, 147-160.
- Blake, W.R., Jr., Boucherle, M.M., Fredskild, B., Janssens, J.A. and Smol, J.P. (1992). The geomorphological setting, glacial history and Holocene development of "Kap

- Inglefield Sø" North-West Greenland. *Meddelelser om Grønland, Geoscience*, **27**, 41p.
- Clark, J.A., Farrell, W.E. and Peltier, W.R. (1978). Global changes in postglacial sea level: a numerical calculation. *Quaternary Research*, **9**, 265-287.
- De Freitas, T.A. (1990). Implications of glacial striae on Hans Island, between Greenland and Ellesmere Island (Nares Strait). *Journal of Glaciology*, **36**, 129-130.
- Dyck, W., Fyles, J.G. and Blake, W., Jr. (1965). Geological Survey of Canada radiocarbon dates IV. *Radiocarbon*, **7**, 24-46.
- Dyke, A.S. (1983). *Quaternary Geology of Somerset Island, District of Franklin*. Geological Survey of Canada, Memoir 403, 32p.
- Dyke, A.S. (1984). *Quaternary geology of Boothia Peninsula and northern District of Keewatin, central Canadian Arctic*. Geological Survey of Canada, Memoir 407, 26p.
- Dyke, A. S. (*in press a*). The last glacial maximum and deglaciation of Devon Island: Support for an Innuitian Ice Sheet. *Quaternary Science Reviews*.
- Dyke, A. S. (*in press b*). Holocene delevelling of Devon Island, Arctic Canada: implications for ice sheet geometry and crustal response. *Canadian Journal of Earth Sciences*.
- Dyke, A.S., Morris, T.F. and Green, D.E.C. (1991). *Postglacial tectonic and sea level history of the central Canadian Arctic*. Geological Survey of Canada, Bulletin 397, 56p.
- England, J. (1976a). Late Quaternary glaciation of the eastern Queen Elizabeth Islands, Northwest Territories, Canada: alternative models. *Quaternary Research*, **6**, 185-202.
- England, J. (1976b). Postglacial isobases and uplift curves from the Canadian and Greenland High Arctic. *Arctic and Alpine Research*, **8**, 61-78.
- England, J. (1978). The glacial geology of northeastern Ellesmere Island, NWT, Canada. *Canadian Journal of Earth Sciences*, **15**, 603-617.
- England, J. (1983). Isostatic adjustments in a full glacial sea. *Canadian Journal of Earth Sciences*, **20**, 895-917.
- England, J. (1987). Glaciation and the evolution of the Canadian high arctic landscape. *Geology*, **15**, 419-424.

- England, J. (1990). The late Quaternary history of Greely Fiord and its tributaries, west-central Ellesmere Island. *Canadian Journal of Earth Sciences*, **27**, 255-270.
- England, J. (1992). Postglacial emergence in the Canadian High Arctic: integrating glacioisostasy, eustasy and late deglaciation. *Canadian Journal of Earth Sciences*, **29**, 984-999.
- England, J. (1996). Glacier dynamics and paleoclimatic change during the last glaciation of eastern Ellesmere Island, Canada. *Canadian Journal of Earth Sciences*, **33**, 779-799.
- England, J. (1997). Unusual rates and patterns of Holocene emergence, Ellesmere Island, Arctic Canada. *Journal of the Geological Society*, London, **154**, 781-792.
- England, J. (1998). Support for the Innuitian Ice Sheet in the Canadian High Arctic during the Last Glacial Maximum. *Journal of Quaternary Science*.
- England, J. (*In press*). Coalescent Greenland and Innuitian Ice during the Last Glacial Maximum: revising the Quaternary of the Canadian High Arctic. *Quaternary Science Reviews*.
- England, J. and Ó Cofaigh, C. (1998). Deglacial sea level along Eureka Sound: the effects of ice retreat from a central basin to alpine margins. *Geological Association of Canada and Mineralogical Association of Canada Annual Meeting, abstract volume*, Quebec City, A-52.
- England, J., Sharp, M.J., Lemmen, D.S. and Bednarski, J. (1991). On the extent and thickness of the Innuitian Ice Sheet: a postglacial-adjustment approach: Discussion. *Canadian Journal of Earth Sciences*, **28**, 1689-1695.
- Forman, S.L. (1990). Postglacial relative sea-level history of northwestern Spitsbergen, Svalbard. *Bulletin of the Geological Society of America*, **102**, 1580-1590.
- Forman, S.L., and Polyak, L. (1997). Radiocarbon content of pre-bomb marine mollusks and variations in the ¹⁴C reservoir age for coastal areas of the Barents and Kara seas, Russia. *Geophysical Research Letters*, **24**, 885-888.
- Forman, S.L., Lubinski, D., Miller, G.H., Snyder, J., Matishov, G., Korsun, S., and Myslivets, V. (1995). Postglacial emergence and distribution of late Weichselian ice-loads in the northern Barents and Kara seas. *Geology*, **23**, 113-116.

- Forman, S.L., Lubinski, D., Miller, G.H., Matishov, G.G., Korsun, S., Snyder, J., Herlihy, F., Weihe, R., and Myslivets, V. (1996). Postglacial emergence of western Franz Josef Land, Russia, and retreat of the Barents Sea Ice Sheet. *Quaternary Science Reviews*, **15**, 77-90.
- Forman, S.L., Weihe, R., Lubinski, D., Tarasov, G., Korsun, S., and Matishov, G. (1997). Holocene relative sea-level history of Franz Josef Land, Russia. *Bulletin of the Geological Society of America*, **109**, 1116-1133.
- Funder, S. and Hansen, L. (1996). The Greenland ice sheet - a model for its culmination and decay during and after the last glacial maximum. *Bulletin of the Geological Society of Denmark*, **42**, 137-152.
- Fyles, J.G. (1962). In: Jenness, S.E. (ed.), *Field Work, 1961; Geological Survey of Canada Information Circular No.5*, 4-6.
- Hättestrand C. and Stroeven, A.P. (1996). Field evidence for wet-based ice-sheet erosion from the south-central Queen Elizabeth Islands, Northwest Territories, Canada. *Arctic and Alpine Research*, **28**, 466-474.
- Hodgson, D.A. (1985). The last glaciation of west-central Ellesmere island, Arctic Canada. *Canadian Journal of Earth Sciences*, **22**, 347-368.
- Hodgson, D.A., St-Onge, D.A. and Edlund, S.A. (1991). Surficial materials of Hot Weather Creek basin, Ellesmere Island, Northwest Territories. In: *Current Research, Part E, Geological Survey of Canada Paper 91-1E*, 157-163.
- Koerner, F.M., Fisher, D.A. and Patterson, W.S.B. (1987). Wisconsinan and pre-Wisconsinan ice thickness on Ellesmere Island, Canada: inferences from ice cores. *Canadian Journal of Earth Sciences*, **24**, 296-301.
- Lemmen, D.S. (1989). The last glaciation of Marvin Peninsula, northern Ellesmere Island, High Arctic, Canada. *Canadian Journal of Earth Sciences*, **26**, 2578-2590.
- Lemmen, D.S., Aitken, A.E. and Gilbert, R. (1994). Early Holocene deglaciation of Expedition and Strand fiords, Canadian High Arctic. *Canadian Journal of Earth Sciences*, **31**, 943-958.
- McNeely, R. (1989). *Geological Survey of Canada Radiocarbon Dates XXVIII*. Geological Survey of Canada Paper 88-7, 93p.

- Quinlan, G. and Beaumont, C. (1981). A comparison of observed and theoretical postglacial relative sea level in Atlantic Canada. *Canadian Journal of Earth Sciences*, **18**, 1146-1163.
- Reeh, N. (1984). Reconstruction of the glacial ice covers and Greenland by three-dimensional, perfectly plastic ice-sheet modelling. *Annals of Glaciology*, **5**, 115-121.
- Stuiver, M. and Reimer, P.J. (1993). Extended ^{14}C data base and revised CALIB 3.0 ^{14}C age calibration program. *Radiocarbon*, **35**, 215-230.
- Trettin, H. P. (1991). *Geology of the Inuitian Orogen and Arctic Platform of Canada and Greenland*. Geological Survey of Canada, Geology of Canada, No.3, 569p.
- Tushingham, A. M. (1991). On the extent and thickness of the Inuitian Ice-Sheet: a postglacial-adjustment approach. *Canadian Journal of Earth Sciences*, **28**, 231-239.
- Walcott, R.I. (1970). Isostatic response to loading of the crust in Canada. *Canadian Journal of Earth Sciences*, **7**, 716-727.
- Walcott, R.I. (1972). Late Quaternary vertical movements in eastern North America: quantitative evidence of glacio-isostatic rebound. *Reviews of Geophysics and Space Physics*, **10**, 849-884.

CHAPTER FIVE

Conclusions

The subject of this thesis is the reconstruction of high latitude Quaternary glaciation and postglacial relative sea level change. Its geographic focus on southern Eureka Sound, High Arctic Canada, was driven by the potential of this largely unstudied area for linking the glacial and sea level records of the alpine sector of the Queen Elizabeth Islands with that of the central and western Arctic Archipelago. Briefly reiterated, the objectives of this research were:

- (1) to reconstruct the configuration and dynamics of late Wisconsinan glaciation in southern Eureka Sound.
- (2) to investigate whether evidence is preserved in the study area for (a) pre-late Wisconsinan glaciations (cf. Lemmen and England 1992; Bednarski 1995), and (b) a “full glacial sea” (England 1983, 1992).
- (3) to determine the principal controls on early Holocene deglacial sedimentation and ice dynamics in High Arctic fiords from glacial geomorphological and sedimentological studies.
- (4) to determine the magnitude and chronology of postglacial emergence throughout southern Eureka Sound, reconstruct the pattern of early Holocene shoreline delevelling, and link this reconstruction to published data from the north and south to obtain a comprehensive picture of differential unloading for greater Eureka Sound.

5.1 LATE WISCONSINAN GLACIATION OF SOUTHERN EUREKA SOUND

During the late Wisconsinan, southern Eureka Sound supported extensive regional glaciation. Ice-divides were located along the highlands of Ellesmere and Axel Heiberg islands from which ice-flow converged on Eureka Sound. Westerly ice-flow across Ellesmere Island is recorded by two granite dispersal trains resting on striated and ice-moulded carbonate bedrock, one centred along the axis of Bay Fiord, and the second extending across northern Svendsen and southern Raanes peninsulas. The intervening area on Raanes Peninsula was

covered by a local ice-mass, which was coalescent with the regional granite-carrying ice. Along Eureka Sound, ice emanating from Bay Fiord bifurcated, flowing north towards Nansen Sound (Fyles in Jeness 1962; Bell 1992) and south towards Norwegian Bay. Granite erratics on the Ringnes islands may record the extension of granite-carrying Ellesmere Island ice across Norwegian Bay and into the western Arctic Archipelago.

Marine limit, which is superimposed onto the dispersal trains in the form of raised deltas and beaches, dates early Holocene. It is noteworthy that logged stratigraphic exposures never show more than one basal till in section, and this is typically overlain by early Holocene deglacial sediments. This implies that the ice responsible for deposition of granite erratics in the study area retreated during the early Holocene, and therefore that southern Eureka Sound was inundated by late Wisconsinan glaciation. There is no litho- or morphostratigraphic evidence to ascribe deposition of the dispersal trains, or parts thereof, to different glaciations, or to indicate that they were deposited at different times. Several surface exposure dates obtained on samples of erratics and bedrock collected during this study also support a late Wisconsinan age. A single AMS date of 27.3 ka BP, obtained from glaciofluvial outwash in Bay Fiord, provides a maximum age for the onset of the last ice advance in this area.

This date, in conjunction with data from Bednarski (1998), indicates that the onset of the Last Glacial Maximum in Eureka and Nansen sounds occurred sometime after 28-27 ka BP, and perhaps even as late as <20 ka BP (Blake 1992a). The reconstruction advocated here for extensive late Wisconsinan glaciation in southern Eureka Sound on the basis of glacial geological and chronological evidence and associated postglacial emergence of up to ~150 m asl, most closely approximates the *Inuitian Ice Sheet* model of Blake (1970).

Early Holocene deglaciation in southern Eureka Sound commenced $\geq 9200 \pm 110$ BP [10150 (9940) 9690 cal BP] and was characterised by a two-step retreat pattern. Initial break-up and radial retreat of ice in the larger fiords and inter-island channels may have been driven by the combined effects of eustatic sea level rise >9.2 ka BP coupled to an abrupt increase in early Holocene temperature (Fairbanks 1989; Alley *et al.* 1993; Blanchon and Shaw 1995; Lowe and Walker 1997). In several fiords this initial phase of retreat was rapid (Ó Cofaigh Chapter 3, this volume). Regionally, evidence for an initial phase of rapid deglaciation has also been reported from western Axel Heiberg Island (Lemmen *et al.* 1994) and Nansen

Sound (Bednarski 1998). This initial retreat phase terminated when ice margins stabilised on-land forming the "drift belt" (Hodgson 1985), and was succeeded by subsequent slower retreat. Terrestrial stabilisation lasted (locally) until 7180 ± 65 BP [7840 (7660) 7530 cal BP]. Two-step deglaciation is expressed by prominent contrasts in glacial geomorphology between the inner and outer parts of many fiords on western Ellesmere and Axel Heiberg islands (Hodgson 1985; England 1987, 1990; Lemmen *et al.* 1994; Ó Cofaigh Chapter 3, this volume; England *in press*).

Definitive stratigraphic evidence for pre-late Wisconsinan glaciation in southern Eureka Sound was not found. Bedded gravel and sand containing paired bivalves with radiocarbon ages of 46 and 47 ka BP on Stor Island may record deposition by pre-late Wisconsinan ice on the island, but as till is absent from the associated stratigraphic sequence, a glaciogenic interpretation for the sediments is equivocal. No chronologic or stratigraphic evidence in support of a full glacial sea was found in the study area.

The reconstruction advocated here for an extensive late Wisconsinan glaciation in southern Eureka Sound, in conjunction with evidence for a similar extensive Last Glacial Maximum in Nansen Sound to the north (Bednarski 1998), implies that glacial landforms and sediments assigned to pre-late Wisconsinan glaciations along northern Eureka Sound (Bell 1992) also date from the late Wisconsinan. The presence of shelly till along the length of the sound demonstrates that the channel existed prior to the first till-depositing glaciation in the region. Bathymetric evidence from the floor of the channel and on-shore glacial geomorphic evidence (*e.g.*, striae, plucked bedrock) demonstrates erosional modification during glacial inundation of Eureka Sound. Late Pliocene deposits with *in-situ* marine macrofauna from Hvitland Peninsula, Nansen Sound (Fyles *et al.* 1998) indicates that the Eureka Sound/Nansen Sound fiord system is at least that old.

5.2 CONTROLS ON EARLY HOLOCENE DEGLACIAL SEDIMENTATION AND ICE DYNAMICS

Glacial geomorphological and sedimentological studies in two adjacent fiords (Starfish Bay and Blind Fiord) on southwestern Ellesmere Island demonstrate that early Holocene deglaciation was characterised by a two-step retreat pattern, where rapid recession of trunk

glaciers, probably driven by eustatic sea level rise and abrupt early Holocene warming, preceded terrestrial stabilisation and deposition. The location of early Holocene deglacial depocentres was predominantly controlled by *fiord bathymetry*, specifically the presence or absence of pinning points. Pinning points facilitated glacier stabilisation, and therefore fiord heads, and the narrow and shallow inner parts of fiords were especially favourable depocentre locations. Two-step retreat resulted in a landscape zonation in which a well-defined belt of glaciogenic landforms in inner fiords records topographically-controlled terrestrial stabilisation, and contrasts with outer fiords where a common absence of pinning points allowed rapid glacier retreat, predominantly by calving, which precluded extensive deglacial sedimentation in these areas.

Although the location of deglacial landform/sediment assemblages and associated radiocarbon dates in both fiords record two-step deglaciation, marked differences in glacial geomorphology and sedimentology indicate that the retreating trunk glaciers were characterised by different *basal thermal regimes*. In Starfish Bay, abundant fine-grained subaquatic outwash indicates the presence of a well-developed subglacial drainage system and a predominantly warm-based thermal regime. In contrast, in Blind Fiord, the dominance of lateral meltwater channels and lack of fine-grained subaquatic outwash indicate that trunk ice was predominantly cold-based during retreat. Collectively these observations demonstrate that early Holocene deglaciation in High Arctic fiords was characterised by significant variations in basal thermal regime which controlled the nature of associated glacial landform/sediment assemblages, the location of which was intimately related to local variations in fiord bathymetry.

This contrast in basal thermal regime is proposed to reflect the thickness and areal extent of the two glaciers' accumulation areas. Directional ice-flow indicators show that Blind Fiord was fed by locally-nourished ice on Raanes Peninsula, while Starfish Bay was fed by regional flow from an expanded Prince of Wales Icefield. It is possible that this latter source was thicker and more extensive than that on Raanes Peninsula. Convergent flow from an extensive, thick icefield would have resulted in increased internal deformation and strain heating, particularly where fiords were narrow. This would have promoted frictional heating and sliding, and facilitated development of warm-based conditions. In Blind Fiord, rapid

retreat by calving may have resulted in increased extensional flow with overall thinning of the trunk glacier, particularly in the lower part of the ablation zone, and would have facilitated down-glacier advection of cold ice to glacier margins. Thinning of the glacier would also reduce insulation of the bed from colder surface temperatures.

5.3 POSTGLACIAL EMERGENCE OF SOUTHERN EUREKA SOUND

Postglacial emergence of 140-150 m asl is recorded along southern Eureka Sound by raised marine deltas, beaches and washing limits which date early Holocene. Marine limit throughout this area is metachronous and formed successively with glacier retreat. Marked contrasts in the form and rate of initial unloading are exhibited by emergence curves from the study area. In Blind Fiord, relative sea level exhibits a continuous fall since deglaciation and marine limit formation (cf. Type A curve of Quinlan and Beaumont 1981). Initial unloading was characterised by rates of ≥ 5 m/century. This contrasts with curves from Starfish and Irene bays, where the rate of initial emergence was ≤ 1 m/century. It is noteworthy that the timing of initial emergence at all three sites is similar, slow initial emergence in Irene and Starfish bays was concurrent with rapid initial emergence in Blind Fiord. The validity of this variation is considered uncertain, pending determination of the marine reservoir effect for *Portlandia arctica* in the region, and given the similar radiocarbon chronologies and proximity between sites (with respect to the spatial integration of unloading).

Isobases drawn on the 8.5 ka shoreline for greater Eureka Sound demonstrate that a cell of highest emergence extends along the length of the channel, and closes in the vicinity of the entrance to Norwegian Bay. This pattern is inferred to be compatible with glacial geological evidence for extensive late Wisconsinan glaciation in southern Eureka Sound (Ó Cofaigh Chapter 2, this volume) and is attributed to a solely glacioisostatic origin, indicating a loading centre over Eureka Sound during the late Wisconsinan (cf. Blake 1970).

5.4 RECOMMENDATIONS FOR FUTURE RESEARCH

(1) Collectively, independent glacial geological investigations from several locations (Blake 1992a and b, 1993; Blake *et al.* 1992; Bednarski 1998; England 1998, *in press*, Dyke *in press*; Ó Cofaigh this study), indicate an extensive Last Glacial Maximum for the alpine

sector of the Queen Elizabeth Islands (Ellesmere and Axel Heiberg islands), extending into the central Arctic. However, the extent and dynamics of late Wisconsinan glaciation further west in the archipelago remains unknown. Future priority should therefore be placed on Quaternary geologic studies throughout the western Arctic Archipelago. For example, a key question is the age and source of granite erratics which occur on many of the islands in this region (Craig and Fyles 1965; St.-Onge 1965, Balkwill *et al.* 1974; Hodgson 1989, 1990). Utilisation of surface exposure dating methods would allow direct assessment of the age of these erratics for the first time.

(2) With few exceptions (*e.g.*, McLean *et al.* 1989; Lemmen 1990; Hein and Mudie 1991) the Quaternary marine record of the Canadian High Arctic remains largely unknown. Although logistically challenging, a detailed program of coring and seismic investigation has the potential to provide new insights on the extent of late Wisconsinan glaciation in the archipelago, as well as information on glacier-dynamics, chronology and sedimentation. A key aspect of this would involve sedimentological analysis and radiocarbon dating of cores from the continental shelf off Prince Patrick Island eastwards to the Ringnes islands. If the *Inuitian Ice Sheet* model is accurate with respect to maximum late Wisconsinan ice extent, evidence for glacial expansion and sedimentation should be preserved there, as well the earliest dates on deglaciation. In this regard, the origin of canyons on the continental shelf that extend in towards the fiords and inter-island channels (Johnson *et al.* 1990) should be investigated. Zarkhidze *et al.* (1991) also show shelf-transverse channels extending across the outer part of the continental shelf off Ellesmere and Axel Heiberg islands which continue down the continental slope, and similar channels extend down the continental slope north of Prince Patrick and Borden islands. Many channels have sediment fans at their mouths. The origin and significance of these channels and fans *vis-a-vis* past glacier extent, dynamics and sedimentation (*cf.* Dowdeswell *et al.* 1996; Vorren *et al.* 1998) is uninvestigated.

(3) Finally, a continuing problem for Quaternary glacial geological studies in the Canadian High Arctic is the lack of research on many aspects of contemporary glaciogenic sedimentation in this region. For example, reconstructions of past glaciological information such as basal thermal regime or subglacial drainage from the study of early Holocene glaciomarine sedimentology would be strengthened by reference to appropriate modern

analogues of ice-proximal glaciomarine sedimentary processes and products in the Canadian High Arctic. However, no research has been conducted on this topic. Thus what constitutes the ice-proximal deposits of a modern marine-terminating glacier in the Canadian High Arctic is unknown, and this constrains our ability to interpret the ancient record. Future research on modern ice-proximal glaciomarine sedimentation is therefore particularly desirable.

5.5 REFERENCES

- Alley, R.B., Meese, D.A., Shuman, C.A., Gow, A.J., Taylor, K.C., Grootes, P.M., White, J.W.C., Ram, M., Waddington, E.D., Mayewski, P.A. and Zielinski, G.A. (1993). Abrupt increase in Greenland snow accumulation at the end of the Younger Dryas event. *Nature*, **362**, 527-529.
- Balkwill, H.R., Roy, K.J., Hopkins, W.S. and Sliter, W.V. (1974). Glacial features and pingos, Amund Ringnes Island, Arctic Archipelago. *Canadian Journal of Earth Sciences*, **11**, 1319-1325.
- Bednarski, J. (1995). Glacial advances and stratigraphy in Otto Fiord and adjacent areas, Ellesmere Island, Northwest Territories. *Canadian Journal of Earth Sciences*, **32**, 52-64.
- Bednarski, J. (1998). Quaternary history of Axel Heiberg Island bordering Nansen Sound, Northwest Territories, emphasising the last glacial maximum. *Canadian Journal of Earth Sciences*, **35**, 520-533.
- Bell, T. (1992). *Glacial and sea level history of western Fosheim Peninsula, Ellesmere Island, Arctic Canada*. Unpublished PhD thesis, University of Alberta, Edmonton, 172pp.
- Bell, T. (1996). Late Quaternary glacial and sea level history of Fosheim Peninsula, Ellesmere Island, Canadian High Arctic. *Canadian Journal of Earth Sciences*, **33**, 1075-1086.
- Blake, W.R., Jr. (1970). Studies of glacial history in arctic Canada. I. Pumice, radiocarbon dates, and differential postglacial uplift in the eastern Queen Elizabeth Islands. *Canadian Journal of Earth Sciences*, **7**, 634-664.
- Blake, W.R., Jr. (1977). Glacial sculpture along the east-central coast of Ellesmere Island, Arctic Archipelago. *Geological Survey of Canada Paper 77-1C*, 107-115.
- Blake, W.R., Jr. (1992a). Shell-bearing till along Smith Sound, Ellesmere Island - Greenland: age and significance. *Sverigies Geologiska Undersökning*, **81**, 51-58.
- Blake, W.R., Jr. (1992b). Holocene emergence at Cape Herschel, east central Ellesmere Island, Arctic Canada: implications for ice sheet configuration. *Canadian Journal of Earth Sciences*, **29**, 1958-1980.

- Blake, W.R., Jr. (1993). Holocene emergence along the Ellesmere Island coasts of northernmost Baffin Bay. *Norsk Geologisk Tidsskrift*, **73**, 147-160.
- Blake, W.R., Jr., Boucherle, M.M., Fredskild, B., Janssens, J.A. and Smol, J.P. (1992). The geomorphological setting, glacial history and Holocene development of "Kap Inglefield Sø" North-West Greenland. *Meddelelser om Grønland, Geoscience*, **27**, 41p.
- Blanchon, P. and Shaw, J. (1995). Reef-drowning events during the last deglaciation: evidence for catastrophic sea-level rise and ice-sheet collapse. *Geology*, **23**, 4-8.
- Craig, B.G. and Fyles, J.G. (1960). Pleistocene Geology of Arctic Canada. *Geological Survey of Canada, Paper 60-10*, 21 p.
- Dowdeswell, J.A., Kenyon, N.H., Elverhøi, A., Laberg, J.S., Hollender, F.-J., Mienert, J. and Siegert, M.J. (1996). Large-scale sedimentation on the glacier-influenced Polar North Atlantic margins: long-range side-scan sonar evidence. *Geophysical Research Letters*, **23**, 3535-3538.
- Dyke, A. S. (*in press*). The last glacial maximum and deglaciation of Devon Island: Support for an Inuitian Ice Sheet. *Quaternary Science Reviews*.
- England, J. (1983). Isostatic adjustments in a full glacial sea. *Canadian Journal of Earth Sciences*, **20**, 895-917.
- England, J. (1987). Glaciation and the evolution of the Canadian high arctic landscape. *Geology*, **15**, 419-424.
- England, J. (1990). The late Quaternary history of Greely Fiord and its tributaries, west-central Ellesmere Island. *Canadian Journal of Earth Sciences*, **27**, 255-270.
- England, J. (1992). Postglacial emergence in the Canadian High Arctic: integrating glacioisostasy, eustasy and late deglaciation. *Canadian Journal of Earth Sciences*, **29**, 984-999.
- England, J. (1998). Support for the Inuitian Ice Sheet in the Canadian High Arctic during the last Glacial Maximum. *Journal of Quaternary Science*, **13**, 275-280.
- England, J. (*in press*). Coalescent Greenland and Inuitian Ice during the Last Glacial Maximum: revising the Quaternary of the Canadian High Arctic. *Quaternary Science Reviews*.

- Fairbanks, R. G. (1989). A 17,000 year glacio-eustatic sea level record: influence of glacial melting rates on the Younger Dryas event and deep ocean circulation. *Nature*, **342**, 637-642.
- Fortier, Y.O. and Morley, L.W. (1956). Geological units of the Arctic Islands. *Transactions of the Royal Society of Canada*, **50**, 3-12.
- Fyles, J.G. (1962). In: Jenness, S.E. (ed.), *Field Work, 1961; Geological Survey of Canada Information Circular No.5*, 4-6.
- Fyles, J.G., McNeil, D.H., Matthews, J.V., Jr., Barendregt, R.W., Marincovich, L., Jr., Brouwers, E., Bednarski, J., Brigham-Grette, J.M., Oviden, L.O., Baker, J. and Irving, E. (1998). *Geology of Hvitland beds (late Pliocene), White Point Lowland, Ellesmere Island, Northwest Territories*. Geological Survey of Canada Bulletin 512, 35p.
- Hattersley-Smith, G. (1969). Glacial features of Tanquary Fiord and adjoining areas of northern Ellesmere Island, NWT. *Journal of Glaciology*, **8**, 23-50.
- Hättestrand C. and Stroeven, A.P. (1996). Field evidence for wet-based ice-sheet erosion from the south-central Queen Elizabeth Islands, Northwest Territories, Canada. *Arctic and Alpine Research*, **28**, 466-474.
- Hein, F.J. and Mudie, P.J. (1991). Glacial-marine sedimentation, Canadian polar margin, north of Axel Heiberg Island. *Géographie Physique et Quaternaire*, **45**, 213-227.
- Hodgson, D.A. (1985). The last glaciation of west-central Ellesmere island, Arctic Canada. *Canadian Journal of Earth Sciences*, **22**, 347-368.
- Hodgson, D.A. (1989). Quaternary geology of the Queen Elizabeth Islands. In: Fulton, R.J. (ed.), *Quaternary Geology of Canada and Greenland*, Geological Survey of Canada, Geology of Canada, no. 1, 441-477.
- Hodgson, D.A. (1990). Were erratics moved by glaciers or icebergs to Prince Patrick Island, western Arctic Archipelago, Northwest Territories? In: *Current research, Part D, Geological Survey of Canada, Paper 90-1D*, 67-70.
- Horn, D.R. (1963). *Marine geology, Peary Channel, District of Franklin*. Geological Survey of Canada, Paper 63-11, 33p.

- Johnson, G.L., Grantz, A. and Weber, J.R. (1990). Bathymetry and physiography. In Grantz, A., Johnson, L. and Sweeny, J.F. (eds.), *The Arctic Ocean Region*, Geological Society of America, The Geology of North America, 63-78.
- Lemmen, D.S. (1990). Glaciomarine sedimentation in Disraeli Fiord, High Arctic Canada. *Marine Geology*, **94**, 9-22.
- Lemmen, D.S. and England, J. (1992). Multiple glaciations and sea level changes, northern Ellesmere Island, high arctic Canada. *Boreas*, **21**, 137-152.
- Lemmen, D.S., Aitken, A.E. and Gilbert, R. (1994). Early Holocene deglaciation of Expedition and Strand fiords, Canadian High Arctic. *Canadian Journal of Earth Sciences*, **31**, 943-958.
- Lowe, J.J. and Walker, M.J.C. (1997). *Reconstructing Quaternary Environments*. Second edition, Longman, 446p.
- McLean, B., Sonnichsen, G., Vilks, G., Powell, C., Moran, K., Jennings, A., Hodgson, D.A. and Deonarine, B. (1989). Marine geological and geotechnical investigations in Wellington, Byam Martin, Austin, and adjacent channels, Canadian Arctic Archipelago. *Geological Survey of Canada, Paper 89-11*, 69p.
- Marlowe, J.I. (1968). Sedimentology of the Prince Gustaf Adolf Sea area, District of Franklin. *Geological Survey of Canada, Paper 66-29*, 83p.
- Miller, G.H. and Brigham-Grette, J.B. (1989). Amino acid geochronology: resolution and precision in carbonate fossils. *Quaternary International*, **1**, 111-128.
- Praeg, D. (1989). Geomorphic and geologic evidence for a fluvial/glacial origin of submarine troughs in southern Norwegian Bay, Canadian Arctic Archipelago. *18th Annual Arctic Workshop, Program with Abstracts*, Department of Geography, University of Lethbridge, Alberta, (abstract).
- Quinlan, G. and Beaumont, C. (1981). A comparison of observed and theoretical postglacial relative sea level in Atlantic Canada. *Canadian Journal of Earth Sciences*, **18**, 1146-1163.
- St. Onge, D. (1965). *La geomorphologie de l'Ile Ellef Ringnes Territoires du Nord-Ouest, Canada*. Geographical Branch, Paper 38, 58p.

- Sugden, D.E. (1978) Glacial erosion by the Laurentide Ice Sheet. *Journal of Glaciology*, **20**, 367-391.
- Trettin, H.P. (1991). Middle and late Tertiary tectonic and physiographic developments. In Trettin, H.P. (ed.), *Geology of the Inuitian Orogen and Arctic platform of Canada and Greenland*. Geological Survey of Canada, Geology of Canada, No. 3, 493-496.
- Vorren, T.O., Laber, J.S., Blaume, F., Dowdeswell, J.A., Kenyon, N.H., Mienert, J., Rumohr, J. and Werner, F. (1998). The Norwegian-Greenland Sea continental margins: morphology and late Quaternary sedimentary processes and environment. *Quaternary Science Reviews*, **17**, 273-302.
- Zarkhidze, V.S., Fulton, R.J., Mudie, P.J., Piper, D.J.W., Musatov, E.E., Naryshkin, G.D. and Yashin, D.S. (compilers) (1991). *Circumpolar map of Quaternary deposits of the Arctic*. Geological Survey of Canada, Map 1818A, scale 1: 6 000 000.

APPENDIX A

CHAPTER TWO

Radiocarbon dates and Chlorine-36 dates

Table A.1 Pre-Holocene radiocarbon dates, southern Eureka Sound

Site	Location	Laboratory dating No. ^a	Material ^b	Age (years BP)	Enclosing material	Sample elev. (m asl)	Related RSL (m asl)	Comments
1	Bay Fiord 78°54'N, 85°00'W	AA-23607	<i>Chlamys islandica</i> fragment	37,130±1000	Surface	128	na	Glacially-redeposited sample from granitic till veneer over ice moulded bedrock
2a	Bay Fiord 78°54'N, 85°00'W	AA-23608	<i>H. arctica</i> fragment	33,030±610	Surface	137	na	As above
2b	As above	AA-23609	<i>H. arctica</i> fragment	38,490±1100	Surface	137	na	As above
3a	Bay Fiord 78°51'N, 84°32'W	AA-23605	<i>M. truncata</i> fragment	27,380±360	Surface	198	na	Glacially redeposited sample from sandy gravel outwash
3b	Bay Fiord 78°51'N84°32'W	AA-23606	<i>M. truncata</i> fragment	37,910±960	Surface	198	na	As above
4a	Bay Fiord 78°50'50"N 84°33'00"W	AA-23601	<i>M. truncata</i> fragment	34,830±850	Surface	176	na	Glacially redeposited sample from sandy gravel outwash
4b	As above	AA-23602	<i>M. truncata</i> fragment	30,930±420	Surface	176	na	As above
4c	As above	AA-23603	<i>H. arctica</i> fragment	35,510±730	Surface	176	na	As above
4d	As above	AA-23604	<i>H. arctica</i> fragment	41,690±1700	Surface	176	na	As above

1
3
3

5	Bear Corner 78°10'N, 87°24'W	TO-5602	<i>M. truncata</i> fragment	35,310±400	Surface	191	na	Glacially redeposited sample from till veneer
6a	Baumann Fiord 78°09'N, 87°46'W	TO-5600	<i>M. truncata</i> fragment	36,910±410	Surface	199	na	Glacially redeposited sample from till veneer
6b	Baumann Fiord 78°09'N, 86°46'W	TO-5615	<i>H. arctica</i> ? fragment	36,160±430	Surface	190	na	Glacially redeposited sample from till veneer
7	Bjorne Peninsula 77°29'N, 85°45'W	GSC-2700	<i>H. arctica</i>	30,100±750 ^c	Surface	103-108	?	Whole valves and fragments from gravelly silt on hilltop.
8a	Stor Island 78°58'N, 86°17'W	AA-27489	<i>H. arctica</i> ^b	47,790±3500	Sand	15	>15	Paired valves from bedded sands.
8b	As above	AA-23585	<i>H. arctica</i> ^b	46,850±2800	Sand	15	>15	As above.

^a Laboratory designations: GSC = Geological Survey of Canada; TO = IsoTrace Laboratory, University of Toronto; AA = University of Arizona. TO and AA samples were dated by accelerator mass spectrometry, and corrected for isotopic fractionation to a base of ¹³C = -2.5‰. A reservoir correction of 410 years was then applied, which is equivalent to corrections to a base of ¹³C = 0‰. GSC shell samples were dated conventionally and corrected for fractionation to a base of ¹³C = 0‰.

^b Denotes sample consisting of paired valves found within, or deflating from, enclosing sediment.

^c GSC uncorrected date (Hodgson 1985). This date has not been corrected for isotopic fractionation or a marine reservoir effect.

Table A.2 Holocene radiocarbon dates, southern Eureka Sound.

Sources (including this paper): (Dyck and Fyles 1964; Dyck *et al.* 1965; Lowden and Blake 1968, 1978; Hodgson 1985)

Site	Location	Laboratory dating No. ^a	Material ^b	Age (years BP)	Enclosing material	Sample elev. (m asl)	Related RSL (m asl)	Calibrated age (cal BP) ^d
1	Bay Fiord 78°43.5'N, 82°34'W	GSC-3823 (outer fraction)	<i>M. truncata</i> + fragments	6110±70 ^c	Surface	92	≥ 92 ≤ 100	
1a	As GSC-3823	GSC-3823 (inner fraction)	<i>M. truncata</i> + fragments	7590±80 ^c	Surface	92	≥ 92 ≤ 100	
2	Bay Fiord 78°53'30"N, 82°23'45"W	GSC-5991	<i>M. arenaria</i> ^b	5300±70	Sand and silt	13	≥ 13 ≤ 96	5900 (5720) 5580
3a	Irene Bay 78°03'18"N, 81°28'38"W	GSC-5897	<i>Astarte borealis</i> , <i>H. arctica</i> ^b	5200±70	Sand and silt	55	≥ 55 ≤ 78	5840 (5620) 5460
3b	Irene Bay 78°03'18"N, 81°28'38"W	GSC-5966	Driftwood	6360±100	Sand	55	≥ 55 ≤ 78	7400 (7230) 7010
4	Irene Bay 78°03'11"N, 81°28'52"W	GSC-5955	Driftwood	1790±160	Sand	9	9	2050 (1710) 1340
5	Irene Bay 79°01'N, 81°31'W	GSC-1978	<i>P. arctica</i> ^b	8820±90	Silt	70-74	>80	9810 (9490) 9340
6	Irene Bay 79°01'N, 81°28'W	GSC-3397	<i>H. arctica</i>	7340±170	Surface	66-70	≥75	8170 (7830) 7500

7	Augusta Bay 78°51'N, 81°48'W	GSC-118	<i>H. arctica</i> , <i>M. truncata</i>	6370±100°	Silt	33	≥37	
8a	Strathcona Fiord 78°36'20"N, 82°18'10"W	TO-5143	<i>H. arctica</i> fragment	7740±70	Diamict	17	≥17 ≤ 74	8400 (82.50) 8060
8b	Strathcona Fiord 78°36'20"N, 82°18'30"W	GSC-5937	<i>M. truncata</i> ^b	5220±80	Sand	13	≥13 ≤ 74	5870 (5640) 5470
9	Strathcona Fiord 78°34'N, 82°19'W	GSC-3765	<i>H. arctica</i>	6780±80	Surface	56	>56	7480 (7330) 7170
10	Strathcona Fiord 78°32' 30"N, 82°16'45"W	TO-5144	<i>P. arctica</i> ^b	6700±100	Silt	54	> 54 ≤ 67	7450 (7250) 7030
11	Strathcona Fiord 78°33'N, 82°20'W	GSC-175	Moss peat	7680±150°	Sand	395	na	
12	Strathcona Fiord 78°34' 10"N, 82°20'00"W	TO-5145	<i>Macoma</i> <i>calcareo</i> ^b	5480±60	Silt	7	≥ 7 ≤ 82	6140 (5930) 5760
13	Strathcona Fiord 78°37'N, 82°42'W	AA-23596	<i>P. arctica</i> ^b	7785±65	Silt	24	≥ 24 ≤ 84	8420 (8300) 8110
14a	Strathcona Fiord 78°40'N, 82°45'W	AA-23589	<i>P. arctica</i> ^b	5945±70	Silty sand	16	≥ 16 ≤ 92	6620 (6410) 6270
14b	Strathcona Fiord 78°40'30"N, 82°45'30"W	GSC-5960	<i>Astarte</i> <i>borealis</i>	6110±80	Surface	21	≥ 21 ≤ 92	6820 (6630) 6410
15	Strathcona Fiord 78°42'N, 82°51'W	GSC-170	<i>M. truncata</i> ^b	7750±160°	Silt	75	≥ 77 ≤ 98	

16a	Strathcona Fiord 78°45'N, 83°23'W	AA-23599	<i>M. truncata</i> ^b	7480±65	Silty sand	53	≥ 53 ≤ 122	8130 (7950) 7820
16b	Strathcona Fiord 78°45'N, 83°23'W	GSC-3728	Twig, <i>Salix</i> sp.	7280±90	Silty pebbly sand	70	≥ 53 ≤ 85 (1227)	8250 (8060, 8040, 8000) 7850
17	Bay Fiord 78°49'N, 84°03'W	AA-23586	<i>P. arctica</i> ^b	7140±55	Silty sand	48	≥ 48 ≤ 120	7780 (7630) 7520
18	Bay Fiord 78°51'N, 84°33'W	AA-23598	<i>H. arctica</i> fragment	7180±65	Silt	6	>6≤112	7840 (7660) 7530
19	Bay Fiord 78°54'N, 85°10'W	GSC-452	Whale skull	1380±130 ^c	Surface	2.5	≥ 2.5	
20	Bay Fiord 78°55'N, 85°13'W	AA-23588	<i>H. arctica</i> fragment	8190±60	Gravel	98	≥ 98 ≤ 120	8970 (8740) 8540
21	Eureka Sound 78°50'N, 85°44'W	AA-23590	<i>H. arctica</i>	7745±60	Surface	71	≥ 71 ≤ 76	8380 (8260) 8090
22	Stor Is. 78°53'N, 86°14'W	AA-23584	<i>M. truncata</i> fragment	7615±60	Gravel	49	>49 ≤ 109	8280 (8110) 7950
23	Trapper's Cove 78°39'N, 86°43'W	AA-23587	<i>P. arctica</i> ^b	9030±70	Silt	72	> 72 ≤ 118	9930 (9810) 9540
24	Trapper's Cove 78°32'N, 86°41'W	AA-23593	<i>P. arctica</i> ^b	8925±70	Silt	97	> 97 ≤ 110	9850 (9630) 9460
25	Eureka Sound 78°31'N, 87°14'W	AA-23592	<i>M. truncata</i> fragment	8245±90	Surface	99	99	9140 (8910) 8540
26	Bear Corner 78°08'N, 87°29'W	GSC-6067	<i>M. truncata</i> ^b	6040±60	Sand	23	>23	6710 (6530) 6380

27	Bear Corner 78°07'N, 87°27'W	GSC-6028	<i>M. truncata</i> , <i>H. arctica</i> + fragments	8750±100	Surface	132	≥132 ≤ 142	9760 (9440) 9200
28	Baumann Fiord 78°08'N, 86°45'W	TO-5610	<i>Macoma</i> <i>calcareo</i>	8160±70	Sand	65	>65	8960 (8700) 8500
29	Baumann Fiord 78°08'N, 86°40'W	TO-5862	<i>M. truncata</i> fragment	8590±70	Gravel	128	≥128 ≤ 138	9460 (9330) 9060
30	Blind Fiord 78°23'N, 85°40'W	GSC-5896	<i>M. truncata</i> , <i>H. arctica</i> + fragments	8090±110	Surface	95	≥95 ≤ 120	8950 (8560) 8370
31	Blind Fiord 78°24'N, 85°48'W	TO-5863	<i>H. arctica</i> fragment	7090±70	Surface	109	≥ 109 ≤ 125	7760 (7580) 7440
32	Blind Fiord 78°22'N, 85°48'W	GSC-6054	<i>M. truncata</i> , <i>H. arctica</i>	8220±100	Surface	107	≥ 107 ≤ 124	9100 (8830) 8470
33	Blind Fiord 78°20'45"N, 85°52'30"W	GSC-5924	<i>M. truncata</i> + fragments	7990±140	Surface	86	≥ 86 ≤ 124	8920 (8460) 8190
34	Blind Fiord 78°22'N, 85°50'W	TO-5608	<i>H. arctica</i> fragment	8310±80	Surface	123	≥ 123 ≤ 129	9210 (8950) 8630
35	Blind Fiord 78°20'10"N, 85°50'58"W	GSC-5990	<i>M. truncata</i> <i>H. arctica</i> + fragments	8020±90	Surface	76	≥ 76 ≤ 129	8860 (8490) 8310
36	Blind Fiord 78°19'N, 85°52'W	TO-5598	<i>H. arctica</i> fragment	8670±190	Surface	122	≥ 122 ≤ 128	9850 (9390) 8930
37	Blind Fiord 78°14'N, 85°56'W	TO-5861	<i>H. arctica</i> fragment	5410±70	Surface	122	≥ 122 ≤ 133	6060 (5880) 5670

38	Blind Fiord 78°14'N, 85°57'W	GSC-6047	<i>H. arctica</i> , <i>M. truncata</i>	8550±80	Gravel	119	≥ 119 ≤ 133	9420 (9250) 9000
39	Blind Fiord 78°13'N, 86°04'W	GSC-6102	<i>H. arctica</i> , <i>A. borealis</i> ^b	5640±110	Silt	31	≥ 31 ≤ 39	6360 (6140) 5870
40	Blind Fiord 78°11'N, 86°04'W	TO-5612	<i>M. truncata</i> fragment	8510±80	Surface	127	≥ 127 ≤ 133	9400 (9220) 8970
41	Baumann Fiord 78°06'N, 85°52'W	GSC-244	<i>H. arctica</i> , <i>M. truncata</i> + fragments	8480±140 ^c	Surface	116	≥ 116	
42	Baumann Fiord 78°06'N, 85°28'W	AA-23583	<i>H. arctica</i> fragment	8725±65	Surface	133	≥ 133 ≤ 143	9600 (9430) 9250
43	Trold Fiord 78°06'N, 85°27'W	AA-23591	<i>H. arctica</i> fragment	8645±60	Gravel	131	≥ 131 ≤ 143	9500 (9370) 9180
44	Trold Fiord 78°36'N, 84°30'W	BETA-91868	<i>H. arctica</i> , <i>A. borealis</i> ^b	6320±80	Sand	51	≥ 51	7080 (6850) 6650
45a	Trold Fiord 78°37'N, 84°28'W	TO-5594	<i>P. arctica</i> ^b	8250±450	Silts	83	> 83 ≤ 99	9830 (8920) 7930
45b	Trold Fiord 78°37'N, 84°28'W	AA-23594	<i>P. arctica</i> ^b	8510±75	Silts	76	> 76 ≤ 99	9390 (9220) 8980
46	Trold Bay 78°29'N, 84°34'W	AA-23597	<i>H. arctica</i> ^b	8020±65	Silt	88	> 88 ≤ 92	8810 (8500) 8350
47	Starfish Bay, 78°13'N, 84°34'W	GSC-6037	<i>H. arctica</i> , <i>M. truncata</i>	7740±90	Silt	78	> 78 ≤ 101	8410 (8230) 8000
48	Starfish Bay 78°11'N, 84°08'W	GSC-2719	<i>P. arctica</i> ^b	8710±120	Silt	68	> 72	9730 (9420) 9060

49	Starfish Bay 78°11'N, 84°01'W	TO-5606	<i>H. arctica</i> ^b	5460±60	Silt	18	> 18 ≤ 86	6110 (5910) 5740
50	Starfish Bay 78°10'35"N, 84°02'00"W	GSC-5907	<i>M. truncata</i> ^b + fragments	4800±120	Silt	6	> 6 ≤ 86	5460 (5210) 4840
51	Starfish Bay 78°12'N, 84°00'W	TO-5596	<i>H. arctica</i>	7240±80	Silt	71	>71	7910 (7730) 7570
52a	Starfish Bay 78°10'20"N, 84°03'15"W	GSC-5936	<i>M. truncata</i> ^b + fragments	4630±80	Silt	3	>3 ≤ 80	5240 (4880) 4710
52b	Starfish Bay 78°10'20"N, 84°03'15"W	GSC-5941	<i>M. truncata</i> <i>H. arctica</i> ^b	4950±70	Silt	9	>9 ≤ 80	5570 (5320) 5140
53	Starfish Bay, 78°10'45"N, 84°18'20"W	GSC-5967	<i>M. truncata</i> , <i>M. calcarea</i>	5130±90	Silt	7	>7 ≤ 98	5760 (5570) 5310
54	Troid Fiord, 78°10'45"N, 84°18'20"W	TO-5590	<i>H. arctica</i> fragment	7470±70	Surface	102	≥ 102 ≤ 110	8130 (7950) 7800
55	Troid Fiord, 78°08'0"N, 84°59'30"W	TO-5592	<i>P. arctica</i> ^b	8840±80	Silt	71	>71	9810 (9510) 9380
56	Troid Fiord, 78°08'N, 84°59'W	TO-5604	<i>P. arctica</i> ^b	9200±110	Silt	41	>41	10150 (9940) 9690
57	Troid Fiord 78°07'N, 85°02'W	GSC-6034	<i>M. truncata</i> ^b	8210±90	Sand	75	≥ 75 ≤ 95	9050 (8810) 8480

58	Jaeger Bay 78°03'N, 84°47'W	AA-23600	<i>H. arctica</i> fragment	7795±60	Surface	77	≥ 77 ≤106	8420 (8310) 8120
59	Vendom Fiord 78°04'N, 82°06'W	GSC-1858	<i>H. arctica</i> ^b	7010±80	Sand	52	>54	7680 (7520) 7370
60	Vendom Fiord 78°07'N, 82°08'W	GSC-1957	<i>H. arctica</i>	6980±90	Surface	48-53	>53 (>63?)	7670 (7500) 7320

^a Laboratory designations: GSC = Geological Survey of Canada; TO = IsoTrace Laboratory, University of Toronto; AA = University of Arizona. TO and AA samples were dated by accelerator mass spectrometry. These samples were corrected for isotopic fractionation to a base of ¹³C = -2.5‰; a reservoir correction of 410 years was then applied, which is equivalent to corrections to a base of ¹³C = 0‰; GSC shell samples were dated conventionally and corrected for fractionation to a base of ¹³C = 0‰. GSC terrestrial organic samples were dated conventionally and corrected for fractionation to a base of ¹³C = -2.5‰.

^b Denotes sample consisting of paired valves found within, or deflating from, enclosing sediment.

^c 1960's GSC uncorrected dates (Hodgson 1985). These dates have not been corrected for isotopic fractionation or a marine reservoir effect. Approximate corrections could be made for isotopic fractionation to a base of ¹³C = -2.5‰ by adding 400-410 years to this uncorrected age (R. McNeely, unpublished communication to GSC clientele, 1991). A similar amount could then be subtracted to account for the marine reservoir effect. However, such a correction has not been applied as the result would be approximately the same as the uncorrected raw date reported here. GSC dates obtained during the course of this study (1990's) typically show differences between raw and corrected ages (to a base of ¹³C = 0‰) which are well within the reported standard errors of the individual dates.

^d Dates were calibrated using CALIB 3.0 (Stuiver and Reimer 1993) and calibrated dates are reported at 2 standard deviations.

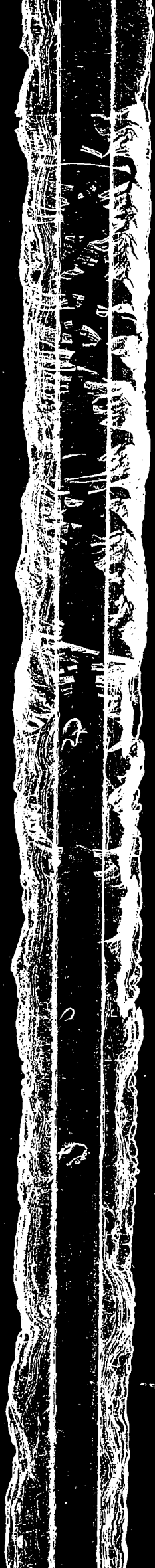
Table A.3 Chlorine-36 surface exposure dates, southern Eureka Sound

Site	Location	Landform	Elevation (m asl)	Age (ky) with zero erosion	Age (ky) with erosion of 5mm/ky	Error (ky)	Comments
1	Bay Fiord 78°53'30"N, 85°18'00"W	Granite erratic	158	11.1	10.8	0.6	Granite boulder resting on surface of till veneer and ice-moulded bedrock.
2	Bay Fiord 78°51'20"N, 84°23'45"W	Granite erratic	155	21.0	20.7	1.0	Granite boulder on summit plateau protruding 0.5m from surface of till.
3	Between Starfish and Jaeger Bays 78°09'20"N, 84°27'00"W	Granite erratic	762	28.0	29.9	0.9	Granite boulder resting on surface of summit regolith.
4	Baumann Fiord, 78°05'00"N, 86°12'00"W	Bedrock	381	16.0	15.6	0.9	Gabbro dyke.
5	Baumann Fiord, 78°08'45"N, 86°49'00"W	Bedrock	234	29.7	27.6	1.3	Gabbro dyke. Shelly granitic till veneer occurs nearby.
6	Baumann Fiord, 78°08'30"N, 87°12'00"W	Gabbro erratic	324	46.4	38.9	2.2	Gabbro boulder resting on sandstone bedrock. Gabbro dykes outcrop nearby.

Table A.4 Early Holocene radiocarbon dates, Eureka Sound and Nansen Sound. Sources (including this paper): (Hodgson *et al.* 1991; Hein and Mudie 1991; Bell 1996; Bednarski 1995, 1998).

Site	Location	Laboratory dating No. ^a	Material	Age (years BP)	Enclosing material	Sample elev. (m asl)	Related RSL (m asl)	Calibrated age (cal BP) ^b
1	Axel Heiberg Shelf ~80°58'N, 97°25'W	TO-1148	Foraminifera	9955±80	Mud	Marine core	-	11220 (10940) 10550
2	Nansen Sound 81°01'N, 91°40'W	GSC-4740	<i>Yoldia</i> sp.	10,300±100	Silt	45	≥45	11950 (11460) 11010
3	Otto Fiord 81°03'N, 88°41'W	TO-1110	<i>Portlandia</i> sp.	11,660±80	Silt	72	>104	13510 (13250) 13040
4	Otto Fiord 81°07'N, 87°04'W	S-2646	<i>M. truncata</i>	9115±130	Surface	77	>77-115	10100 (9870) 9490
5	Fosheim Peninsula 79°56'N, 84°17'W	TO-2240	<i>P. arctica</i>	9560±90	Mud	90	>88 ≤141	10780 (10320) 10030
6	Fosheim Peninsula 79°58.2'N, 84°29'W	GSC-4784	<i>H. arctica?</i>	10,600±90	Surface	122-123	≥123	12420 (12110) 11610
7	Trapper's Cove 78°59'N, 86°43'W	AA-23587	<i>P. arctica</i>	9030±70	Silt	72	>72 ≤118	9930 (9810) 9540
8	Bear Corner 78°07'N, 87°27'W	GSC-6028	<i>M. truncata</i> <i>H. arctica</i> + fragments	8750±100	Surface	132	≥132 - ≤142	9760 (9440) 9200
9	Troid Fiord 78°08'N, 84°59'W	TO-5604	<i>P. arctica</i>	9200±110	Silt	41	>41 ≤143	10220 (9940) 9630

1
4
3



^a Laboratory designations: GSC = Geological Survey of Canada; TO = IsoTrace Laboratory, University of Toronto; S = Saskatchewan Research Council; AA = University of Arizona. TO and AA samples were dated by accelerator mass spectrometry. These samples were corrected for isotopic fractionation to a base of $^{13}\text{C} = -2.5\text{‰}$; a reservoir correction of 410 years was then applied, which is equivalent to corrections to a base of $^{13}\text{C} = 0\text{‰}$; GSC and S shell samples were dated conventionally and corrected for fractionation to a base of $^{13}\text{C} = 0\text{‰}$.

^b Dates were calibrated using CALIB 3.0 (Stuiver and Reimer 1993) and calibrated dates are reported at 2 standard deviations.

APPENDIX B

CHAPTER THREE

Radiocarbon dates

Table B.1: Radiocarbon dates, Starfish Bay and Blind Fiord, southwestern Ellesmere Island.

Site	Location ^a	Laboratory dating No. ^b	Material	Age (years BP)	Enclosing material	Sample elevation (m asl)	Related RSL (m asl)	Calibrated age (cal BP) ^d
1	Starfish Bay (a) 78°08'N, 84°59'W	TO-5604	<i>P. arctica</i> ^c	9200±110	Silt	41	>41	10150 (9940) 9690
2	Starfish Bay (a) 78°08'N, 84°59'W	TO -5592	<i>P. arctica</i> ^c	8840±80	Silt	71	>71	9810 (9510) 9380
3	Starfish Bay (a) 78°09'N, 84°59'W	TO-5590	<i>H. arctica</i>	7470±70	Surface	102	>102 ≤ 110	8130 (7950) 7800
4	Starfish Bay (b) 78°13'N, 84°34'W	GSC-6037	<i>M. truncata</i> , <i>H. arctica</i>	7740±90	Silt	78	>78 ≤ 101	8410 (8230) 8000
5	Starfish Bay (c) 78°11'N, 84°08'W	GSC-2719	<i>P. arctica</i> ^c	8710±120	Silt	68	>72	9730 (9420) 9060
6	Starfish Bay (c) 78°12'N, 84°00'W	TO-5596	<i>H. arctica</i>	7240±80	Silt	71	>71	7910 (7730) 7570
7	Blind Fiord (a) 78°09'N, 86°46'W	TO-5600	<i>Mya truncata</i>	36,910±410	Surface	199	-	-
8	Blind Fiord (a) 78°09'N, 86°46'W	TO-5615	Shell fragment	36,160±430	Surface	190	-	-
9	Blind Fiord (a) 78°08'N, 86°40'W	TO-5862	<i>M. truncata</i>	8590±70	Surface	128	≥128 ≤ 138	9460 (9330) 9060
10	Blind Fiord (a) 78°08'N, 86°45'W	TO-5610	<i>M. calcarea</i>	8160±70	Sand	65	>65	8960 (8700) 8500
11	Blind Fiord (b) 78°11'N, 86°04'W	TO-5612	<i>M. truncata</i>	8510±80	Surface	127	≥127 ≤ 133	9400 (9220) 8970
12	Blind Fiord (b) 78°14'N, 85°57'W	GSC-6047	<i>M. truncata</i> , <i>H. arctica</i>	8550±80	Gravel	119	≥119 ≤ 133	9420 (9250) 9000

13	Blind Fiord (b) 78°19'N, 85°52'W	TO-5598	<i>H. arctica</i>	8670±190	Surface	122	≥122 ≤ 128	9850 (9390) 8930
14	Blind Fiord (c) 78°22'N, 85°50'W	TO-5608	<i>H. arctica</i>	8310±80	Surface	123	≥123 ≤ 129	9210 (8950) 8630
15	Blind Fiord (c) 78°20'N, 85°52'W	GSC-5924	<i>M. truncata</i> + frags.	7990±140	Surface	86	≥86 ≤ 124	8920 (8460) 8190
16	Blind Fiord (c) 78°22'N, 85°48'W	GSC-6054	<i>M. truncata</i> , <i>H. arctica</i>	8220±100	Surface	107	≥107 ≤ 124	9100 (8830) 8470
17	Blind Fiord (c) 78°24'N, 85°48'W	TO-5863	<i>H. arctica</i>	7090±70	Surface	109	≥109 ≤ 125	7760 (7580) 7440
18	Blind Fiord (c) 78°23'N, 85°48'W	GSC-5896	<i>M. truncata</i> , <i>H. arctica</i> + frags.	8090±110	Surface	95	≥95 ≤ 120	8950 (8560) 8370

1-47
a Letters in parentheses designate sectors A, B, and C from both fiords referred to in text.

b Laboratory designations: TO samples were dated by accelerator mass spectrometry at IsoTrace, University of Toronto; GSC are conventionally dated samples by the Geological Survey of Canada. IsoTrace dates have been corrected for fractionation to a base of $^{13}\text{C} = -25\text{‰}$; a reservoir correction of 410 years was then applied which is equivalent to a base of $^{13}\text{C} = 0\text{‰}$. GSC dates were corrected for fractionation to a base of 0‰ .

c Denotes samples consisting of paired valves found within, or deflating from, enclosing sediment.

d Dates were calibrated using CALIB 3.0 (Stuiver and Reimer 1993), and calibrated ages are reported to two standard deviations.

APPENDIX C
CHAPTER FOUR
Radiocarbon dates

Table C.1 Holocene radiocarbon dates, greater Eureka Sound

Sources (incl. this paper): (Dyck *et al.* 1965; Hodgson 1985; Hodgson, in McNeeley 1989; England 1990, 1992; Lemmen *et al.* 1994; Bednarski 1995; Bell 1996)

Site	Location	Laboratory dating No. ^a	Material	Age (years BP)	Enclosing material	Sample elev. (m asl)	Related RSL (m asl)	Calibrated age (cal BP) ^c
1	Ellesmere Island Baumann Fiord 78°08'N, 86°40'W	TO-5862	<i>M. truncata</i> fragment	8590±70	Surface	128	≥128 - ≤138	9460 (9330) 9060
2	Ellesmere Island Blind Fiord 78°11'N, 86°04'W	TO-5612	<i>M. truncata</i> fragment	8510±80	Surface	127	≥127 - ≤133	9400 (9220) 8970
3	Ellesmere Island Blind Fiord 78°14'N, 85°57'W	GSC-6047	<i>H. arctica</i> , <i>M. truncata</i>	8550±80	Gravel	119	≥119 - ≤133	9420 (9250) 9000
4	Ellesmere Island Blind Fiord 78°22'N, 85°50'W	TO-5608	<i>H. arctica</i> fragment	8310±80	Surface	123	≥123 - ≤129	9210 (8950) 8630
5	Ellesmere Island Blind Fiord 78°22'N, 85°48'W	GSC-6054	<i>M. truncata</i> , <i>H. arctica</i>	8220±100	Surface	107	≥107 - ≤124	9100 (8830) 8470
6	Ellesmere Island Blind Fiord 78°23'N, 85°40'W	GSC-5896	<i>M. truncata</i> , <i>H. arctica</i> , fragments	8090±110	Surface	95	≥95 - ≤120	8950 (8560) 8370
7	Ellesmere Island Blind Fiord 78°13'N, 86°04'W	GSC-6102	<i>H. arctica</i> , <i>A. borealis</i>	5640±110	Silt	31	≥31 - ≤39	6360 (6140) 5870
8	Ellesmere Island Starfish Bay, 78°13'N, 84°34'W	GSC-6037	<i>H. arctica</i> , <i>M. truncata</i>	7740±90	Silt	78	>78 - ≤101	8410 (8230) 8000

9	Ellesmere Island Starfish Bay 78°11'N, 84°08'W	GSC-2719	<i>P. arctica</i>	8710±120	Silt	68	>68 - ≤89	9730 (9420) 9060
10	Ellesmere Island Starfish Bay 78°12'N, 84°00'W	TO-5596	<i>H. arctica</i>	7240±80	Silt	71	≥71	7910 (7730) 7570
11	Ellesmere Island Irene Bay 79°01'N, 81°31'W	GSC-1978	<i>P. arctica</i>	8820±90	Silt	70-74	≥80 (≤92)	9810 (9490) 9340
12	Ellesmere Island Irene Bay 79°01'N, 81°28'W	GSC-3397	<i>H. arctica</i>	7340±170	Surface	66-70	≥70 - ≤75	8170 (7830) 7500
13	Ellesmere Island Irene Bay 78°03'N, 81°28'W	GSC-5897	<i>Astarte borealis,</i> & <i>H. arctica</i>	5200±70	Sand and silt	55	≥55 - ≤78	5840 (5620) 5460
14	Ellesmere Island Irene Bay 78°03'N, 81°28'W	GSC-5966	Driftwood	6360±100	Sand	55	≥55 - ≤78	7400 (7230) 7010
15	Ellesmere Island Irene Bay 78°03'N, 81°28'W	GSC-5955	Driftwood	1790±160	Sand	9	9	2050 (1710) 1340
16	Ellesmere Island Eureka Sound 79°14'N, 85°30'W	TO-2245	<i>H. arctica</i>	8430±70	Silt	101	>101	9350 (9090) 8920
17	Ellesmere Island Cafion Fiord 79°35'N, 80°31'W	TO-2339	<i>M. truncata</i>	8380±80	Sand	98	>98 - ≤114	9310 (9000) 8740
18	Ellesmere Island Fosheim Peninsula 79°48'N, 86°18'W	GSC-5156	<i>H. arctica</i>	8680±80	Silt	132	>132 - ≤150	9560 (9390) 9150

19	Ellesmere Island Fosheim Peninsula 79°50'N, 85°13'W	TO-2241	<i>M. truncata</i>	8480±80	Silt	93	>93	9380 (9190) 8950
20	Ellesmere Island Fosheim Peninsula 79°58'N, 85°22'W	GSC-4708	<i>M. truncata</i>	8520±80	Silt	100	>100 - ≤146	9400 (9210) 8970
21	Ellesmere Island Fosheim Peninsula 79°58'N, 84°26'W	GSC-5155	<i>M. truncata</i>	8570±120	Silt	100	>100 - ≤145	9500 (9270) 8950
22	Ellesmere Island Fosheim Peninsula 80°11'N, 86°33'W	TO-2233	<i>M. truncata</i>	8440±80	Surface	94	≥94	9370 (9140) 8900
23	Ellesmere Island Fosheim Peninsula 80°15'N, 85°02'W	TO-2229	<i>M. truncata</i>	8450±80	Silt	94	>94 - ≤149	9370 (9150) 8920
24	Ellesmere Island Greely Fiord 80°24'N, 81°30'W	GSC-2369	<i>M. truncata</i>	8450±100	Surface	127	≥127 - ≤146	9400 (9140) 8820
25	Ellesmere Island d'Iberville Fiord 80°43'N, 80°35'W	S-2640	<i>H. arctica</i>	8415±130	Silt	88	>88 - ≤139	9390 (9030) 8660
26	Ellesmere Island Greely Fiord 80°43'N, 80°35'W	S-2645	<i>M. truncata</i>	8465±130	Sand	95	>95 - ≤124	9430 (9160) 8730

27	Ellesmere Island Hare Fiord 81°05'N, 85°14'W	S-2641	<i>H. arctica</i>	8590±130	Silt	88	>88 - ≤110	9540 (9320) 8940
28	Ellesmere Island Nansen Sound 81°06'N, 90°10'W	S-2639	<i>M. truncata</i>	8370±130	Silt	103-105	>105	9360 (8980) 8600
29	Axel Heiberg Is. Strand Fiord 91°47'N, 79°10'W	GSC-5408	<i>M. truncata</i> , <i>H. arctica</i>	8390±100	Sand and gravel	37-63	>63 - ≤105	9340 (9000) 8700
30	Axel Heiberg Is. Strand Fiord 90°17'N, 79°15'W	GSC-5411	<i>M. truncata</i>	8430±80	Surface	84-93	≥93 - ≤124	9360 (9080) 8850
31	Ellesmere Island Baumann Fiord 78°06'N, 85°52'W	GSC-244	<i>H. arctica</i> , <i>M. truncata</i> , fragments	8480±140 ^b	Surface	116	≥116 - ≤122	
32	Ellesmere Island Told Fiord 78°06'N, 85° 27'W	AA-23591	<i>H. arctica</i> fragment	8645±60	Gravel	131	≥131 - <143	9500 (9370) 9180
33	Ellesmere Island Norwegian Bay 77°07'N, 87°42'	GSC-840	<i>H. arctica</i> , <i>M. truncata</i> , + fragments	8590±150 ^b	Surface	107	≥107	
34	Graham Island 77°16'N, 89°57'W	GSC-2253	<i>M. truncata</i>	8420±160	Sand	102	>102	9430 (9040) 8600

^a Laboratory designations: GSC = Geological Survey of Canada; TO = IsoTrace Laboratory, University of Toronto; S = Saskatchewan Research Council; AA = University of Arizona. TO and AA samples were dated by accelerator mass spectrometry. These samples were corrected for isotopic fractionation to a base of $^{13}\text{C} = -25\text{‰}$; a reservoir correction of 410 years was then applied, which is equivalent to correction to a base of $^{13}\text{C} = 0\text{‰}$; GSC and S samples were dated conventionally and corrected for fractionation to a base of $^{13}\text{C} = 0\text{‰}$. GSC terrestrial organic samples were dated conventionally and corrected for fractionation to a base of $^{13}\text{C} = -25\text{‰}$.

^b 1960's GSC uncorrected dates (Hodgson 1985). These dates have not been corrected for isotopic fractionation or a marine reservoir effect. Approximate corrections could be made for isotopic fractionation to a base of $^{13}\text{C} = -25\text{‰}$ by adding 400-410 years to this uncorrected age (R. McNeely, unpublished communication to GSC clientele, 1991). A similar amount could then be subtracted to account for the marine reservoir effect. However, such a correction has not been applied as the result would be approximately the same as the uncorrected raw date reported here. GSC dates obtained during the course of this study (1990's) typically show differences between raw and corrected (to a base of $^{13}\text{C} = 0\text{‰}$) ages which are well within the reported standard errors of the individual dates.

^c Dates were calibrated using CALIB 3.0 (Stuiver and Reimer 1993) and calibrated dates are reported at 2 standard deviations.